1977

Coulometric detection in liquid chromatography

John H. Larochelle
Iowa State University

INFORMATION TO USERS

This material was produced from a microfilm copy of the original document. While the most advanced technological means to photograph and reproduce this document have been used, the quality is heavily dependent upon the quality of the original submitted.

The following explanation of techniques is provided to help you understand markings or patterns which may appear on this reproduction.

1. The sign or "target" for pages apparently lacking from the document photographed is "Missing Page(s)". If it was possible to obtain the missing page(s) or section, they are spliced into the film along with adjacent pages. This may have necessitated cutting thru an image and duplicating adjacent pages to insure you complete continuity.

2. When an image on the film is obliterated with a large round black mark, it is an indication that the photographer suspected that the copy may have moved during exposure and thus cause a blurred image. You will find a good image of the page in the adjacent frame.

3. When a map, drawing or chart, etc., was part of the material being photographed the photographer followed a definite method in "sectioning" the material. It is customary to begin photoing at the upper left hand corner of a large sheet and to continue photoing from left to right in equal sections with a small overlap. If necessary, sectioning is continued again — beginning below the first row and continuing on until complete.

4. The majority of users indicate that the textual content is of greatest value, however, a somewhat higher quality reproduction could be made from "photographs" if essential to the understanding of the dissertation. Silver prints of "photographs" may be ordered at additional charge by writing the Order Department, giving the catalog number, title, author and specific pages you wish reproduced.

5. PLEASE NOTE: Some pages may have indistinct print. Filmed as received.

University Microfilms International
300 North Zeeb Road
Ann Arbor, Michigan 48106 USA
St. John's Road, Tyler's Green
High Wycombe, Bucks, England HP10 8HR

Coulometric detection in liquid chromatography

by

John H. Larochelle

A Dissertation Submitted to the
Graduate Faculty in Partial Fulfillment of
The Requirements for the Degree of
DOCTOR OF PHILOSOPHY

Department: Chemistry
Major: Analytical Chemistry

Approved:

Signature was redacted for privacy.

In Charge of Major Work

Signature was redacted for privacy.

For the Major Department

Signature was redacted for privacy.

For the Graduate College

Iowa State University
Ames, Iowa

1977

TABLE OF CONTENTS

LIST OF FIGURES

LIST OF TABLES

I. INTRODUCTION

Advances in the development of high performance liquid chromatography (HPLC) have been restricted by the lack of suitable detectors for the large variety of analytical problems of interest. As the performance of liquid chromatographs has been improved and interest has increased in the analysis of complex samples with very low analyte concentrations, the requirements on the detector have increased. Requirements for detectors which are suitable for use with modern liquid chromatography include high sensitivity, a large linear dynamic range, and a small internal volume.

At the present time, the most popular detector for use with HPLC is the photometric detector which is based on the absorption of electromagnetic radiation by analyte species in the chromatographic effluent. Analytes which are not colored can be detected photometrically if they are caused to react with color-forming reagents in the effluent stream of the chromatograph to form colored products prior to passage through the detector. The output of the photometric transducer, P, is a non-linear function of the concentration of the analyte in the sample cell as described by Equation I.1.

$$P = P_o \cdot 10^{-\varepsilon b C} \qquad \text{(I.1)}$$

In Equation I.1, P_o = output signal when C = 0;

C = concentration of absorbing species in

the detector cell (mole/l);

b = path length of optical beam in the detector cell (cm);

ε = molar absorptivity of the absorbing species (l/mole-cm).

The change in the output signal from the transducer, ΔP, is related to the change in concentration of the absorbing species within the detector cell, ΔC, as described by Equation I.2.

$$\Delta P = -\varepsilon b P_o \cdot 10^{-\varepsilon b C} \Delta C \qquad (I.2)$$

The value of ΔP is a non-linear function of concentration, according to Equation I.2, and is seldom applied directly for quantitation. Associated electronic circuitry is used to calculate the absorbance, A, of the absorbing species by electronically computing the logarithm of the ratio P_o/P. The output of the detector is thus linearized with respect to C as given by Equation I.3.

$$A = \log(P/P_o) = \varepsilon b C \qquad (I.3)$$

The absorbance is proportional to the cell path length and efforts to minimize the internal volume of the detector result in increasing demands on the photometric detector to maintain high sensitivity with a minimum of electrical noise. At the present time, photometric detectors are available with b = 1.0 cm and internal volumes of 10 µl for which the minimum detectable A is approximately 0.001.

Use of detectors based on the electrochemical principle of amperometry can offer some advantages for HPLC in comparison with photometric detectors. Sensitivities of amperometric detectors for electroactive species are very great and relatively independent of the chemical identity, whereas the molar absorptivity is a direct consequence of chemical structure and may differ by several orders of magnitude for two analyte species. Furthermore, a simple linear relationship between the detector output and the amount of analyte passing through the detector is predicted, thus eliminating the need for electronic signal modification which may introduce error. Response of an amperometric detector for an electroactive analyte is described by Faraday's law as given be Equation I.4.

$$I = nFJ \qquad (I.4)$$

In Equation I.4, I = electrical current (coul/sec);
F = the Faraday constant (96,487 coul/equiv);
J = flux of electroactive analyte at the detector surface (moles/sec);
n = number of electrons in the half reaction (equiv/mole).

A direct comparison of the sensitivities and limits of detection of the photometric and amperometric detectors is easily illustrated. The accurate measurement of an electrode current as small as 10^{-9} coul/sec is possible using modern

inexpensive electronic devices. For this example, a value of 10 µl/sec is chosen as the rate of flow of effluent in the detectors. The corresponding concentration of Ag^+ detected electrochemically is 10^{-7} g/l (0.1 part per billion). The value of ε necessary for photometric detection of this concentration in a 1.0-cm cell is 10^6 l/mol-cm, a value larger than any reported for synthetically produced compounds to my knowledge.

The design and several applications of amperometric detectors suitable for use in HPLC are described in this manuscript.

II. LITERATURE REVIEW

A. Requirements of a Detector

General acceptance of liquid chromatography as an instrumental method of chemical analysis has been retarded by the lack of suitable detectors. Many detectors for liquid chromatography have been developed (1-10), but none have universal applicability with high sensitivity. Consequently, commercially produced liquid chromatographs are available with a choice of detectors. The variety of detectors available for liquid chromatography have been extensively reviewed in the analytical literature (11-19).

Several workers in the field of liquid chromatography have proposed procedures and criteria for the evaluation of detectors for chromatography (20-24). The following parameters should be considered when selecting a detector for use with liquid chromatography:

1. sensitivity and limit of detection,
2. linear dynamic range,
3. calibration and precision,
4. signal to noise ratio,
5. response to parameters other than solute concentration,
6. internal volume and
7. ease of operation.

Detectors may be divided into two classes depending on the scope of application: general detectors and selective detectors. General detectors have similar sensitivity for a broad spectrum of analyte species while selective detectors have a high sensitivity only for a specific group of analytes. A sacrifice in sensitivity usually accompanies the change from a selective detector to a general detector. The two most common general detectors for liquid chromatography are the refractive index detector and the micro-adsorption detector. Because these detectors also respond to changes of the mobile phase and are very sensitive to temperature changes, they do not have as low a detection limit as certain selective detectors and they are usually not used with gradient elution or when analyte concentration is extremely low. When using a general detector, the chromatographic system must be able to separate the analyte of interest from the other constituents of the sample. However, if a selective detector is used the chromatographic system need only separate the analyte of interest from other members of the class of compounds for which the detector is sensitive. For complex mixtures, selectivity can be a distinct advantage. The photometric detector is the most commonly used selective detector in liquid chromatography. Not only is the photometric detector selective to those solutes which absorb radiation at the chosen wavelength, but the sensitivity of

the detector may be changed by adjusting the wavelength of the photometric beam. Selective detectors, such as the photometric detector, generally are favored over general detectors where applicable (21).

The limit of detection for instrumental methods of analysis is determined by the sensitivity and noise of the system. The sensitivity is the response per unit of analyte concentration. The detection limit is taken as that sample size which will produce a detector response which is some multiple of the standard deviation of the background signal. In gas chromatography, for example, the multiple is usually two. However, this custom is not so well established in liquid chromatography.

A linear detector is one for which the detector output is proportional to the amount of the analyte passing through the detector. Although the output signal of the transducer element in the detector may not be linear with the amount of analyte present, a specified function of the transducer output may be used which is linear with the amount of analyte. For example, the photo-transducer of a photometric detector has a response which is proportional to the transmittance of the solution and an exponential function of analyte concentration. However, the negative logarithm of the transmittance, the absorbance, is a linear function with respect to the concentration of the analyte. Hence, most modern

photometric detectors are constructed with an electronic circuit which automatically computes the logarithm of the transmittance.

The upper limit of linearity is the maximum amount of analyte which results in a detector response which is linear within the specified confidence limits. The lower limit of the linear range may be considered the detection limit (23).

Almost all chromatographic systems must be calibrated at some time and it is desirable that the detector be easily calibrated and that the sensitivity remain constant for a long period of time.

Noise is the variation of the output of the detector which is not directly related to the concentration of the analyte. Noise can be classified as short-term noise, long-term noise or drift. Short-term noise has a period which is much less than the time period for detector response to the analyte and introduces uncertainty in the shape of the chromatographic peak. Long-term noise has a period on the order of the time for the chromatographic peak and introduces uncertainty in the baseline of the chromatographic peak. Drift has a period which is much greater than the time for the chromtographic peak. As for long-term noise, drift can obscure broad peaks with low peak heights. Although drift is not necessarily linear with time, the assumption is

usually made that drift is linear within the time period of a chromatographic peak. The baseline for a chromatographic peak, therefore, is conveniently assumed to be represented by a straight line drawn to superimpose the baseline immediately before and after the peak. Drift does not cause much uncertainty in the baseline determined in this manner but may interfere with techniques of peak integration which cannot account for the change in baseline which occurs with time. Drift may also require the occasional offsetting of the recorder baseline so that the chromatographic peak remains on the chart.

Detector noise results from the response of the detection system to changes in experimental parameters or from change in the sensitivity of the detector due to changes in experimental parameters. For example, the refractive index detector and the micro-adsorption detector are very sensitive to changes in temperature and may respond to a change in temperature as small as 10^{-4} °C. The sensitivities of the refractive index detector and the micro-adsorption detector are also a function of the flow rate of the eluent (21) and, therefore, changes in flow rate result in noise and loss of precision. Noise in electrochemical systems has been reviewed by Tyagai (25).

Most detectors, including the photometric detector, respond to the concentration of the analyte passing through

the detector. Some detectors, such as the flame ionization detector for gas chromatography and the coulometric detector, which will be described in this manuscript, do not respond to concentration but rather to the total flux of analyte. The number of moles of analyte, N, in the solvent stream is related to the concentration of the analyte, C, and the volume flow rate, V_f by Equation II.1.

$$N = \int C V_f dt \qquad \text{(II.1)}$$

In general practice, V_f is assumed to be constant and the time integral of the detector response, or the area of the recorded chromatographic peak, is taken to be proportional to N. When using peak area for quantitation with a concentration-sensitive detector, change in V_f will lead to error. However for detectors which respond to the total flux of analyte, the peak area is proportional to the number of moles of analyte which have passed through the detector regardless of fluctuations in V_f.

The internal volume of the detector should be small to keep the chromatographic resolution high. Furthermore in modern high performance liquid chromatography, an analyte peak may be entirely contained in 0.1 ml of effluent. It is desirable, therefore, that the volume of the detector be minimal, e.g., 10 µl or less, so sensitivity is a maximum.

Finally, the operation of the detector should be considered. Detectors can be destructive or non-destructive.

Non-destructive detectors may be put in series to make available the particular advantages of each. The detector should be continuous in operation and have a response time which is fast enough to follow the fastest change in analyte concentration.

Also of importance to the analyst is the cost, ease of operation and maintenance required of the detector system.

B. Amperometric Detectors

Amperometric detectors are selective in operation. The sensitivity for a potentially electroactive analyte may be controlled by the selection of electrode potential, electrode material, electrolyte, and the pretreatment of the electrode. The electrochemical response of an amperometric detector can be related to the flux of electroactive species on the basis of Faraday's law of electrolysis and Fick's laws of diffusion as given by Equation II.2.

$$I = nFJ = nFAD(dC/dx) \qquad \text{(II.2)}$$

In Equation II.2, A = area of the electrode (cm^2);

D = diffusion coefficient (cm^2/sec);

dC/dx = concentration gradient at electrode surface (moles/cm^2).

The constants n, F, and J, have the meaning described previously for Equation I.4.

The concentration gradient at the electrode surface is related to a distance, δ, which is equivalent to the thickness of the quiescent fluid layer at the electrode surface through which diffusion is the primary mechanism of mass transport.

$$dC/dx = \frac{C^b - C^o}{\delta} \qquad \text{(II.3)}$$

In Equation II.3, C^b = bulk concentration of electroactive species;

C^o = surface concentration of electroactive species.

When concentration values are given in units of moles/liter, the current is in mA. The value of δ is uniquely dependent on the geometry of the electrode and the conditions of fluid flow at the electrode surface.

Levich examined many electrode designs under conditions of convective mass transport and demonstrated that the electrode currents are a function of the fluid velocity in the vicinity of the electrode. A popular form for an electrochemical detector is a tube through which the electrolyte passes with electrolysis occurring at the inner surface of the tube. Levich (26) solved the equations of mass transport for the tubular electrode under conditions of laminar fluid flow and the limiting current ($C^o = 0$) was predicted to be given by Equation II.4.

$$I_l = 5.43nFD^{2/3}L^{2/3}V_f^{1/3}C^b \qquad \text{(II.4)}$$

In Equation II.4, L = length of tube (cm);

V_f = fluid flow rate (ml/sec).

The derivation of Equation II.4 was made assuming a negligible consumption of the electroactive analyte from the electrolytic solution flowing through the tubular electrode. Blaedel and co-workers (27-29) confirmed Equation II.4 and demonstrated the application of a tubular electrode for analysis of several electrochemical systems.

The tubular electrodes usually applied for electroanalysis electrolyze only a fraction of the electroactive species, in accordance with the assumption of Levich, and, therefore, do not realize the maximum sensitivity possible. For example, the tubular electrode of Blaedel and Boyer (29) electrolyzed 0.4% of the electroactive species at V_f = 3.5 ml/min.

As predicted by Equation II.4, the sensitivity of a tubular detector is a function of fluid flow rate, V_f. Assuming the value of V_f to be constant during the period of electrolysis, the number of coulombs of charge, Q, which pass in the electrode during application for chromatographic detection is given by Equation II.5.

$$Q = 5.43nFD^{2/3}L^{2/3}V_f^{1/3}\int C^b(t)\,dt \qquad (II.5)$$

The number of moles of analyte in the peak, N, is related to time-dependent concentration by Equation II.6.

$$N = V_f\int C^b(t)\,dt \qquad (II.6)$$

The combination of Equations II.5 and II.6 yields Equation II.7 relating the area of the detection peak to the moles of analyte in the peak.

$$Q = 5.43nFD^{2/3}L^{2/3}V_f^{-2/3}N \qquad \text{(II.7)}$$

As seen in an examination of Equation II.7, V_f must be held constant during calibration and analysis with the tubular detector for maximum precision and accuracy. Amperometric detectors with designs different than the tubular electrode will also have response characteristics which are strongly dependent on V_f.

Müller (30) in 1947 first reported the use of an electrode for amperometric electroanalysis in a flowing stream. Although Muller's work employed a platinum electrode, subsequent work focused primarily on using the dropping mercury electrode (DME) for electroanalysis of flowing streams. The first application of the DME for continuous analysis of a flowing stream was reported by Kemula (31) in 1952. Kemula applied the DME to the effluent of a liquid chromatographic column. Other workers have since reported numerous designs of detectors for flowing streams based on the DME (32-39). These detectors have been used for monitoring a large variety of analytes: sulfur dioxide (40), uranium in process streams (41), various other inorganic metal ions (37, 42-48), nitro compounds (32), amino acids

(49, 50), proteins (51), pesticides (52, 53), aldehydes and ketones (54) and alkaloids (55).

The major benefit to be derived from the use of a Hg electrode is the large cathodic range available for applied voltage. However, the disadvantages of the DME as a detector in flowing streams include the periodic nature of the electrode, the large residual current due to the charging of the electrical double layer of the growing electrode, and the irregular drop times obtained in a flowing stream. The periodic nature of the drop sets a limit to the response time of the detector. The combination of the charging current and the irregular drop time generates noise which can obscure small faradaic signals. Mercury pools have also been applied as electrodes for stream analysis (56). The Hg-pool electrode is free of some of the above interferences, but motion of the pool surface caused by the incident fluid causes irregular limiting currents and large background currents (56).

The disadvantages listed for Hg detectors are not observed for solid electrodes. Solid electrodes based on carbon have a much larger anodic working range while still retaining an appreciable overvoltage for the reduction of hydrogen ion. Adams, et al. (57, 58) described an inexpensive detector based on carbon paste for the detection of biogenic amines in physiological samples and reported a

sensitivity which rivals that for gas chromatography of the derivatives with mass spectrometric detection. Carbon-based electrodes have been used for the detection of inorganic ions (59-62) and organic compounds (63-67). The carbon paste electrode has found wide application for the detection of biogenic compounds (58, 65, 68-76) and has been reviewed by Kissinger et al. (77).

Yamada and Matsuda (78) described and evaluated a detector called a "wall jet electrode" in which a jet of the electrolyte issued forth from a circular nozzle with axisymmetrical laminar flow onto a stationary electrode in the shape of a disk. Matsuda (79) showed that I_l was related to C^b by Equation II.8.

$$I_l = knFV_f^{3/4}a^{-1/2}R^{3/4}C^b \qquad \text{(II.8)}$$

In Equation II.8, a is the diameter of the nozzle and R is the radius of the disk. Yamada and Matsuda verified Equation II.8 and applied it to the determination of ferricyanide. Fleet and Little (80) described the application of a wall jet detector to the effluent of a HPLC.

C. Coulometric Detectors

The so-called "coulometric detector" is an amperometric detector in which all of the electroactive analyte in the electrolyte stream is electrolyzed. The response of a coulometric detector is predicted by Equation II.9.

$$I = nFV_fC^b \qquad \text{(II.9)}$$

For the application of a coulometric detector in liquid chromatography, the charged passed for elution of an electroactive species is given by Equation II.10.

$$Q = nFN \qquad \text{(II.10)}$$

The sensitivity of a coulometric detector is, therefore, independent of experimental parameters and the need for calibration is eliminated. The coulometric detector can potentially be the most accurate and precise of the many detectors available for quantitative analysis by liquid chromatography. This advantage is in addition to the fact of very high sensitivity as already discussed for amperometric detectors.

Efforts to develop coulometric detectors which can operate at high values of V_f have centered on increasing the surface area of the electrode while minimizing the internal volume of the detector and the cell resistance. The total flux can be increased by increasing the electrode surface or by decreasing the thickness of the diffusion layer at the electrode-solution interface. Eckfeldt (81) described an electrode having an appearance similar to a rat maze through which the electrolyte passed in contact with a gold electrode. Bard (82) proposed the use of ultrasonic waves in the vicinity of a gauze electrode to reduce the diffusion layer thickness by disrupting the laminar flow patterns over the surface of the electrode. Johansson (83) described a device for

increasing the flux of analyte to the surface of a cylindrical electrode by rotating a concentric rod within the electrode at a high velocity. Electrodes which are simple in design and operation and yet retain coulometric efficiency at high flow rates have been those electrodes which have been constructed by packing a detection cavity with finely divided electrode material as particles (84-91), wire mesh or gauze (92), and porous or fritted metals (93). These types of packing have large surface areas and contain minimal volumes of electrolyte. The packing also disrupts the laminar flow patterns of the electrolyte and, therefore, promotes a smaller value of the diffusion layer thickness.

The first reported application of a coulometric detector was by Shaffer, Briglio and Brockman (94) in 1948 for use in the continuous analysis of a gas stream. Eckfeldt and Shaffer (84) reported the use of a coulometric electrode for determining dissolved oxygen. Sioda used a granular graphite electrode (88) for the determination of $Fe(CN)_6^{3-}$ and discussed the theory of that detector, and electrodes constructed from rolled 80-mesh platinum gauze. Taylor and Johnson (95) used the coulometric detector constructed in my research to determine antimony in alloys and in human hair. Takata and Muto (96) developed a coulometric detector for use with liquid chromatography and demonstrated its use in the detection of a variety of substances including metal

cations, inorganic anions, organic acids and sugars. Fujinaga (59) has reviewed the use of coulometric detectors and electrochromatography.

III. INSTRUMENTATION

A. Electronic Circuitry

1. Three-electrode potentiostat

A schematic diagram of the three-electrode potentiostat used for voltammetric and chromatographic experiments is shown in Figure III.1. The operational circuit maintains the potential difference between the working and reference electrodes ($E_{we} - E_{ref}$) at the value of the signal voltage (E_{sig}) applied at the input terminal. The signal voltage is connected by a 10K-Ω precision resistor to the summing junction of the control amplifier, A-1 (Analog Devices 119A). Amplifier A-2 (Analog Devices 40J) measures the potential of the reference electrode with respect to the working electrode and the output of A-2 is connected to the summing junction of A-1 through a 10K-Ω precision resistor. An Analog Devices 40J amplifier was chosen for the potential follower because this amplifier has a large input resistance (10^{11} Ω) and draws very little current (< 50 pA) from the reference electrode. Amplifier A-3 (Analog Devices 119A) is a current-to-voltage converter. The output voltage from A-3 is proportional to the current in the indicating electrode with the proportionality constant being equal to R_f. The Analog Devices 119A was selected for the control

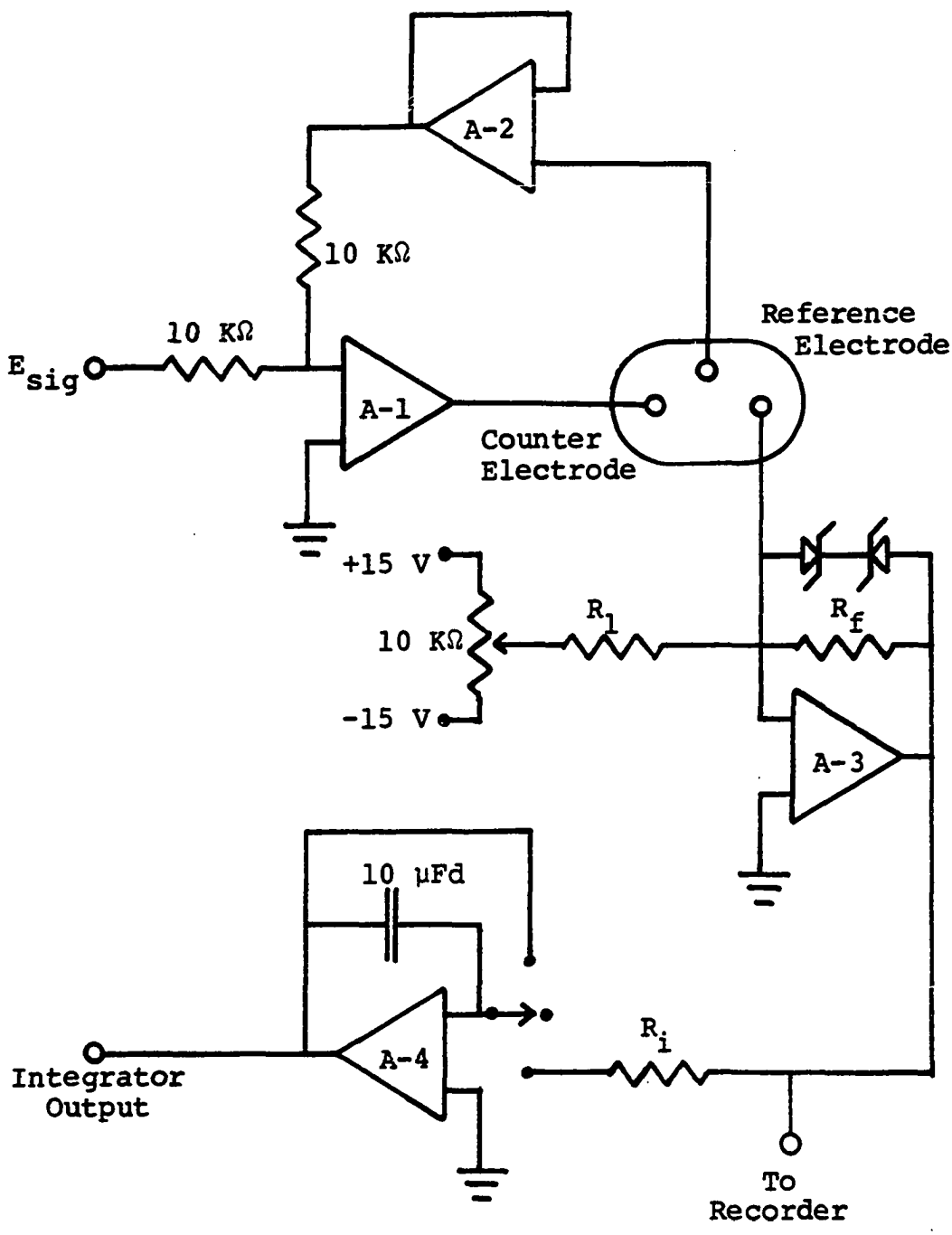

Figure III.1. Schematic diagram of the three-electrode potentiostat and integrator

amplifier and the current-to-voltage converter because this amplifier is capable of delivering relatively high output currents (± 20 mA).

The output of the current-to-voltage converter was connected to the input of a strip chart recorder and an electronic integrator. Residual currents were electronically subtracted from the total current using a voltage divider consisting of a ten-turn potentiometer connected to the supply voltages (± 15 V). The adjustable output of the divider was connected to the summing junction of the current-to-voltage converter through resistor R_1. The value of resistor R_1 was selected to give optimum range and sensitivity by a series of switches which are not shown in Figure III.1. The appropriate feedback resistor, R_f, for the current-to-voltage converter was also selected by a switch which is not shown in the figure. The feedback resistors, R_f, were calibrated by the Physics Instrument Shop at Iowa State University.

2. Integrator

The circuit for electronic integration of the output signal of the current-to-voltage converter (E_i) is also shown in Figure III.1. Amplifier A-4 (Analog Devices AD 503) was chosen for this application because the presence of a very low bias current (15 pA max) in the amplifier required no external compensation when integrating the chromatographic

signals. The result was a simple, stable, electronic integrator with an output drift of only 2 mV/hr. A 10.0 ± 0.01 μFd capacitor from Electronics Associates, Inc., was used as the feedback element for the integrator. This capacitor was chosen for its extremely low leakage and stable value of capacitance. The input resistor for the integrator, R_i, was one of a series of precision resistors which could be selected by a switch to give the desired value for the integration constant, RC. RC constants were calibrated by integrating constant and standard voltages for a known period of time.

Voltages were measured using a 3½-digit, digital voltmeter from Systron Donner (Model 7050).

B. Liquid Chromatograph

1. Construction

The liquid chromatograph used in this research utilized gas pressure, from a tank of compressed helium from Air Products Corp., to produce fluid flow in the manner described by Seymour, Sickafoose and Fritz (97). The chromatograph is shown schematically in Figure II.2. The eluents and reagents contacted only glass, Teflon, or Kel-F. The components of the chromatograph were connected by Teflon tubing (0.063" o.d. x 0.031" i.d.) and Kel-F tube-end fittings from Chromatronix, Inc. It was found desirable to keep all connecting tubes as

Figure III.2. Schematic diagram of the liquid chromatograph

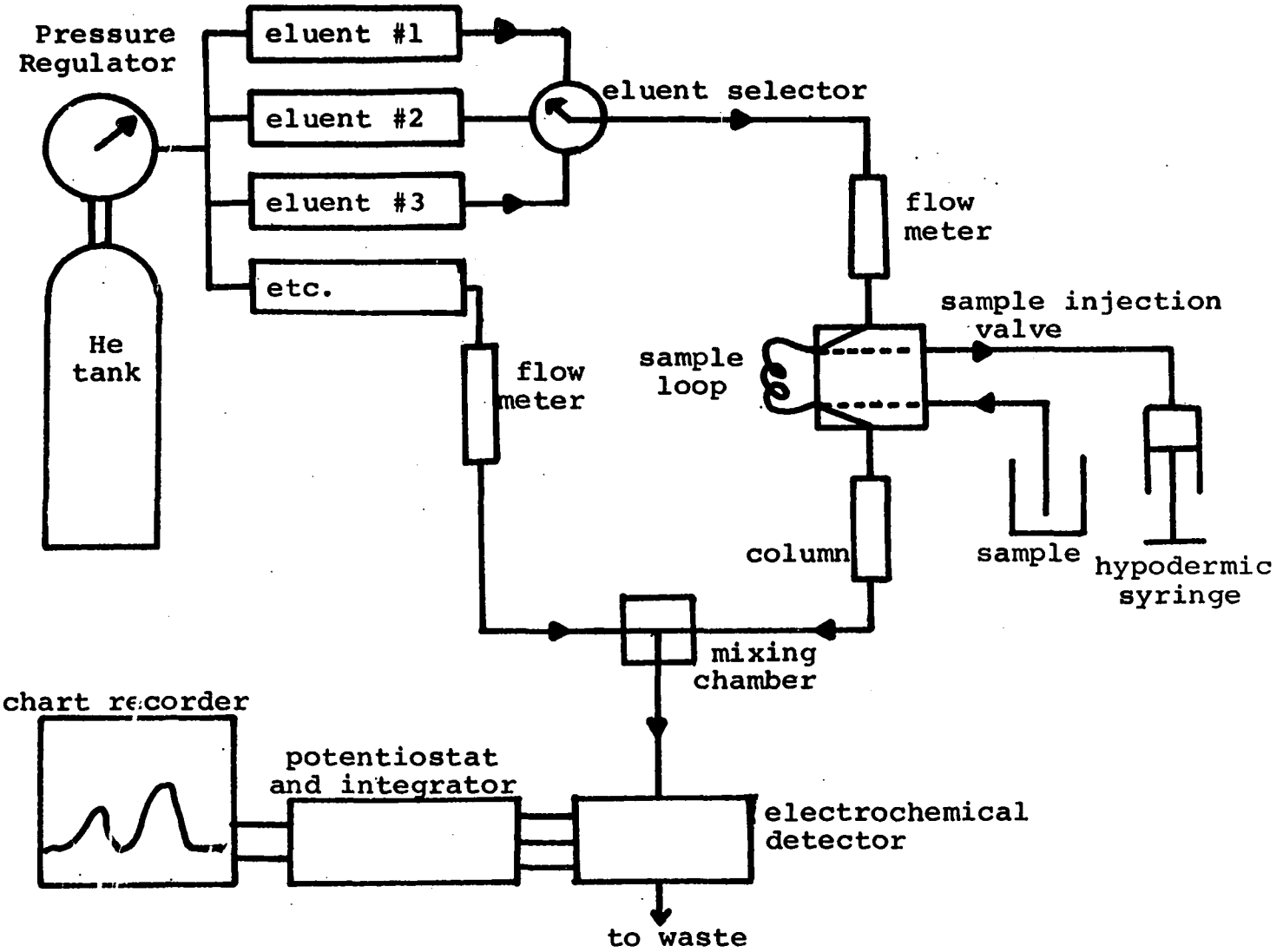
Pressure Regulator
eluent #1
eluent #2
eluent #3
etc.
eluent selector
flow meter
He tank
flow meter
sample loop
sample injection valve
column
sample
hypodermic syringe
mixing chamber
chart recorder
potentiostat and integrator
electrochemical detector
to waste

short as possible because oxygen from the surrounding atmosphere readily diffuses through the Teflon tubing and can be electroactive under certain experimental conditions. Short tubes connecting the injection valve, column, and detector also minimize peak spreading. Helium was chosen as the pressurizing gas because of its low solubility in the reagents. Nitrogen was found to be too soluble and resulted in formation of gas bubbles on the low pressure side of the column. These bubbles disrupted fluid flow and caused noise in the detector current when passing through the detector.

The eluent and reagent tanks were made from glass reagent-grade acid bottles having a capacity of 2 l. The caps of the acid bottles were drilled and Teflon tubing inserted through the holes to allow pressurizing gas to flow in and eluent to flow out of the bottles. The caps thus modified were cast in epoxy resin to seal the space between the cap and the Teflon tubing and to give greater mechanical strength to the cap. One reagent bottle was tested by placing it in a safety container and increasing the internal gas pressure until the bottle ruptured. The rupture occurred at about 100 lbs/in^2. Most of the work described in this thesis was done at pressures of 25 lbs/in^2, thus maintaining a safety factor of 4. It is suggested that if higher pressures are to be used, the bottles be located within or behind a

shielding device. The desired eluting reagent was selected by a Chromatronix 6-position rotary valve (Type R60V6K) which was constructed of Kel-F and Teflon.

Flow rates of the eluent were controlled by constricting the Teflon tubing with Hoffman screw clamps. Flow rates were monitored with Gilmont (Model F1100) flowmeters. The sample was injected using a Chromatronix sample injection valve (Type SV-8031) with a 0.5-ml sample loop. The sample valve was obtained from Chromatronix, Inc., with the optional Kel-F body rather than the Delrin body usually supplied with the valve. Delrin is very quickly deteriorated by contact with strong acids.

The ion-exchange column was a borosilicate glass tube (7 mm o.d. x 8 cm) connected to the chromatograph with glass-to-cheminert unions from Chromatronix, Inc. The effluent from the column was mixed with electrolyte solutions in a mixing chamber constructed by Pine Instrument Company (Model 2MC).

2. Calibration of the sample valve

The sample valve is shown schematically in Figure III.3. The flow pattern in the sample valve is directed by passages drilled in a Kel-F slider which is held between the Teflon ports. The valve is operated by pushing the slider in and out between the positions for sample loading and sample injection. The sample is drawn through the sample loop with

Figure III.3. Schematic diagram of sample injection valve

– – – – – – – – Inject sample

———————— Load sample

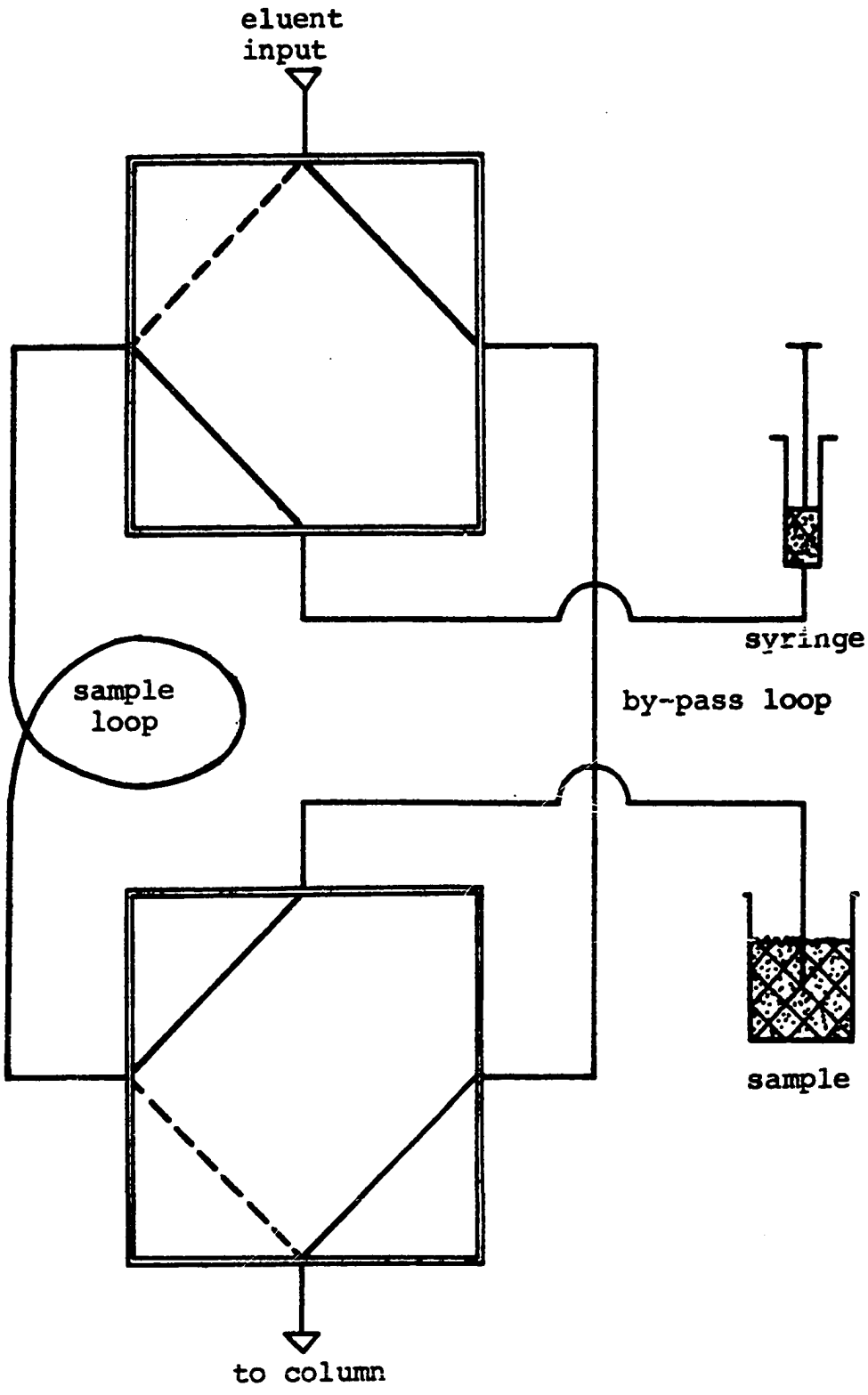
eluent
input
syringe
sample
loop
by-pass loop
sample
to column

a syringe when the slider is in the position for sample loading. The eluent is shunted through the by-pass loop during the sample-loading period to maintain a continuous flow of eluent through the chromatographic system. Bubbles which were occasionally observed to be attached to the wall of the sample loop were removed by sharply tapping the loop while loading the sample loop. The sample was injected into the eluent stream by pushing the slider to the position for sample injection. This operation disconnects the sample-entry tube and syringe from the sample loop and redirects the flow of eluent from the by-pass loop through the sample loop. The volume of the sample loop is adjusted by altering the length of the Teflon tube which constitutes the sample loop. The sample loop was nominally 0.5 ml and was calibrated on the basis of the volume of a 0.1 M solution of sodium hydroxide required to titrate, to the phenolphthalein end point, the quantity of 5 M hydrochloric acid delivered by two injections with the sample valve into distilled water. A 1.0-ml aliquot of 5 M hydrochloric acid was also delivered by a calibrated pipette and titrated with the solution of sodium hydroxide. The volume of the sample loop was calculated as follows:

$$\text{Vol. sample loop} = \text{Vol. pipette}\left[\frac{\text{ml NaOH to titrate 5 M acid delivered by sample loop}}{\text{ml NaOH to titrate 5 M acid delivered by 1 ml pipette}}\right]$$

The 1.0-ml pipette was calibrated by determining the weight of distilled water delivered by the pipette. The apparent density of water was taken to be 0.9920 g/ml at room temperature (27.5°) and, after correcting for the buoyancy of air, the density for water is 0.9952 g/ml. Four measurements of the volume of the pipette were made and the volume was calculated to be 1.0018 ± 0.0002 ml. Four measurements of the sample loop volume were made and the volume calculated to be 0.5040 ± 0.0002 ml.

3. Measurement of flow rates

A calibration curve of flow rate vs. the reading on the flow meter was prepared. The flow meter was calibrated for flow rates with nominal values between 0.5 ml/min to 5.0 ml/min by delivering the eluent into a 10-ml burette and determining the time required to fill the burette. This method was applied with a precision of approximately 1 pph.

C. Detectors

The diagram of a cross section of the detector is shown in Figure III.4. The detector was manufactured by Pine Instrument Co. of Grove City, Pennsylvania. The body of the detector was made of Teflon and the electrode was a platinum tube with a length of 15 mm and an inside diameter of 2.8 mm which was press-fitted into the Teflon body. Fluid connections to the electrode were made with Teflon tubing and

Figure III.4. Cross section of Detector A

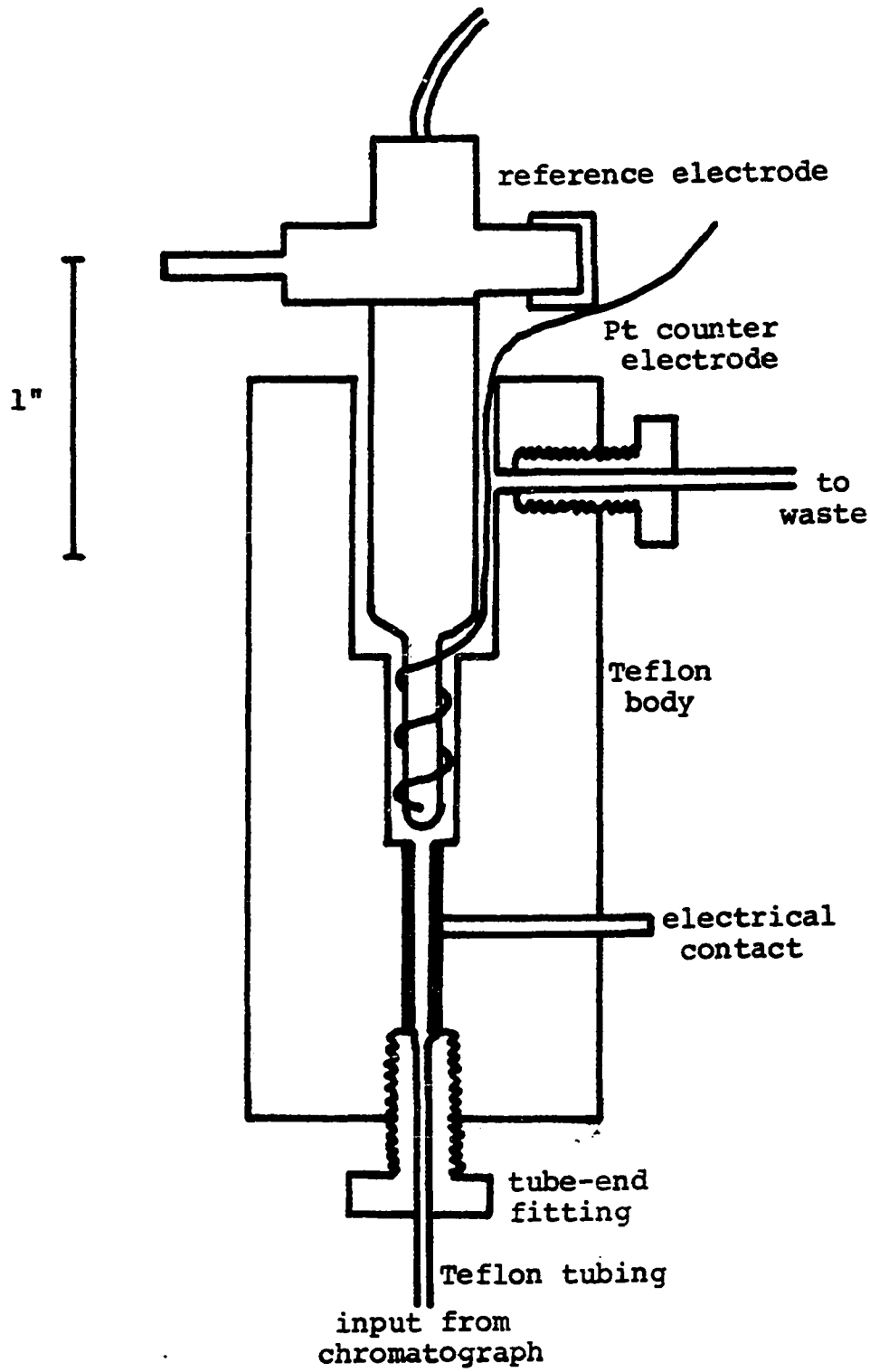
reference electrode
Pt counter electrode
1"
to waste
Teflon body
electrical contact
tube-end fitting
Teflon tubing
input from chromatograph

tube-end fittings from Chromatronix, Inc. Waste effluent was aspirated from the space above the detector into a safety flask with a water aspirator. The reference electrode was a Beckman (Model 39270) saturated calomel electrode (SCE) with a fiber junction. The counter electrode was a coil of 21-gauge platinum wire placed around the body of the reference electrode. The detector, as shown in Figure III.4, is designated Detector A. Detector A was modified by packing the Pt tube with thirty three parallel, 15-mm lengths of 26-gauge Pt wire. This modification is designated Detector B. The Pt tube of Detector A was also packed with short pieces (0.1 mm to 0.5 mm) of 26-gauge and 32-gauge Pt wire. The Pt chips were retained by wads of 31-gauge Pt wire placed at both ends of the tube. This modification is designated Detector C.

IV. EVALUATION OF DETECTORS

A. Introduction

Tubular detectors, such as Detector A in Figure III.4, are easily constructed and their geometric parameters (length, radius, area and internal volume) are readily determined. Furthermore, the theoretical analysis of convective-diffusional mass transport of an electroactive species to the surface of a tubular electrode has been made (26) and verified (98). As discussed previously, the tubular electrode does not function at maximum sensitivity. Other electrode configurations can give greater sensitivity because of increased area of the electrode, increased residence time of the electroactive species in the electrode, or increased flux per unit area of the electroactive species at the electrode surface. In designing electrochemical detectors for maximum sensitivity, the internal volume of the electrode and the electrical resistance of the electrolyte in the detector must remain low. For example, the response of a tubular detector, as given by Equation II.4, is independent of the radius and increases with the length. Therefore, one might choose to design a tubular detector which has a very narrow bore, to keep the internal volume low, and which is very long to achieve greater sensitivity. However, the resulting long, narrow stream of electrolyte would have a high electrical resistance and the interfacial potential

could not be maintained uniform over the entire length of the electrode even for the passage of very small electrical currents. Generally, increased area of the electrode or increased residence time of the electroactive species within the detector is accomplished at the expense of increasing the internal cell volume.

Electrode sensitivity is increased by whatever change in the design or operating parameters which results in a decrease in the thickness of the diffusion layer (see Equation II.3). For conditions of laminar flow, sensitivity is increased for higher flow rates as described by Equations II. 4 and II.5. Detector B was constructed as a first attempt to create many narrow, parallel channels with high flow rates and a large surface area while maintaining a small electrolyte resistance and small internal volume. The value of δ can be further decreased, with a corresponding increase in sensitivity, if the laminar flow is interrupted and turbulence is induced in the fluid stream. Electrode C was constructed in an attempt to maintain a large number of channels with irregular flow patterns. The total surface area of the electrode was large while the cell volume and electrolyte resistance were low.

The efficiency, E, of an amperometric detector is the fraction of the electroactive species which is electrolyzed upon passage through the detector. For a tubular electrode

under conditions of laminar flow, E is predicted by dividing Equation II.7 by Equation II.10 as given by Equation IV.1.

$$E = 5.43D^{2/3}L^{2/3}V_f^{-2/3} \qquad \text{(IV.1)}$$

As predicted by Equation IV.1, the efficiency of the tubular detector decreases as V_f is increased. It is expected that amperometric detectors of other designs have a similar inverse relationship to V_f under laminar conditions of fluid flow.

The electrochemical reaction chosen for the evaluation of the various detectors in this research was the oxidation of iodide to iodine.

$$2I^- \rightarrow I_2 + 2e^-$$

The oxidation of I^- at a Pt electrode surface has been well characterized (99) and is very fast. Consequently, the reaction rate was expected to be limited only by convective-diffusional processes of mass transport. At the electrode potential of 0.800 V vs. SCE used for the oxidation of I^-, dissolved O_2 is not electroactive.

B. Experimental

1. Chemicals and reagents

All chemicals were Mallinckrodt Analyzed Reagents. All solutions were prepared with triply distilled water which was demineralized, following the first distillation, with a

mixed-bed ion-exchange column. The second distillation was from an alkaline permanganate solution.

2. Preparation of solutions

A 10^{-2} M stock solution of NaI was prepared by adding 10 ml of 0.1 N NaOH to 0.750 g of NaI in a 500-ml volumetric flask and diluting to volume with water. The solution was made 10^{-3} M in NaOH to prevent air oxidation of the iodide. The 1 M H_2SO_4 was prepared by boiling the concentrated reagent acid for 15 min to dispel any SO_2 and diluting to 1 M with water. The resulting solution was then deaerated with dispersed He. Solutions of NaI in 1 M H_2SO_4 were prepared immediately before use by dilution of the 10^{-2} M stock solution with 1 M H_2SO_4.

3. Standardization of solutions

The solutions of NaI were standardized by potentiometric titration with 0.1035 M $AgNO_3$. The $AgNO_3$ solution was prepared by dissolving 17.5787 g of $AgNO_3$ in water and diluting to volume in a 1-l volumetric flask. A coiled Ag wire was used as the indicator electrode and a Beckman saturated calomel electrode (SCE) was used as the reference electrode. The indicator potential was monitored with a Corning digital pH meter (Model 119). The inflection point of the graph of millivolts *vs.* volume of titrant added was taken as the end point.

4. Experimental procedures

a. Electrode pretreatment At the start of each experimental day the electrode potential was cycled between the cathodic and anodic limits set by the electrolysis of the 1 M H_2SO_4.

b. Efficiency and precision Samples containing 0.504 ml of 4.73×10^{-5} M NaI in 1 M H_2SO_4 were injected with the chromatronix sample injection valve previously described. The samples passed directly into the detector which was potentiostated at 0.800 V vs. SCE. The flow rates were chosen at random, with no natural sequence. The electrolysis peaks were monitored on a strip chart recorder and the current due to the oxidation of the I^- integrated electronically.

c. Linear dynamic range The following procedure was followed to minimize the effect of trace impurities and to minimize the effect of oxidation of I^- by dissolved O_2 in acidic solutions: Two liters of 1 M H_2SO_4 were prepared as described in Section V.B.2. One liter of the solution was placed in each of two acid bottles which had been washed and rinsed with triply distilled water. The bottles were provided with modified caps as used in the preparation of the eluent tanks. The two solutions were deaerated and pressurized with He. The sample bottle was connected to the sample injection valve at the sample port. When the sample

injection valve was placed in the position for sample loading, the sample solution was drawn through the sample loop there-by rinsing and filling it. The excess sample solution was collected in a graduated cylinder to determine the loss in volume of the sample solution in the bottle. The eluent tank was connected to a flowmeter which was connected to the eluent intake port of the sample injection valve. The eluent exit port of the valve was connected directly to the detector.

Solution of NaI at various concentrations were prepared in the sample tank by successive additions of known volumes of the stock 10^{-2} M solution of NaI. After each addition, the solution was mixed and deaerated by dispersed He. The concentration of the NaI solution was calculated with correction for change in volume.

The NaI solution was injected into the 1 M H_2SO_4 stream flowing through the detector at 3 ml/min. The detector electrode was potentiostated at 0.800 V vs. SCE.

C. Results and Discussion

1. Voltammetry

The electrochemistry of I^- at a platinum electrode in 1 M H_2SO_4 has been described in Reference 99. Current-potential curves for I^- at Detectors A and C were obtained and are compared in Figure IV.1. The large difference in

Figure IV.1. I-E curves for 1.00×10^{-4} M I^- in 1 M H_2SO_4

Anodic scan rate = 0.1 V/min.

Flow rate = 5.0 ml/min.

– – – – – – – – Detector A

———————— Detector C

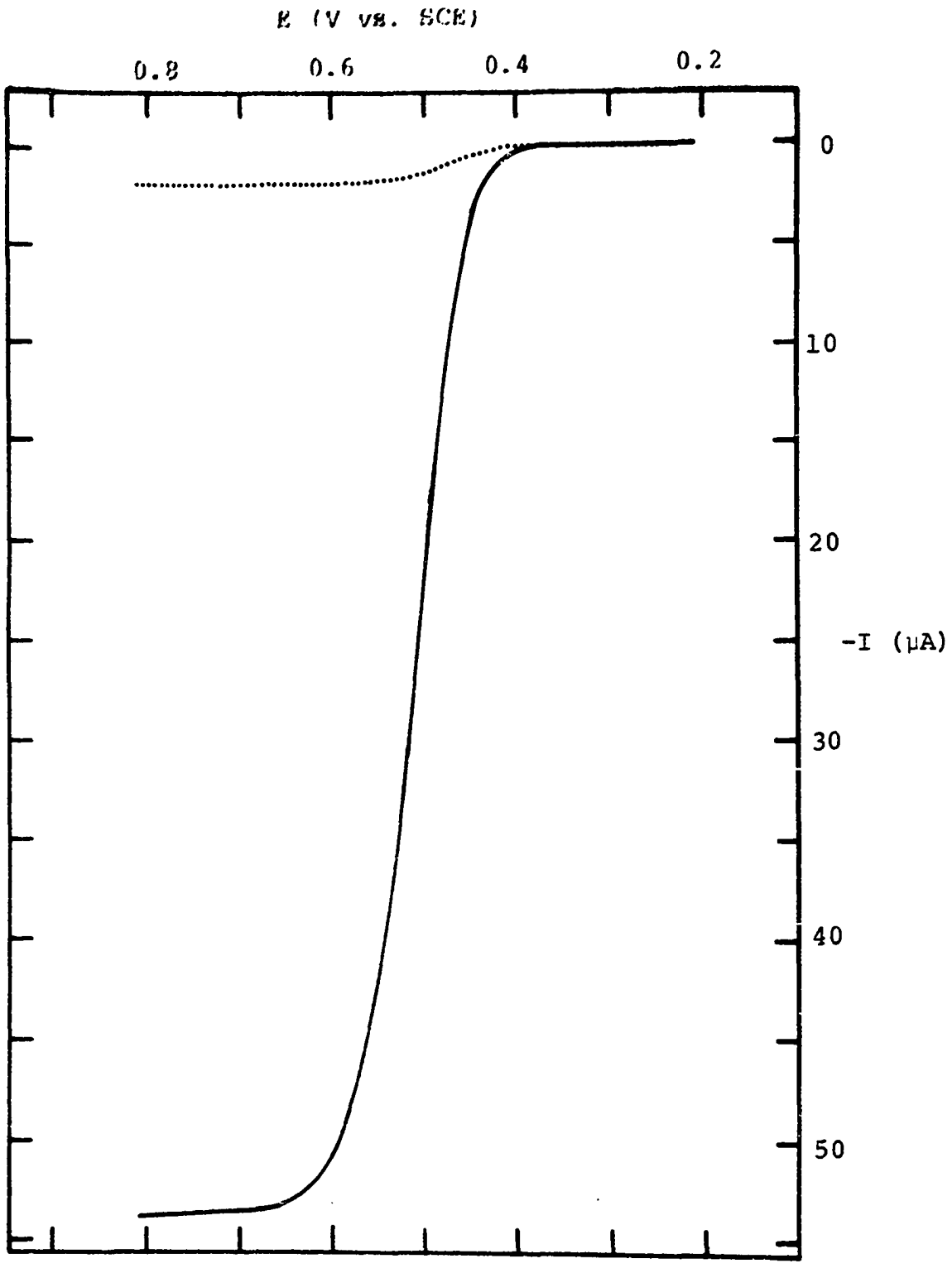
E (V vs. SCE)
0.8
0.6
0.4
0.2
0
10
20
30
40
50
-I (μA)

the electrolytic efficiency of the two detectors is demonstrated by the large differences in the values of the current plateau for the oxidation of I^-. It is clear from an examination of the curves that a detector potential of 0.800 V *vs.* SCE is on the current plateau corresponding to mass-transport limited oxidation of I^-.

2. Detector efficiency and precision

Values of the electrolytic efficiency determined for Detectors A, B and C are shown in Figure IV.2 as a function of flow rate. The plot of log Q *vs.* log V_f for Detector A as linear with a slope of -2/3 in agreement with Equation IV.1. The efficiency of Detector B was greater than that of Detector A due to the greater electrode area and decreased thickness of the diffusion layer. For very low flow rates, the efficiency of Detector B approached 100%. The operation of Detector C was coulometric (100 ± 1%) for V_f < 3.5 ml/min. A plot of the electrolytic efficiency of Detector C *vs.* flow rate is shown with an expanded scale in Figure IV.3 to give a better indication of the change of efficiency with flow rate and the precision of the measurements.

The precision of the analytical application of Detector C was determined from the results of nine injections for V_f in the range of 1.1 to 2.8 ml/min. The results are given in Table IV.1. The relative standard deviation for the series of determinations is 1.8 ppt.

Figure IV.2. Electrolytic efficiency vs. flow rate

▲ - Detector A

● - Detector B

○ - Detector C

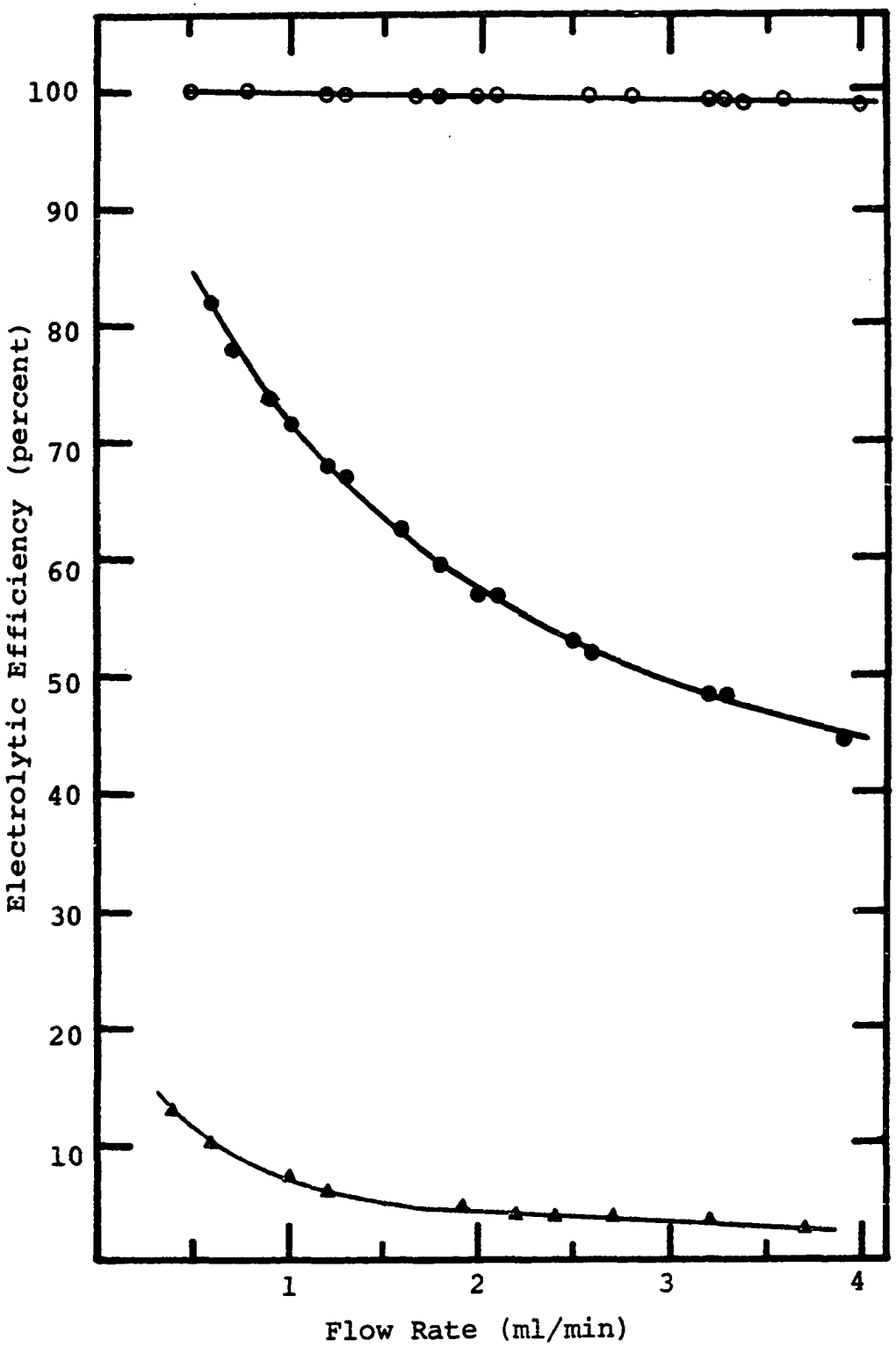
100
90
80
70
60
50
40
30
20
10
Electrolytic Efficiency (percent)
1
2
3
4
Flow Rate (ml/min)

Figure VI.3. Electrolytic efficiency vs. flow rate for Detector C (expanded scale)

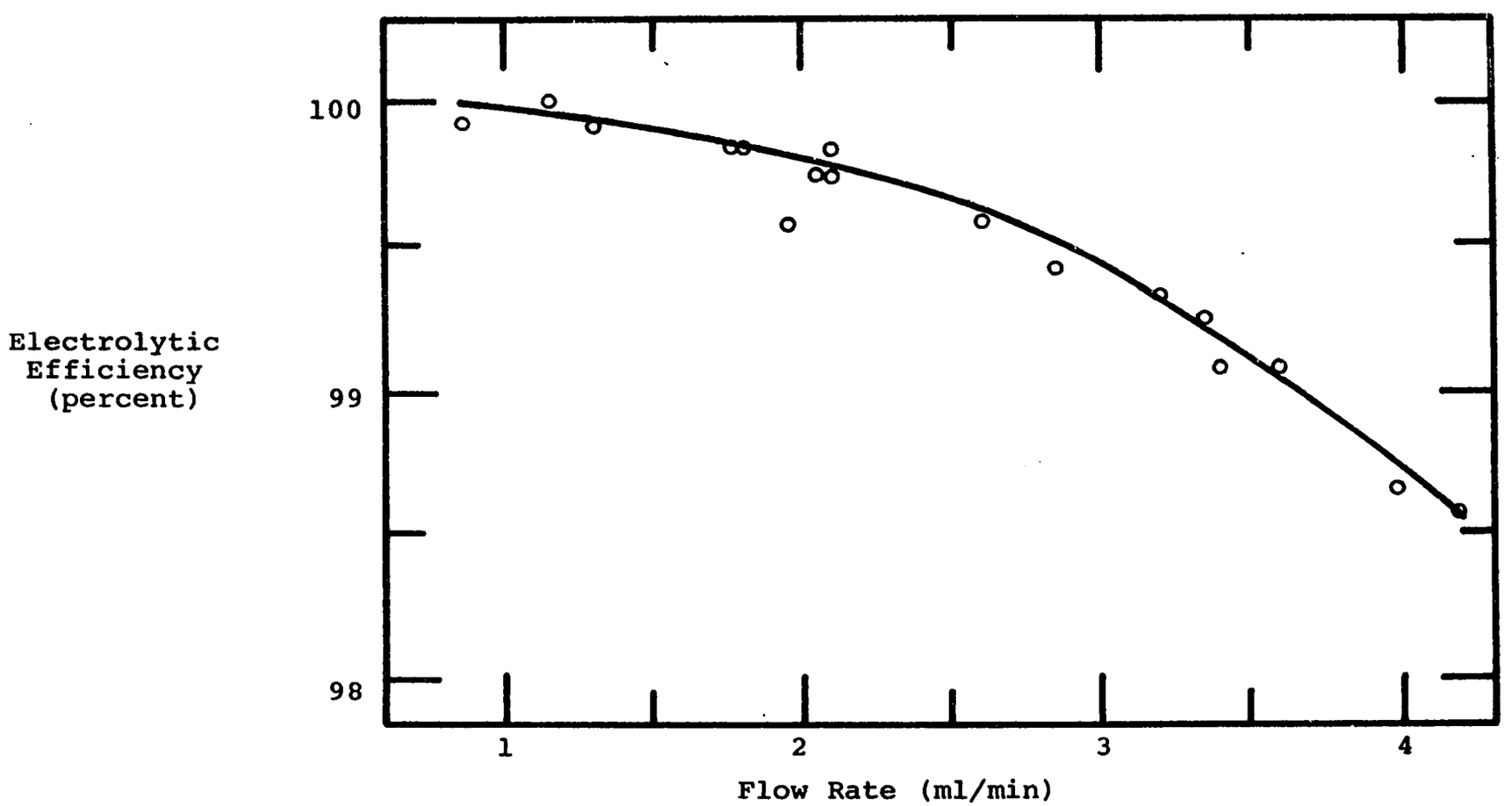
Electrolytic
Efficiency
(percent)
100
99
98
1
2
3
4
Flow Rate (ml/min)

Table IV.1. Precision for Detector C

Flow rate (ml/min)	Charge ($Q \times 10^{-3}$ coul^{-1})	Deviation	Efficiency (%)
1.9	22.91	-.04	99.6
2.1	22.95	.00	99.7
2.1	22.97	.02	99.8
1.8	22.97	.02	99.8
1.1	23.01	.06	100.0
2.0	22.95	.00	99.7
2.8	22.87	-.08	99.4
1.3	22.99	.02	99.9
1.7	22.97	.01	99.8
	avg. = 22.95	avg. = 0.03	avg. = 99.7

A series of injections of 0.504-ml samples of 10^{-4} M NaI into 1 M H_2SO_4 was made at $V_f = 0.85 \pm 0.15$ ml/min. The detector current was integrated electronically. The precision of the determinations was limited by the uncertainty of the least significant digit of the digital voltmeter. This represents a relative standard deviation of less than 1 part per thousand.

The dynamic range of Detector C was determined for solutions of NaI injected into the stream of electrolyte. A logarithmic plot of the integrated electrolysis current vs. concentration of NaI is shown in Figure IV.4. The straight line is the theoretical calibration calculated by Equation II.10. The upper limit of linearity (5×10^{-3} M) was set by the limited output current (20 mA) of the operational amplifiers in the potentiostat. The detection limit was

Figure IV.4. Calibration curve for Detector C

● experimental

—— theory

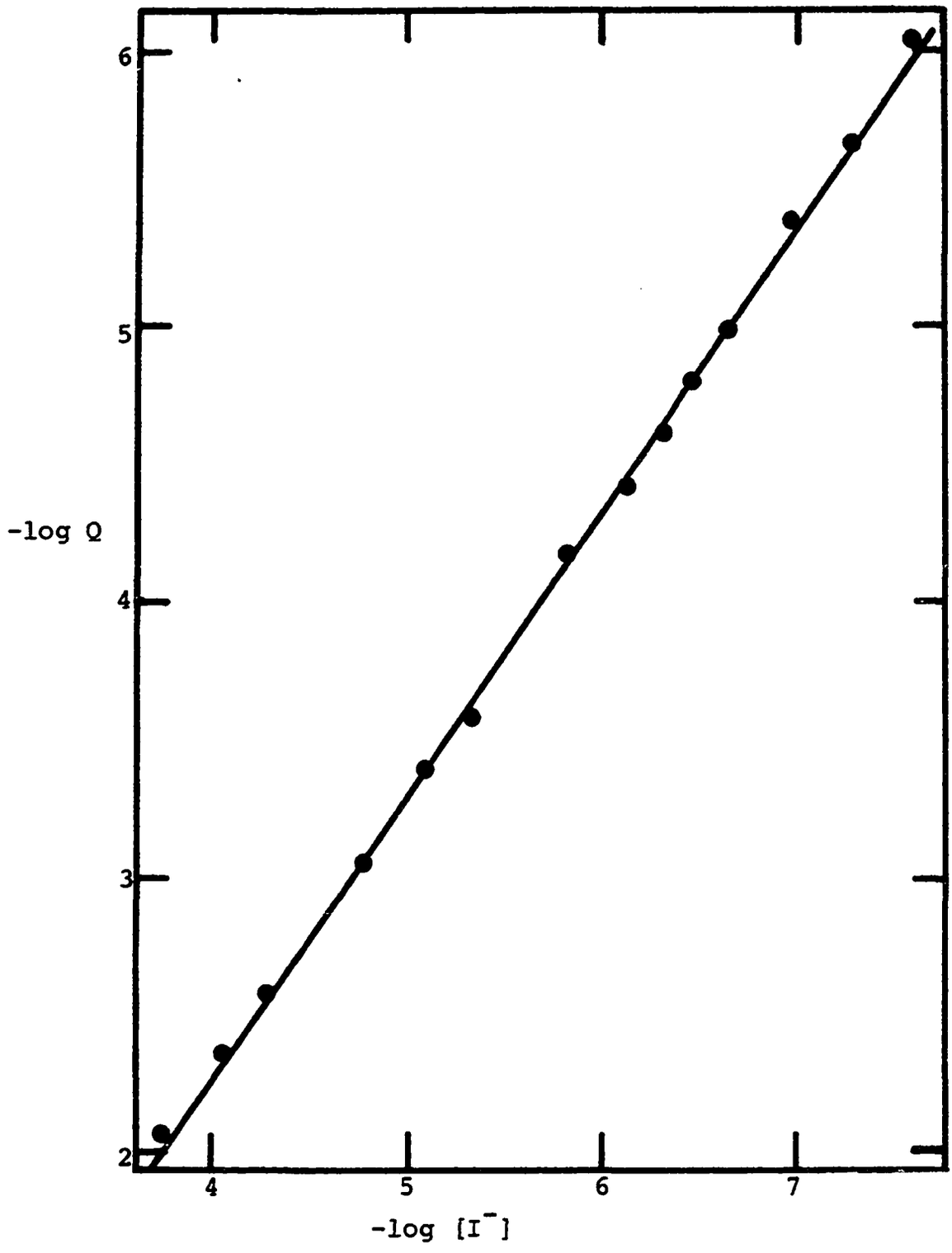
6
5
4
3
2
-log Q
4
5
6
7
-log [I⁻]

taken to be 2.5×10^{-8} M (1.6×10^{-9} g I^-) for which the peak area deviated by more than 10% from the theoretical value. The linear dynamic range of the detector exceeded four decades of concentration giving an impressively large, linear dynamic range. Similar results are expected for all electroactive species which react at the electrode at a rate which is limited by convective diffusional processes to give soluble products.

V. THE DETERMINATION OF COPPER AND IRON

A. Introduction

The separation and coulometric determination of Cu(II) and Fe(III) was chosen as a test system to demonstrate the application of the coulometric detector for liquid chromatography because both Cu(II) and Fe(III) are known to undergo a one electron reduction in the presence of HCl and HBr to give soluble products. Furthermore, the reduction of Cu(II) and Fe(III) at a Pt electrode in HCl and HBr solutions is very fast and, therefore, the reactions were expected to occur at a rate limited by convective-diffusional mass transport.

B. Experimental

1. Chemicals and reagents

A 25% stock solution of HBr (5 M) was prepared by dilution of Baker Analyzed Reagent (47-49%). The acid as received contained variable amounts of Br_2 which is electroactive and purification was required. To remove the Br_2, the solution was first treated with dispersed N_2 for 1 hr. The remaining Br_2 was then electrochemically reduced by stirring the solution over almagamated mossy Zn for 2 hr. During the reduction process, N_2 was slowly passed over the solution to prevent atmospheric O_2 from dissolving in the solution. Following reduction, the solution was filtered

through a bed of glass wool to remove any suspended particles of almagamated Zn and then further treated with dispersed N_2 for 1 hr to remove any dissolved H_2 produced by reduction of hydrogen ions. If not removed, the dissolved H_2 would be oxidized at the electrode potentials used to detect Fe(III) and Cu(II) resulting in large baseline currents. This procedure for solution purification served not only to eliminate the impurity of Br_2, but also to reduce other electroactive impurities which might have been present. Other solutions of HBr were prepared by diluting the 25% stock solution with triply distilled and deaerated water.

A standard solution of Cu(II) containing 5.00 mg Cu/ml was prepared by dissolving 2.500 g of electrolytic Cu from Baker Chemical Co. in 20 ml of concentrated HCl. The resulting solution was diluted to 500.0 ml with 0.1 M HCl. A standard solution of Fe(III) containing 5.00 mg Fe/ml was prepared by dissolving 2.500 g of electrolytic Fe from G. F. Smith Chemical Co. in 20 ml of concentrated HCl with the addition of a few ml of H_2O_2 to oxidize the Fe(II) to Fe(III). The solution was heated to destroy the excess H_2O_2, cooled and diluted to 500.0 ml with 0.1 M HCl.

The macroreticular, strong acid, cation-exchange resin used for chromatographic separations was Amberlite IRA-200 from Rohm and Haas Co. The wet resin was ground with a porcelain mortar and pestle. The ground resin was sieved

using a stream of deionized water to flush the resin through the sieves. This procedure was faster and more convenient than the grinding and sieving of the dry resin. The wet procedure also removed the fine particles which tended to adhere to the larger particles during dry sieving. Inclusion of the fine particles in an ion-exchange column results in excessive resistance to flow of eluents through the column. The 180-250 mesh fraction of ground resin was used to pack the chromatographic column.

2. Standard materials

NBS 87, an aluminum-based standard alloy from the National Bureau of Standards, was analyzed for Cu and Fe. The composition of the alloy, as reported by the certificate of analysis, is given in Table V.1. A 4.0512-g sample of

Table V.1. Composition of NBS 87, an aluminum-based standard alloy

Si	6.22%	Mn	0.30%
Fe	0.46%	Cr	0.17%
Ni	0.59%	Ti	0.16%
Mg	0.39%	Zn	0.075%
Cu	0.30%	Pb	0.07%
		Sn	0.061%

NBS 87 was dissolved by the slow addition of 30 ml of 8 M HCl at room temperature. After sample dissolution, the silica was dehydrated by addition of 100 ml of concentrated $HClO_4$ with gentle boiling until the appearance of the dense white fumes of $HClO_4 \cdot 2H_2O$ marked the completion of the

dehydration. The solution was cooled and filtered with suction through a fine fritted-glass filtering crucible to remove the SiO_2. The removal of SiO_2 was rinsed with distilled water and the combined filtrate was diluted to 500.0 ml. The sample solutions were kept dilute specifically for the reason of preventing the loading of the ion-exchange column.

NBS 169, a Ni-based alloy used for heating elements, was analyzed for Cu and Fe. The composition of the alloy reported by the National Bureau of Standards on the certificate of analysis is given in Table V.2. A 0.8278-g

Table V.2. Composition of NBS 169, a nickel-based alloy

Cr	20.26%	Mn	0.073%
Si	1.42%	Zn	0.042%
Fe	0.54%	V	0.018%
Co	0.19%	Ca	0.015%
Al	0.059%	Cu	0.015%

sample of NBS 169 was dissolved by gentle heating for several hours in 40 ml of aqua regia. The solution was evaporated to 20 ml and diluted to 200 ml.

3. Experimental procedures

a. Voltammetry Fundamental voltammetric studies were performed using the potentiostat described in Section III.A.1 and a platinum, rotating disk electrode (RDE) from Pine Instrument Co. The electrode surface was polished to a mirror finish with Beuhler Handimet 600 paper strips

followed by 30 μm, 6 μm and 1 μm Beuhler AB Metadi diamond polishing compound on a nylon cloth. Water was used as the lubricant for polishing on the paper strips and Behler Metadi fluid lubricant was used for the diamond polish. After each polishing step, the abrasive and lubricant were cleaned from the electrode with an aqueous solution of a liquid detergent applied with a cotton swab. The electrode was then rinsed with distilled water before proceeding to the next polishing step. At the beginning of each series of experiments, the electrode surface was polished using 1 μm Buehler AB polishing alumina on Buehler microcloth with water as a lubricant followed by thorough rinsing with distilled water. The RDE was rotated by a variable speed rotator (Model PIR) from Pine Instrument Co.

The electrochemical cell was fabricated from a borosilicate beaker in the glass shop of the Department of Chemistry and had a capacity of 200 ml. The cell had two side compartments, one for the reference electrode and the other for the counter electrode. The side compartments were separated from the main body of the cell by fritted-glass disks. The glass disks permitted ionic contact without appreciable mixing of the contents of the separated compartments. The cell was also fitted with a glass valve mechanism to either cause N_2 to be dispersed through the solution, by way of a fritted-glass tube sealed low on the

body of the cell, or to cause the N_2 to be passed over the surface of the solution from an orifice high on the body of the cell. During experimentation, the cell was covered with a Teflon cap drilled with a hole through which the electrode was inserted into the cell. Unless otherwise indicated, the solutions were deaerated by dispersing prepurified (99.999%) N_2 through the solution for a minimum of 10 min prior to voltammetric experiments. The N_2 was from Air Products Corp. During all voltammetric experiments, N_2 was passed over the surface of the solution.

All potentials were measured and are reported with respect to a saturated calomel electrode (SCE).

b. Electrode pretreatment At the start of each series of chromatographic determinations, the potential of the detector electrode was cycled between the cathodic and anodic limits for the electrolytic decomposition of the electrolyte. This procedure resulted in the oxidation and reduction of the platinum surface and served to clean the electrode surface of adsorbed impurities. The electrode was then potentiostated at 0.150 V, a potential at which platinum oxide is reduced and hydrogen is not adsorbed. A 0.504-ml sample of 10^{-2} M NaI was injected into the chromatograph. This procedure resulted in the adsorption of a monolayer of iodine at the surface of the electrode. The adsorbed iodine is tightly held by the Pt electrode and is not removed in

pure water or other electrolyte solutions used in experiments described here. The presence of adsorbed iodine inhibits the adsorption of impurities which might otherwise interfere with the reduction of the Cu(II) or Fe(III).

c. Preparation of the chromatographic column A sintered, stainless steel plug supplied by Chromatronix to support the column packing materials was not suitable for use in this research because of the strong acid eluents. One possible procedure to retain the resin in the column might have been the use of a small wad of glass wool in the downstream end of the column. It was difficult to place the glass wool in the end of the narrow column, however. More successful was the preparation of a sintered glass plug as a packing support in the end of the column. Borosilicate glass was crushed with a porcelain mortar and pestle and the 180-250 mesh fraction was used to fill the column. The crushed glass in one end of the column was sintered by rotating that end in the flame of a Meeker burner. The column was cooled and the unsintered glass removed from the column. There remained a ¼-in sintered glass plug in one end of the column. The column was again heated in the flame to insure complete sintering of the remaining glass particles. This procedure formed a durable, porous and effective support for the ion-exchange resin.

The ion-exchange resin was injected as a slurry into the column using a plastic syringe with a Chromatronix luer adapter connected to the column. Air bubbles trapped in the column during the packing or chromatographic operation were easily removed by passing eluent through the column for ½ hr. The procedure apparently resulted in dissolution of the bubbles.

d. Separation procedure The ion-exchange column was pretreated by passing 5 M HBr at a flow rate of 0.5 ml/min until the baseline was steady. An eluent of 0.3 M HBr was then passed at the same flow rate for 3 min. The sample was injected into the stream of 0.3 M HBr and sorbed onto the ion-exchange bed. Four minutes after the sample was injected, the eluent was changed to 1.5 M HBr and the Cu(II) was eluted from the column. After the Cu(II) was completely eluted (approximately 10 min), the eluent was changed to 5 M HBr to elute Fe(III). Succeeding injections of samples could be made without further column pretreatment after the eluent was switched to 0.3 M HBr for 3 min.

e. Reagent addition The effluent from the column was mixed with 5 M HBr in a Teflon mixing chamber (Model 2 MC) from Pine Instrument Co. For noise-free operation, it was necessary that the two streams be mixed thoroughly before entering the detector. The two streams entering the mixing chamber were each split within the chamber and the resulting

streams directed tangentially through four ports in the wall of a cylindrical mixing cavity. The combined streams flowed out through a port which was on the axis of the cylindrical mixing cavity. The volume of the cavity was estimated to be 10-20 μl. The 5 M HBr was introduced into the mixing chamber at the rate of 2 ml/min. The mixture of the effluent and the 5 M HBr streams was passed through the electrochemical detector. The addition of 5 M HBr to the effluent stream was made to provide the optimum electrolyte for the electrochemical reduction of Cu(II) and Fe(III) and to minimize the charging current which resulted from changes in the ionic strength of the solution flowing through the detector. The reagent solution contained 10^{-6} M NaI to provide a continuous supply of I^- for adsorption on the Pt surface.

C. Results and Discussion

1. Voltammetry

The reduction of Cu(II) and Fe(III) to Cu^0 and Fe^0 was undesirable as the deposited metal would change the physical and electrochemical properties of the detector. The presence of HBr as the electrolyte promoted the reduction of Cu(II) and Fe(III) to the corresponding bromide complexes of Cu(I) and Fe(II).

Current-voltage (I-E) curves for the reduction of Cu(II) and Fe(III) in 5 M HBr are shown in Figure V.1. Both curves exhibit current plateaus which are characteristic of very fast electrochemical reactions where the rate of reaction is limited by transport of the electroactive species to the electrode surface. At a detector potential of 0.200 V vs. SCE, the reduction is clearly mass-transport controlled.

2. Response of the detector to changes in eluent

The detector produced a current peak whenever the composition of the stream of electrolyte entering the detector was abruptly changed. This current peak was concluded to result from a change in the charge of the electrical double layer at the electrode surface as a result of the change in electrolyte concentration. The charging currents observed during the elution process were greatly reduced by "buffering" action of the 5 M HBr mixed with the effluent stream.

3. Separation

The first attempt to separate Cu(II) and Fe(III) on a cation-exchange column employed HCl as an eluent. The hydrogen ion from the HCl has less affinity for the column than Cu(II) or Fe(III) but at high acid concentrations the Cu(II) and Fe(III) can be replaced by mass action. Copper(II) has less affinity for the cation exchange resin than Fe(III)

Figure V.1. I-E curves for Cu(II) and Fe(III) at a Pt RDE in 5 M HBr
Anodic scan rate = 0.5 v/min. Rotational velocity = 1600 rev/min.
A. [Fe(III)] = 1.8×10^{-4} M
B. [Cu(III)] = 1.6×10^{-4} M

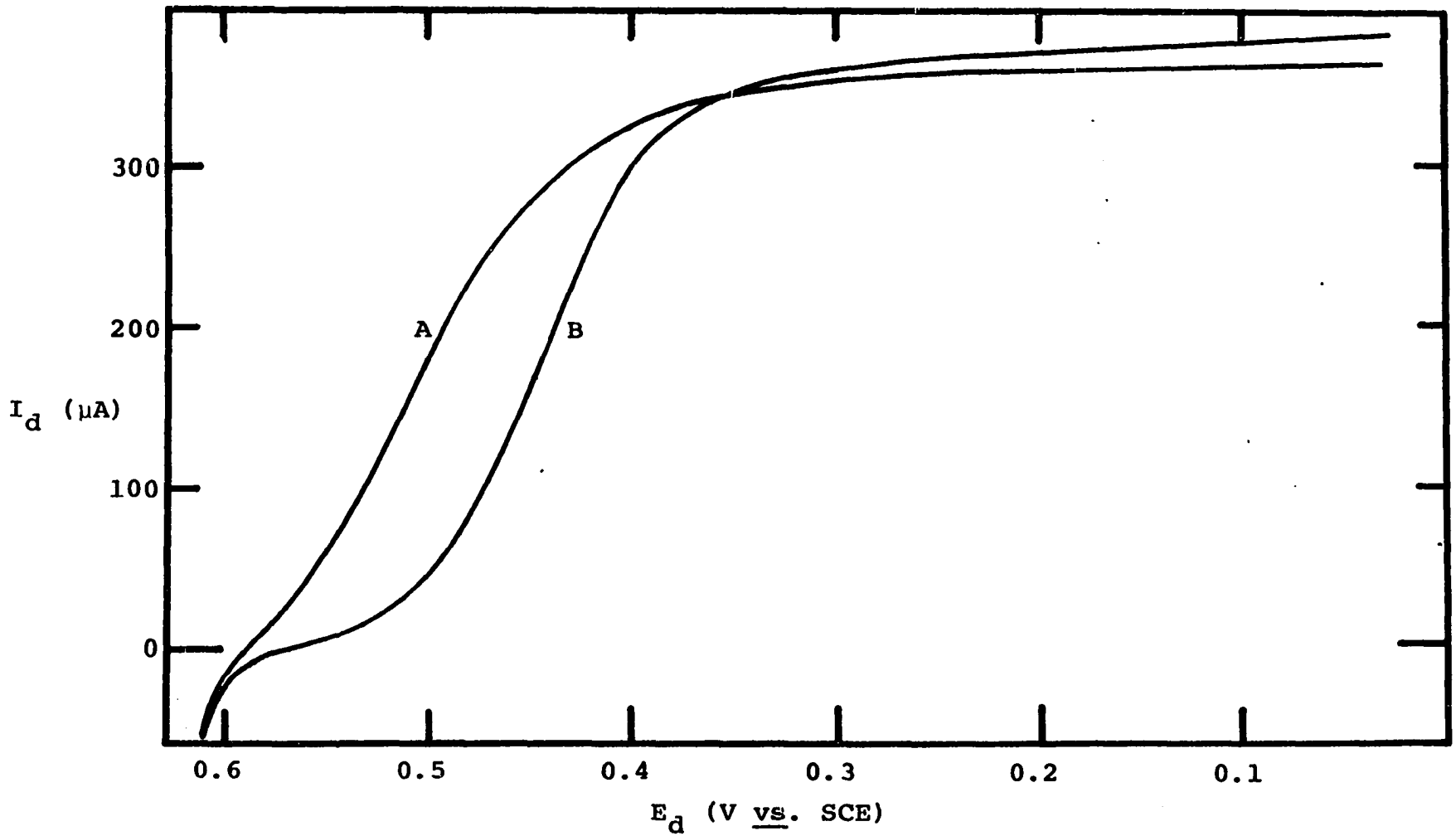
300
200
100
0
A
B
I_d (μA)
0.6
0.5
0.4
0.3
0.2
0.1
E_d (V vs. SCE)

because of the smaller positive charge of Cu(II) and, therefore, might be expected to be eluted at lower concentration of the acid than required for elution of Fe(III). However, Cl^- forms more stable and less positively charged complexes with Fe(III) than Cu(II) which counters the elution order expected on the basis of cation displacement by hydrogen ion. The result is that Cu(II) and Fe(III) are not easily resolved with HCl eluent. Separation of Cu(II) and Fe(III) with HCl as an eluent was not successful. The formation constants for the halide complexes of Fe(III) are generally known to decrease as the halide ion becomes larger and more easily polarized. The alternate choice of HBr as an eluent resulted in successful separations. The use of HBr also resulted in more favorable electrochemistry by permitting the reductions of Cu(II) and Fe(III) at more positive potentials than for the HCl electrolyte.

The Cu(II) was quickly eluted with 1.5 M HBr in a symmetrical peak at flow rates less than 0.5 ml/min. As the flow rate was increased, the Cu(II) peak was observed to tail probably due to incomplete equilibration of the Cu(II) between the stationary and the mobile phases. The Fe(III) peak had considerable tailing at all values of flow rate. The concentration of the HBr solution used to elute the Fe(III) was, therefore, raised to 5 M to minimize the tailing. The relative amount of tailing for the Fe(III) peak

increased for smaller amounts of Fe(III) and for longer columns. The cause of the tailing might be the presence of some ion-exchange sites which have a greater affinity for the Fe(III) than the majority of sites or which have slower exchange kinetics. Another explanation might be found in the ability of Fe(III) to form ion-association complexes, such as $H_3O^+FeBr_4^-$, in acidic solutions of halide ion. Such complexes are known to be soluble in organic solvents. If some ion-association complex were formed, the complex might be soluble in the organic matrix of the ion-exchange resin. The existence of two retention mechanisms could lead to unsymmetrical peaks. For the sake of expedience, the electronic integration of the chromatographic peak for Fe(III) was terminated exactly 8 min after the appearance of the peak maximum.

4. Analysis of an artificial sample

A solution containing 10.00 μg/ml each of Cu(II) and Fe(III) was prepared by diluting the standard solution described in Section V.B.2. The results of the analysis of five 0.504-ml samples of this solution are shown in Table V.3 and a sample chromatogram is shown in Figure V.2. The results for the determination of Cu(II) and Fe(III) in the mixture are in excellent agreement with the known composition. The precision and accuracy obtained with the coulometric detector are about an order of magnitude better than that

Table V.3. Results for standard Cu(II) and Fe(III) (5.040 μg Cu(II) and 5.040 μg Fe(III) per injection)

Injection	$Q_{Cu(II)}$ (mcoul)	$Q_{Fe(III)}$ (mcoul)
1	7.59	8.39
2	7.61	8.42
3	7.64	8.40
4	7.62	8.42
5	7.62	8.43
average	7.62	8.41
relative average deviation	1.6 ppt	1.7 ppt
relative standard deviation	2.5 ppt	2.0 ppt
theoretical	7.65	8.71
relative error	4 ppt	34 ppt
calculated calibration constant	1.512 mC/μg	1.669 mC/μg

Figure V.2. Chromatogram for a standard solution of Cu(II) and Fe(III)
Sample contains 5.040 µg of Cu(II) + 5.040 µg of Fe(III).

A. Injection of sample into stream of 0.3 M HBr.

B. Change of eluent to 1.5 M HBr.

C. Change of eluent to 5.0 M HBr.

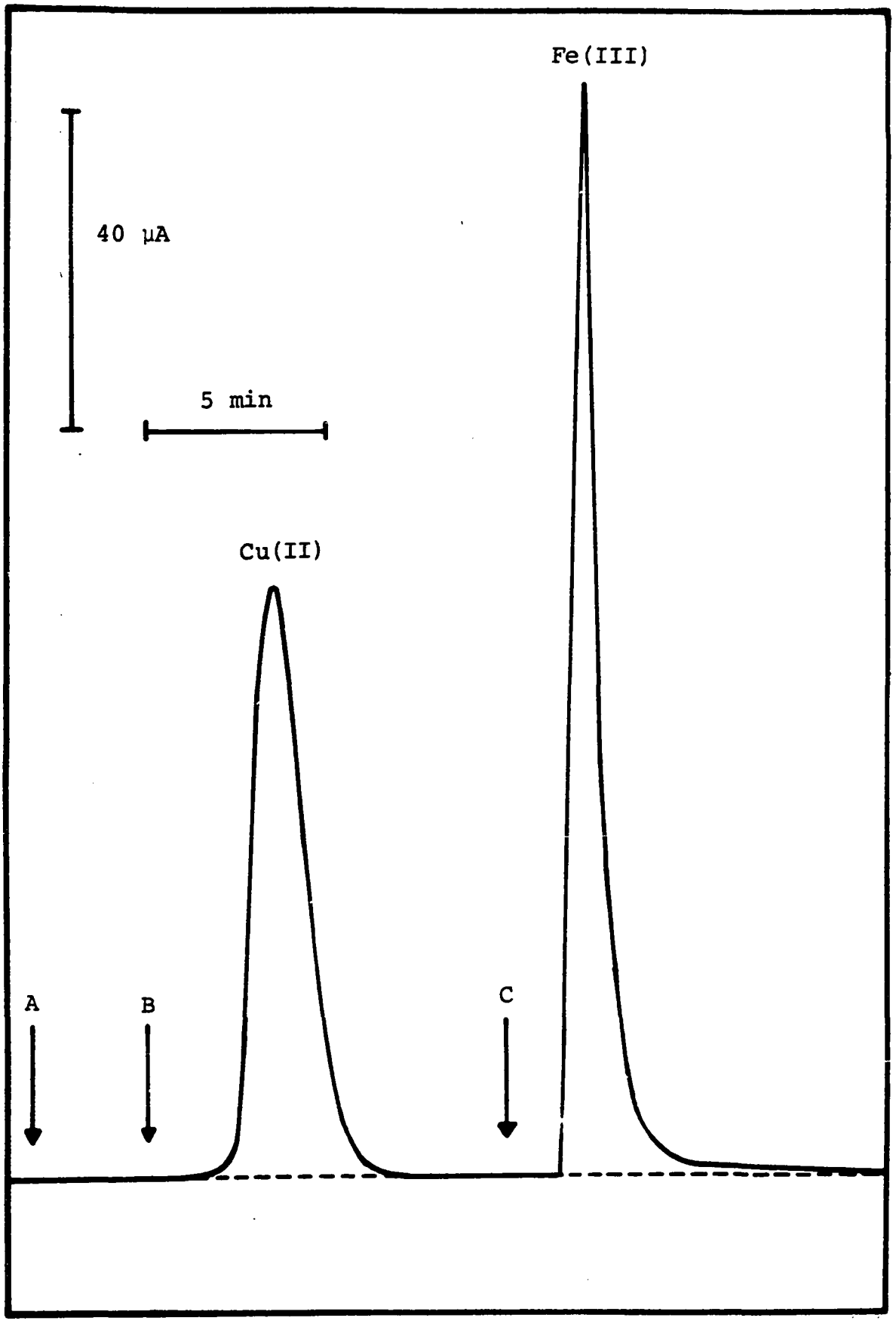
Fe(III)
40 µA
5 min
Cu(II)
A
B
C

which can be obtained by other common detectors for liquid chromatography. In fact, the precision and accuracy of the determination of the Cu(II) are as low as expected for high-quality volumetric determinations of major constituents.

Although the determination of Fe(III) was made with good precision, low results were obtained because part of the chromatographic tail for the Fe(III) peak was not integrated. To attempt a compensation for the amount of Fe(III) lost in the tailing phenomenon, a calibration constant was calculated to relate the number of coulombs determined during the integration of the Fe(III) peak to the actual amount of Fe(III) present in the sample. The value is given in Table V.3. The calibration constant for Fe(III) is a function of the amount of Fe(III) present. The calibration constant was applied in the analysis of the NBS standards. The reader should bear in mind that the low result for Fe(III) was not due to the detector design or operation, but was the result of the poor elution characteristics for Fe(III).

5. Analysis of NBS standards

Because ion-exchange chromatography involves a concentration of the analyte when the sample is adsorbed onto the top of the column, the sensitivity of a chromatographic method may be improved by increasing the sample size. However, in many cases the amount of sample is limited or, as in

the case of NBS 87, the large amounts of other ions present in the sample may result in loading the column thus preventing larger samples from being used. Where the sample size is limited, the sensitivity of the method depends on the sensitivity of the detector. Because larger samples of NBS 87 would load the column with Al(III), the total sample used for analysis was 0.8094 mg. The amount of Cu(II) and Fe(III) in this sample was only 2.5 μg (4.8 ppm) and 3.7 μg (7.4 ppm), respectively. The results of the analysis of five 0.504-ml aliquots of the solution of NBS 87 are given in Table V.4 and a typical chromatogram is shown in Figure V.3. The results were computed on an absolute basis using Equation II.10 and by using the calibration constants given in Table V.2. Even though the amounts of Cu(II) and Fe(III) in the samples were extremely small, the results agree very well with the certificate values. The results for Cu(II), which does not tail during the separation, are excellent for calculations by the absolute method as well as with the calibration constant. In fact, a true judgement of the accuracy is limited by the lack of a third significant figure for the certificate value of the percent Cu supplied by the NBS.

The results for the Fe(III) are slightly low, as expected, when calculated on an absolute basis. This is the result of the tailing for the Fe(III) peak. The analytical results for Fe(III) are excellent when calculated with the calibration constant.

Table V.4. Results for NBS 87 (809.4 μg alloy per injection)

Injection	$Q_{Cu(II)}$ (mcoul)	$Q_{Fe(III)}$ (mcoul)
1	3.66	6.11
2	3.66	6.13
3	3.70	6.13
4	3.68	6.14
5	3.69	6.16
Average	3.68	6.13
Relative average deviation	2.7 ppt	2.0 ppt
Relative standard deviation	4.1 ppt	3.1 ppt
Percent calculated on an absolute basis using Equation II.10	0.300%	0.439%
Certificate value	0.30%	0.46%
Percent calculated using calibration constant from Table V.1	0.302%	0.454%

Figure V.3. Chromatogram for NBS 87
Sample contains 809.4 µg
of NBS 87.
A. Injection of sample into
stream of 0.3 M HBr.
B. Change of eluent to
1.5 M HBr.
C. Change of eluent to
5.0 M HBr.

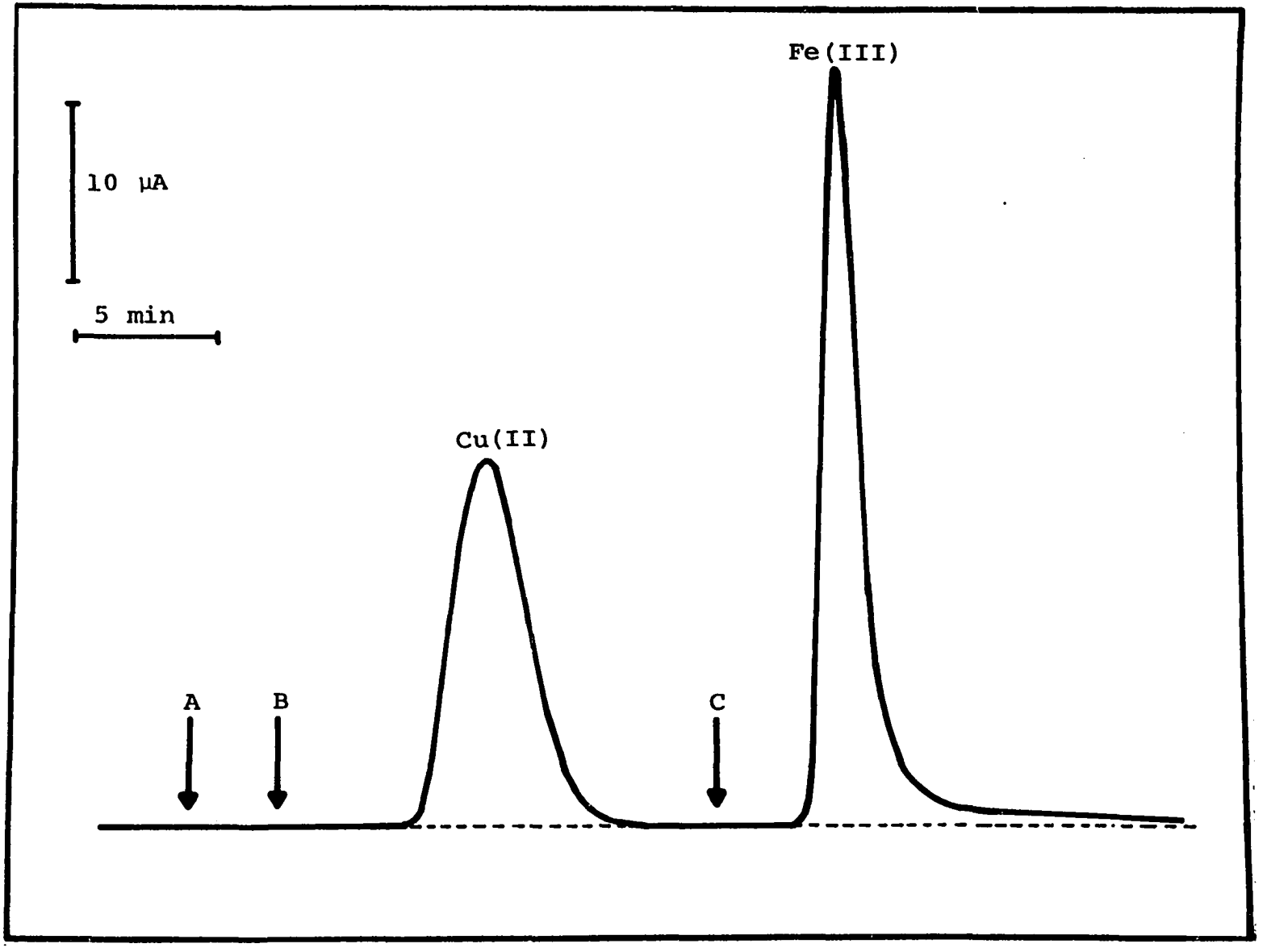
Fe(III)
10 μA
5 min
Cu(II)
A
B
C

NBS 169 is a very interesting sample because of the extremely small amount of copper relative to Fe, Ni and Cr. If a spectrophotometric detector were to be used for the chromatographic analysis, the Ni(II) and Cr(III) present in quantities at least 1000 fold greater than for Cu(II) would have to be masked or separated from the Cu(II) and Fe(III). However, only Cu(II) and Fe(III) are electroactive and no interference results in the electroanalytical detection. The results for five 0.504-ml aliquots of NBS 169 are shown on Table V.5 and a sample chromatogram is shown in Figure V.4. Even though the sample contained only 0.31 μg (0.62 ppm) of Cu(II), the analytical results are in excellent agreement with the certificate value.

The analysis of the National Bureau of Standards reference samples demonstrates the accuracy and precision which can be obtained using the coulometric detector with HPLC for metal ion determinations. This was accomplished without putting severe constraints on the chromatograph such as rigid control of eluent flow rate and temperature.

6. Detection limit

Determination of standard and unknown samples containing as little as 25 ng of Cu(II) were made with less than 10% error. This is concluded to be the absolute detection limit. For a 0.5-ml sample, the relative detection limit is 50 parts per billion. Because of the ability of the

Table V.5. Results for NBS 169 (2.086 mg alloy per injection)

Injection	$Q_{Cu(II)}$ (mcoul)	$Q_{Fe(III)}$ (mcoul)
1	0.455	18.31
2	0.503	18.23
3	0.459	18.27
4	0.439	18.27
5	0.455	18.39
Average	0.462	18.29
Relative average deviation	35 ppt	2.5 ppt
Relative standard deviation	52 ppt	3.5 ppt
Percent calculated on an absolute basis using Equation II.10	0.0146	0.508
Certificate value	0.015	0.54
Percent calculated using calibration constant from Table V.1	0.0147	0.525

Figure V.4. Chromatogram for NBS 169
Sample contains 2.086 mg of alloy.

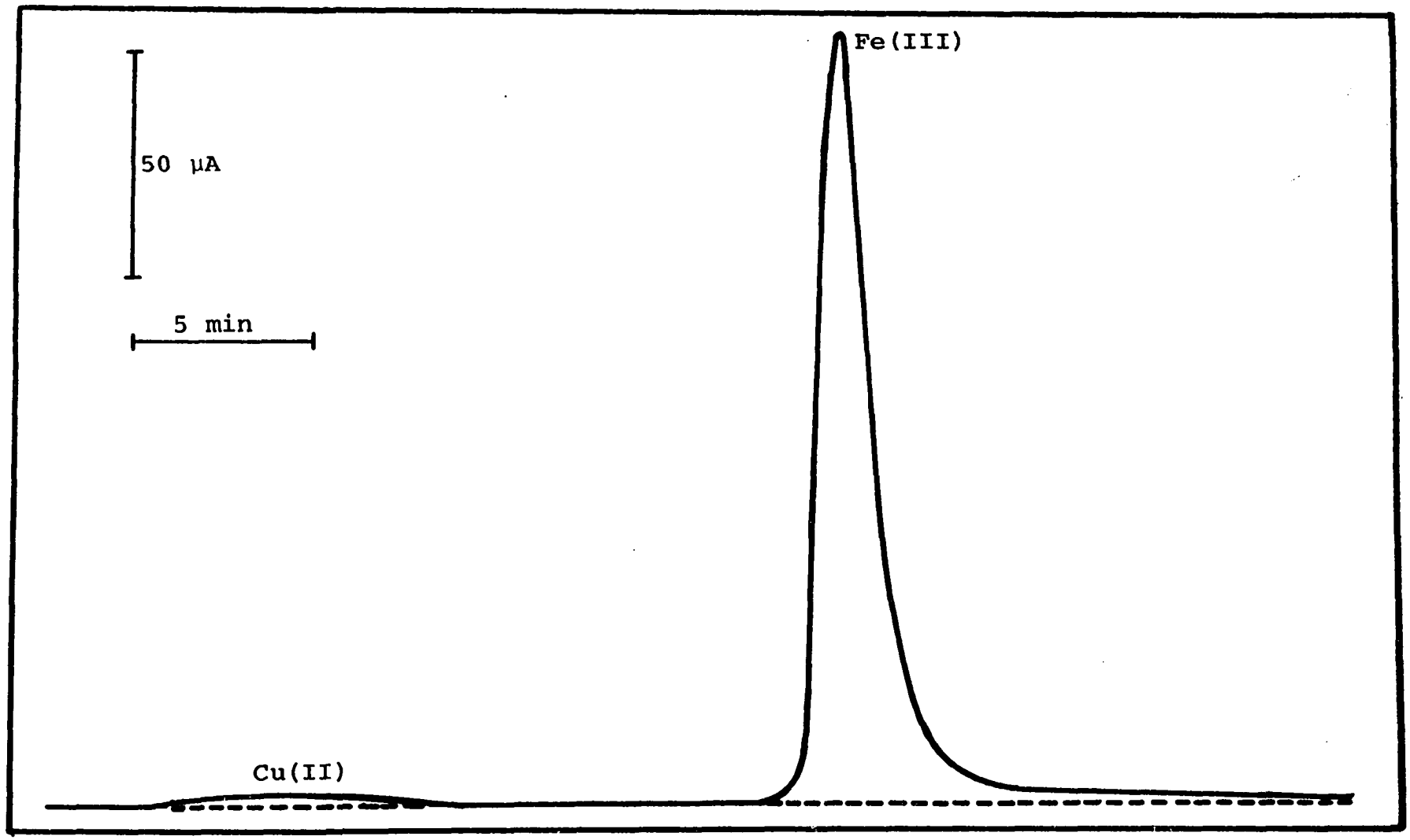
50 µA
5 min
Fe(III)
Cu(II)

ion-exchange resin to concentrate the metals on the resin bed, the relative detection limit can undoubtedly be extended for larger sample volumes. In cases where the amount of sample is not limited and the concentration of other polyvalent cations is not large enough to load the column, the detection limit is limited practically by the maximum time the analyst wishes to spend collecting the sample on the column. For example, 1 hr would be required to inject a 30-ml sample at a rate of 0.5 ml/min. The relative detection limit for such a sample is estimated to be less than 1 part per billion.

No attempt was made to determine the detection limit for Fe(III) because the detection limit is determined by the chromatographic characteristics of the Fe(III) rather than by the detector.

VI. DIFFERENTIAL PULSE VOLTAMMOGRAPH

A. Introduction

Heyrovsky, in 1922, discovered that the electrical current in a dropping mercury electrode (DME), at a constant applied voltage in a solution of electrolyte, is a linear function of the concentration of an electroactive solute in that solution (100). The analytical application of the DME, called "polarography," quickly grew in popularity. For the first time, analysts had available an instrumental technique for determination of a large number of dissolved inorganic species, namely metal ions, at low concentrations. Polarography for determination of metals continued to grow in popularity until the 1950's when it was largely displaced by the competing techniques of atomic absorption and flame emission spectroscopy which have lower detection limits than the conventional polarography.

Polarography as practiced in the conventional manner of Heyrovsky involves recording the electrode current as a function of a slowly varying applied DC voltage. The electrical signal of interest is the current which results from the electrochemical reaction of an electroactive analyte. This current is referred to as the "faradaic current," I_f. In addition to the faradaic current, a residual (background) current is observed which is the current required to "charge" the electrical double layer at the electrode solution

interface. The action of the electrical double layer is much like that of a capacitor which has the electrode surface as one plate and the adjacent solution phase as the other plate. When an electrical potential is applied to the electrode the resulting surface charge is counter balanced by the accumulation of oppositely charged ions in the solution phase in a layer parallel to the electrode surface.

This electrical double layer is modified if ions from the solution are chemisorbed to the electrode surface. Counter ions must also be accumulated in the solution phase so that the entire interfacial region obeys the principle of electrostatic neutrality. The charging current, I_{ch}, is the derivative of the interfacial charge, Q, taken with respect to time according to Equation VI.1.

$$I_{ch} = dQ/dt = \frac{d}{dt}[C_o A(E - E_{ECM})] \qquad \text{(VI.1)}$$

In Equation VI.1: A = electrode area (cm^2);

E = applied potential (V);

E_{ECM} = electrocapillary maximum (V);

C_o = specific capacitance of interfacial region (farads/cm^2).

For application of a slowly varying DC voltage (e.g., 0.1 V/min), the approximations are valid that $dE/dt \approx dC_o/dt \approx dE_{ECM}/dt \approx 0$ and the charging current is primarily the result of the changing area of the mercury drop as given by Equation VI.2. The charging current density (I_{ch}/A) is a

$$I_{ch} = C_o(E - E_{ECM})\,dA/dt \qquad (VI.2)$$

maximum at the start of a new drop when the ratio of area to volume is a maximum. The measurement of electrode current for the purpose of quantitative analysis is made at the end of the drop life when the ratio I_f/I_{ch} is at a maximum. The limit of detection in polarography is set by the charging current and is approximately 10^{-6} M; this is the concentration for which I_f and I_{ch} are approximately equal.

Modifications of polarography have been developed during the last two decades to lower the analytical detection limits to compete with spectroscopic methods of analysis. These modifications include the techniques of pulse polarography and differential pulse polarography. Pulse and differential pulse polarography require moderately sophisticated electronic circuitry and popular acceptance of these analytical techniques has recently been fueled by the revolution in the electronics industry which has given us miniature, integrated, analog and digital circuits.

The analytical techniques of pulse and differential pulse polarography take advantage of the difference in the rate of decay of the faradaic and charging currents in an electrode following a step-wise change in the electrode potential (101-103). The potential step is applied near the end of the lifetime of the mercury drop. The corresponding response of the electrode currents to the potential step is shown

qualitatively in Figure VI.1 and VI.2. Immediately following the potential step, the faradaic current decays with time as the thickness of the diffusion layer grows according to Equation VI.3.

$$I_f = nFAD(C^b - C^o)/\delta = nFAD(C^b - C^o)/\sqrt{\pi Dt} \qquad (VI.3)$$

The charging current decays much more quickly and, after a few milliseconds, is virtually negligible while the faradaic current is relatively large. The value of I_f is measured (sampled) and stored electronically when I_{ch} is virtually zero. The faradaic signal is substantially greater when measured in this manner than for conventional polarography. When the measurement of the electrode current is complete, the mercury drop is mechanically dislodged from the mercury capillary and the cycle repeated with a new value of potential. A complete current-potential curve for potential pulse polarography is obtained by stepping the potential repeatedly from an initial fixed value for no electrolysis to the value of a slowly varying DC ramp voltage. The stored value of the voltage signal which is proportional to the sampled electrode current is recorded as a function of the DC ramp voltage.

Pulse polarography cannot directly resolve the faradaic currents for several electroactive analytes present in a mixture since the faradaic currents are additive. Graphical

Figure IV.1. Currents in a dropping mercury electrode (DME) at constant potential

- - - - - charging current

———— faradaic current

Figure VI.2. Currents in a solid electrode in response to a step-wise change of potential from a region of no electrolysis to a value where electrolysis occurs

- - - - - charging current

———— faradaic current

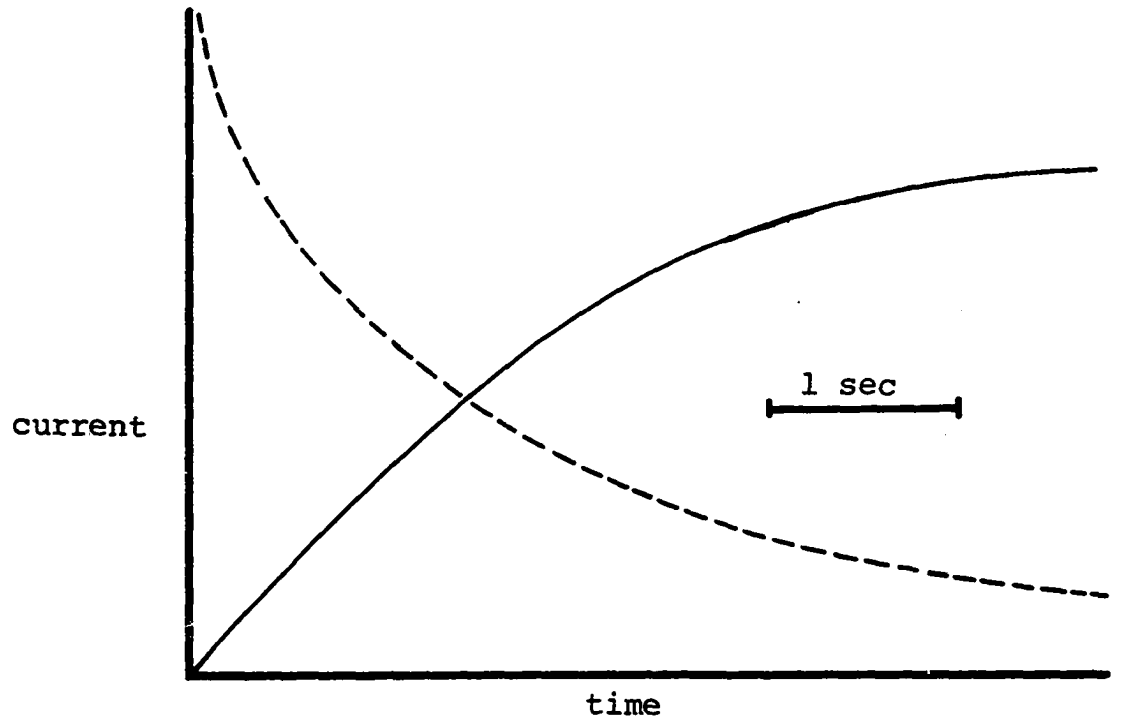
current
1 sec
time

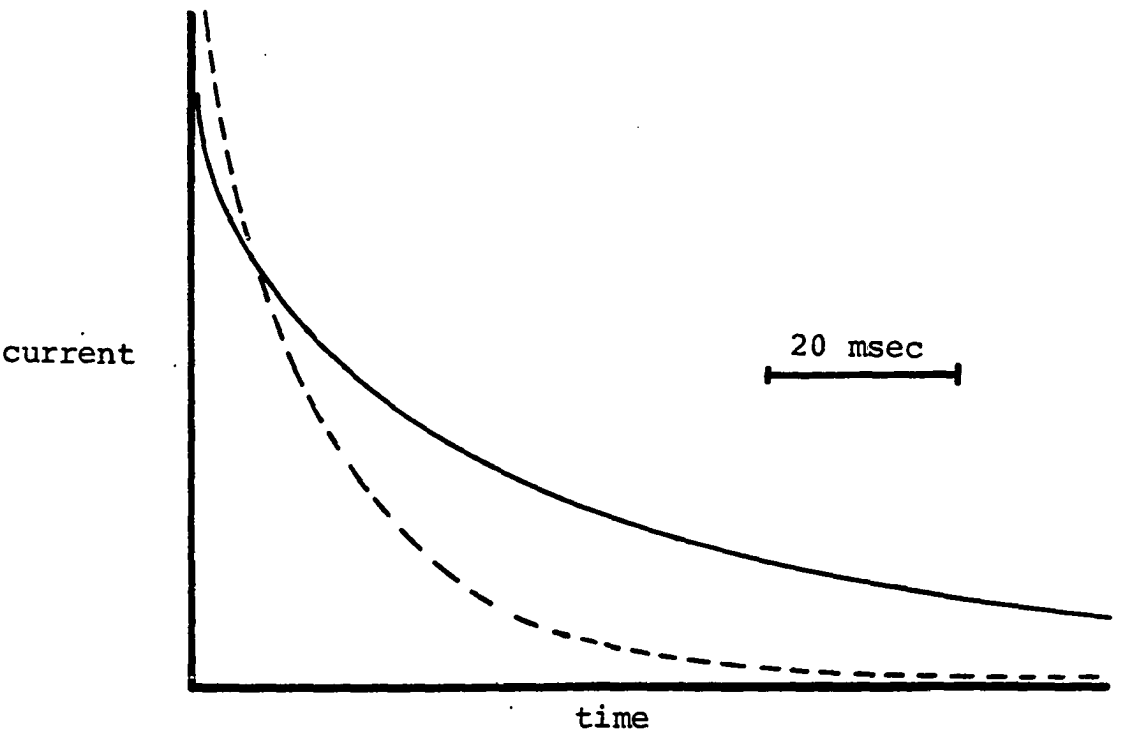
current
20 msec
time

measurement of limiting current for two species can be made only if the respective values of $E_{1/2}$ differ by approximately 200/n mV.

The technique of differential pulse polarography consists of the periodic superposition of a potential pulse on the DC voltage ramp (103). The pulse, ΔE, is relatively small (1-100 mV) and short in duration (1-100 msec). When the technique is used with a DME, the potential pulse is applied just before the end of the lifetime of the drop when the ratio of I_f/I_{ch} is at a maximum. The electrode potential waveform and the resulting electrode currents are shown qualitatively in Figure VI.3. The current is sampled during the period S_1 just prior to the application of the potential pulse and during the period S_2 just before the pulse is removed. The difference between the currents sampled at S_2 and S_1 is computed, the value is stored in an electronic memory and displayed at the output of the instrument until the difference value is updated by the next pulse cycle. The output signal is a result of the change in the electrolysis current due to the change in the degree of polarization of the electrode which results from the application of the pulse potential. A pulse will produce a change in polarization only when the DC voltage ramp is in a potential region for which the electroactive species reacts but not at a transport-limited rate (electrode is not completely polarized).

Figure VI.3. Electrode potential waveform used in differential pulse polarography and the resulting electrode currents

- - - - - charging current

———— total current

S_1 - first sample period

S_2 - second sample period

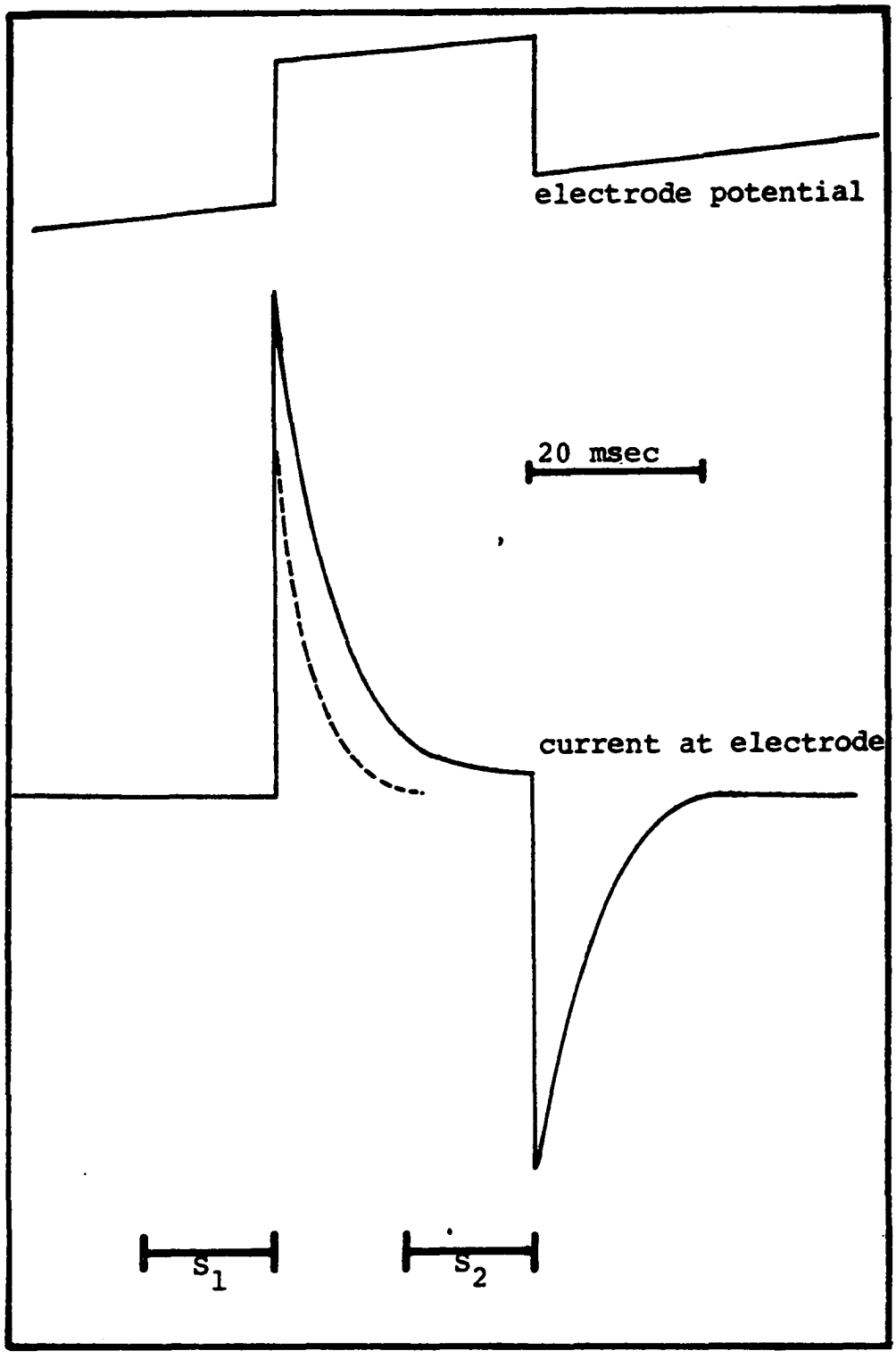
electrode potential
20 msec
current at electrode
S_1
S_2

This region corresponds to the rising part of the current-potential curve for conventional DC polarography. Differential pulse polarography gives a maximum response at the half-wave potential, $E_{1/2}$. Due to the subtraction of the currents before and during the pulse the instrument will give no response when the electrode is at a potential where the electrode is completely polarized. Therefore, the currents due to more easily reduced compounds which are totally polarized at the electrode are subtracted out. A resolution of the signals of electroactive compounds whose half-wave potential differ more than 100/n mV can be made. The recorded wave form for differential pulse polarography is a series of peaks corresponding to the electroactive species. The peak potential is $E_{1/2} \pm 0.5\ \Delta E$ and the peak height is proportional to the concentration of analyte (103).

Pulse and differential pulse techniques can also, in principle, be applied to solid electrodes for electroanalysis. The fact that detection limits for pulse and differential pulse polarography at the DME are lower than for conventional DC polarography was cause for inquiry into the use of these voltammetric techniques in conjunction with amperometric detectors for liquid chromatography.

Commercial instruments are available for pulse and differential pulse polarography (e.g., Princeton Applied Research). However, I chose to design and construct my own

instrument so that I could receive the benefit of the experience and in order that an instrument be obtained with greater flexibility than is commercially available. Solid electrodes can lose electrochemical activity in certain instances because of adsorption of solution impurities and/or the products of electrode reactions. Frequently, electrode activity can be restored if the electrode potential is changed to a value near the limits set for anodic or cathodic decomposition of the electrolytic solution. The instrument was designed to include application of a potential for electrode "cleaning" within each cycle of pulse application.

B. Design and Construction of the Differential Pulse Voltammograph

1. Cycle of operation

An instrument was designed to perform the following sequential operations:

1. potentiostat the electrode at the cleaning potential;
2. step the electrode potential to the value of a DC ramp voltage and allow the subsequent charging current to decay;
3. sample the electrode current;
4. add the potential pulse to the ramp signal and wait for the resulting charging current to decay;

5. sample the current and compute the difference of this current and that measured before the pulse;

6. hold and display this difference value until Steps 1 through 5 have been repeated to give a new value.

Since the instrument was designed for solid electrodes, no mechanism for synchronization with a DME was needed. Because the instrument was not for use with the DME it is called a "differential pulse voltammograph" rather than a "differential pulse polarograph."

The differential pulse voltammograph was designed and constructed as a combination of four functional units:

1. Control Unit,
2. Sample-and-Hold Unit,
3. Potentiostat Unit,
4. Voltage Unit.

The interconnections of the four units is shown in Figure VI.4.

2. Control Unit

The outputs from Jacks A through F of the Control Unit are constructed from transistor-transistor logic (TTL) digital circuits which control operations in the other units. The Control Unit regulates events by using a logic low (0 V) to close logic-driven CMOS electronic switches contained in the circuits of the controlled units.

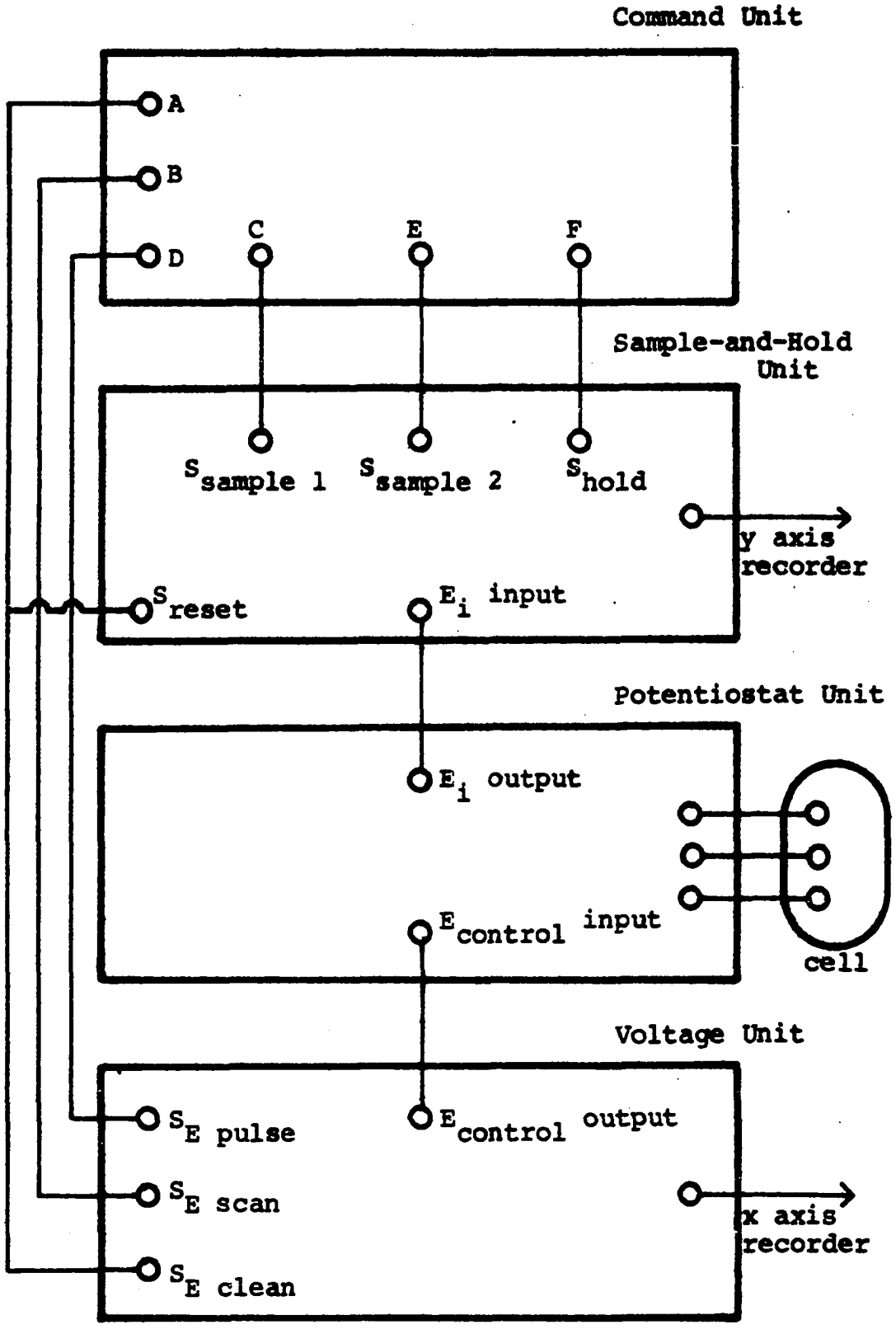

Figure VI.4. Block diagram of differential pulse voltammograph

The cycle of operation is schematically represented in Figure VI.5. The cycle was divided into 16 periods which were in practice the 16 counting states of a TTL four-bit binary counter. NAND gates were used to select the period or group of periods during which an event was permitted to occur.

The periods of operation were chosen to be synchronized with the AC line frequency with each period being one half that of the line frequency (8.33 msec). The prime reason for this choice is that the synchronization of the instrumental events with the line voltage reduces the extent of the pick up of electromagnetic radiation which has its source in the power lines. This time period of 8.33 msec is also reasonable for the decay of the charging current while still being sufficiently short for the sampling of the faradaic current before it has decayed to a negligible value. The 60-Hz radiation is probably the most common source of electrical noise in analytical instruments. The method of current sampling, when combined with the above practice of synchronization, cancels out line frequency noise.

The circuit for the 120-Hz clock used to generate the time base is shown in Figure VI.6. The line voltage is reduced to 12 V RMS by a transformer to isolate the circuit from common ground and to give voltages which are compatible with the amplifiers. The output of the transformer is

Figure VI.5. Cycle of operation. The output signals of a 7493 TTL counter are shown as a function of time and the sequence of events for the differential pulse voltammograph are given

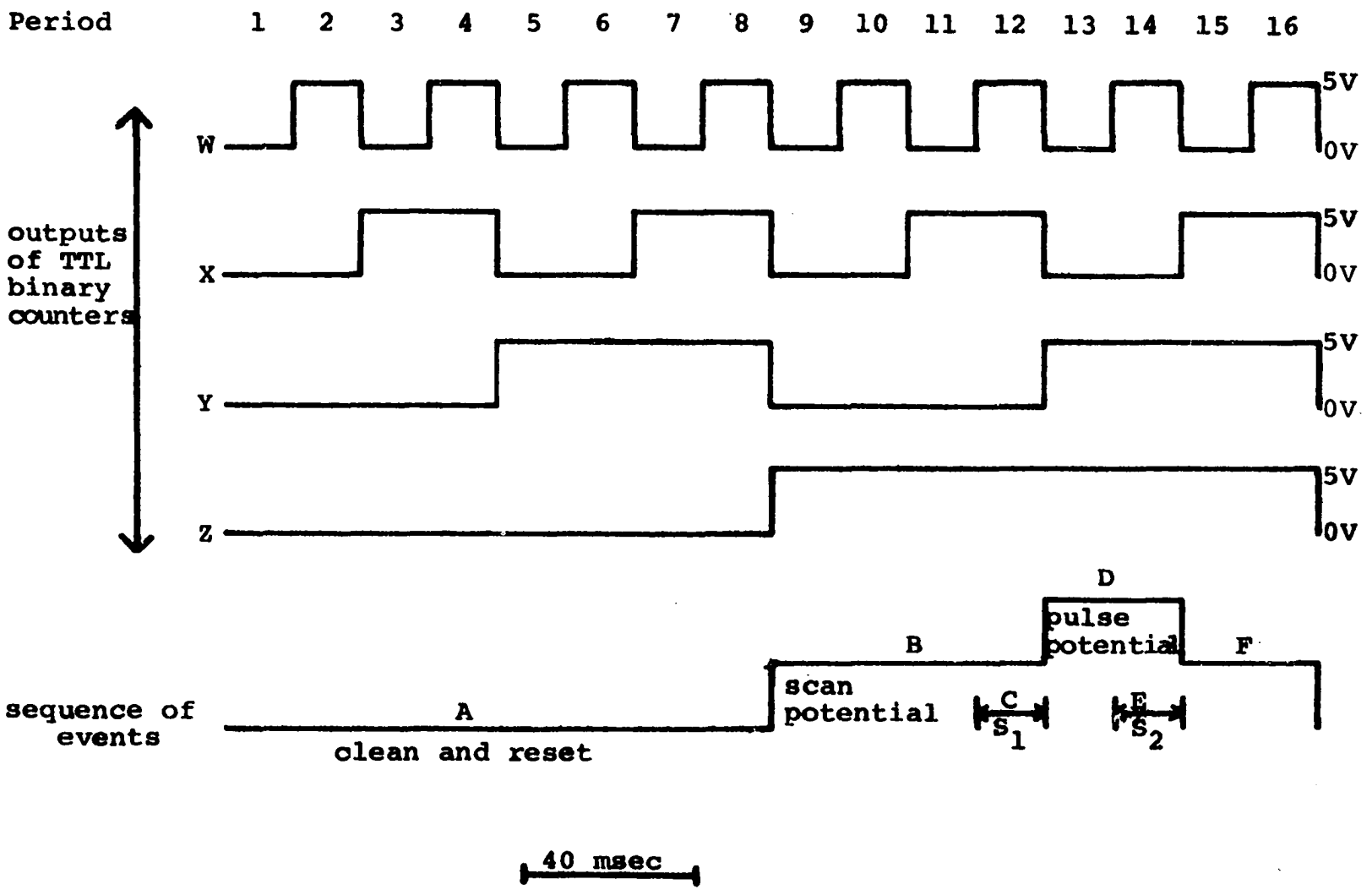
Period
1 2 3 4 5 6 7 8 9 10 11 12 13 14 15 16
outputs of TTL binary counters
W
X
Y
Z
5V
0V
sequence of events
A
clean and reset
B
scan potential
C
S_1
D
pulse potential
E
S_2
F
40 msec

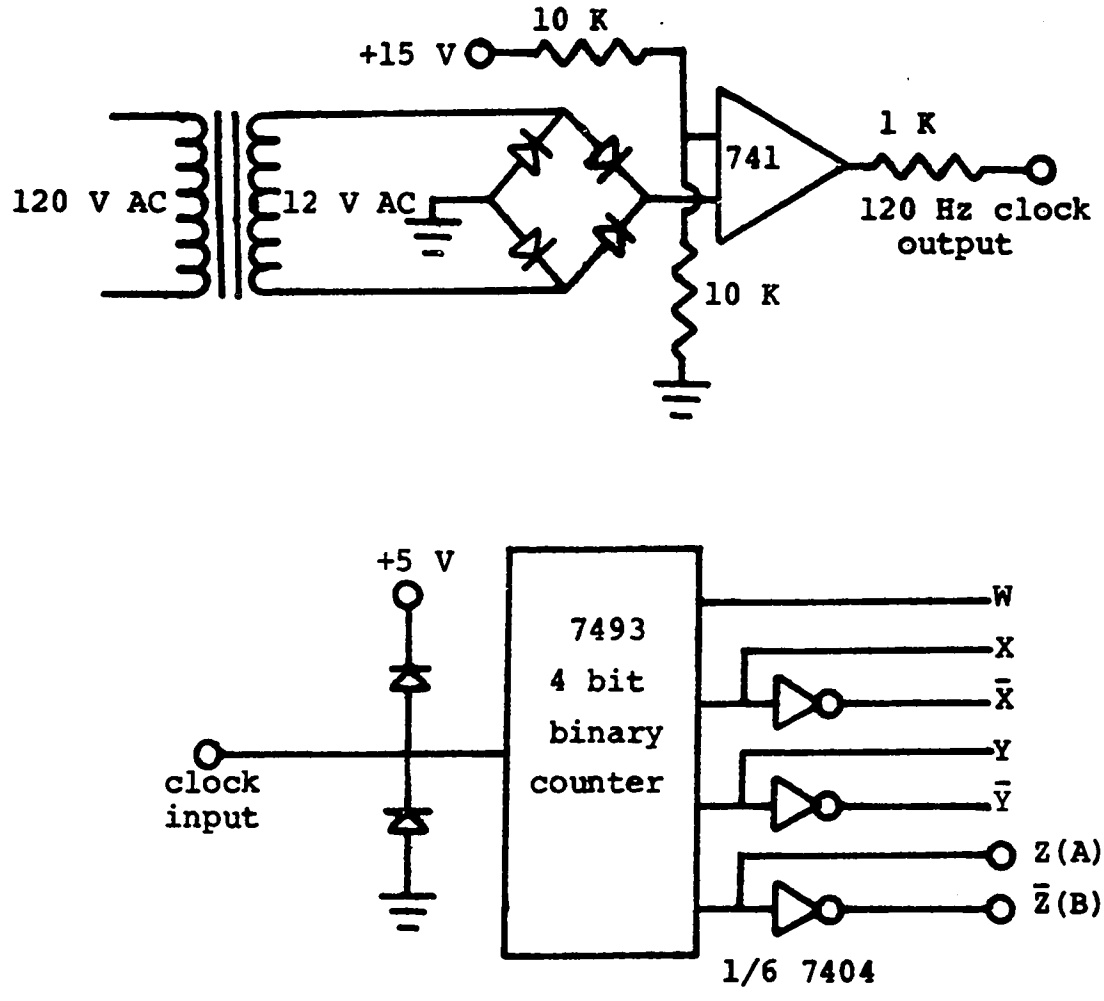

Figure VI.6. Schematic diagram of circuits used in the Control Unit

full-wave rectified by a diode bridge to give 120-Hz pulses. The pulses are transformed into a square wave by a National 741 operational amplifier wired as a comparator. The amplifier switches between its high and low limits when the pulse waveform crosses the comparison voltage of 7.5 V. The output waveform of the amplifier is an asymmetrical square wave with a 120-Hz frequency.

The clock output is applied to the input of a four-bit binary counter (TTL-7493) shown in Figure VI.6. The input is clamped with diodes to ground and to the 5-V power supply to make the signal from the clock compatible with TTL logic levels (0 V and 5 V). The product of the first division, which is at output W, is a symmetrical square wave with a period identical to that of line frequency. Outputs X, Y, and Z of the counter are successive binary divisions. The relationship of the states of the output during the counting is shown in Figure VI.5. The X, Y, and Z outputs are inverted to provide $\bar{X}$, $\bar{Y}$, and $\bar{Z}$ so that events can be switched during the low logic states of the counter.

The desired sequence of events is shown below the timing diagram of the counter in Figure VI.5. Logic commands for the operation in the instrument are generated for particular counting states of the four-bit binary counter by using TTL-7420 NAND gates. A NAND gate has a low output and closes a logic driver switch when all input signals are

high. The cleaning potential for the electrode, which operates during one half of the cycle, is switched directly by the Z output of the counter. The scanning potential for the electrode, which operates during the other half of the cycle, is directly switched by the inverted Z signal, $\bar{Z}$. Thus, when the Z output is high the cleaning potential is off, the signal at the inverted output of $\bar{Z}$ is low, and the scanning potential is summed into the output. Any part of the cycle represented by a logic state of the counter can be chosen for an operation by using the NAND gates. The first sample is taken when the W, X and Z outputs are high and the Y output low (W, X, $\bar{Y}$, Z). In like manner, the pulse potential is applied when X is low and Y and Z are high ($\bar{X}$, Y, Z). During the second half of the pulse, the second sample is taken when W, Y and Z are high and X is low (W, $\bar{X}$, Y, Z). The connection of the counter outputs and the inverted counter outputs to the NAND gates is shown in Figure VI.6. The outputs of the logic elements which will command the various events are labeled chronologically with letters A through F in Figure VI.6. The events are labeled with the corresponding letter in Figure VI.5.

3. Sample-and-Hold Unit

The schematic diagram for the Sample-and-Hold Unit is shown in Figure VI.7. The function of the Sample-and-Hold

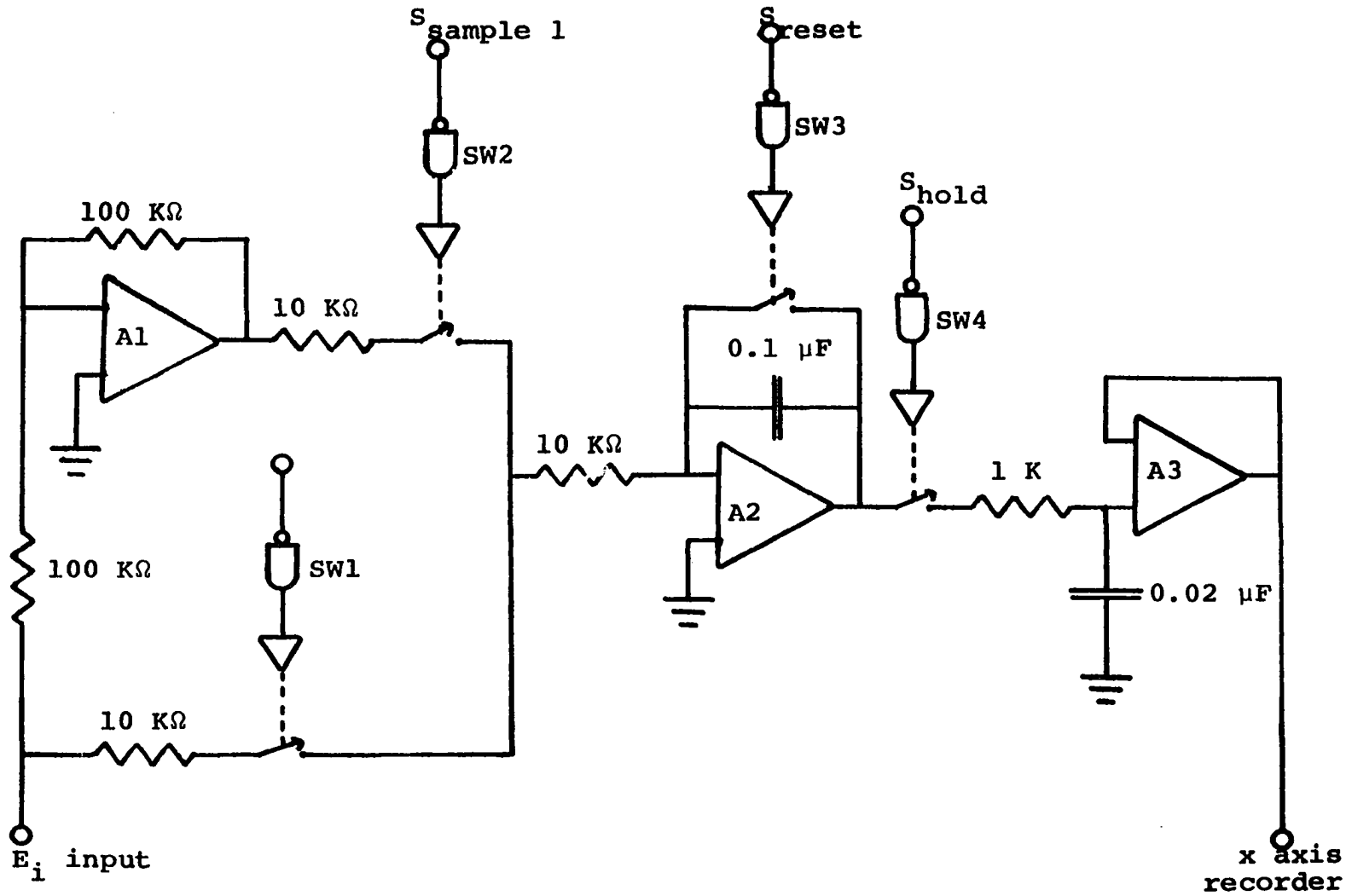

Figure VI.7. Schematic diagram of Sample-and-Hold Unit

Unit is to display an output signal which is proportional to the difference between the current measured before and during the application of the potential pulse.

The sampling periods for two current measurements were chosen to occur during the same relative portion of the line frequency so that pick up of electromagnetic radiation from power lines would be nearly the same during both sampling periods and would, therefore, be subtracted out during the process of computing the difference between the two current signals. Thus the difference would be only the change in the faradaic current resulting from the application of the potential pulse to the electrode. The current signal is integrated electronically to compute the actual average of the current signal during the sampling period. This fact can be recognized from the mathematical definition of the time average, $\bar{X}$, given by Equation VI.4.

$$\bar{X} = \frac{1}{t_p} \int_o^{tp} X(t)\,dt \qquad \text{(VI.4)}$$

$\bar{X}$ is the average value of X during the time period t_p. The integration has the effect of acting as a low pass filter which limits the band pass of the noise to a value proportional to $1/t_p$ without distorting the signal. This method is superior to conventional RC filtering which must use time constants several times larger to obtain an equivalent reduction in noise (104). The heavy filtering by RC networks,

such as that used in commercial instruments, can distort signals which are undergoing rapid changes and cause the treated signal to lag behind the true value. For experiments which require rapid voltage scan rates, such as differential pulse anodic stripping, the integration method provides greater signal fidelity.

The operation of computing the difference of the current signals was effected by integrating the current signal before the pulse (period S_1) and then integrating the inverted (opposite polarity) signal during the later half of the pulse (period S_2). The inversion was effected by using an operational amplifier with unity gain in the inverting configuration. Figure VI.8 shows the relationship of these current signals and the integrator output to the applied potential pulse.

When the current signal is to be sampled before the pulse (S_1), the Control Unit commands switch SW 1 to close and the current is integrated by amplifier A2 for the prescribed period and the integral is stored. When the signal is to be sampled the second time (S_2), switch SW 2 closes and the output of amplifier A1 which is equal in magnitude but of opposite polarity to the current signal, is integrated. Because of the inverted polarity, the second integration proceeds in a direction opposite to the first. This operation provides a true difference of the average current signals.

Figure VI.8. Relationship of Currents, Sample Periods, Voltage Waveforms and Integrator Output

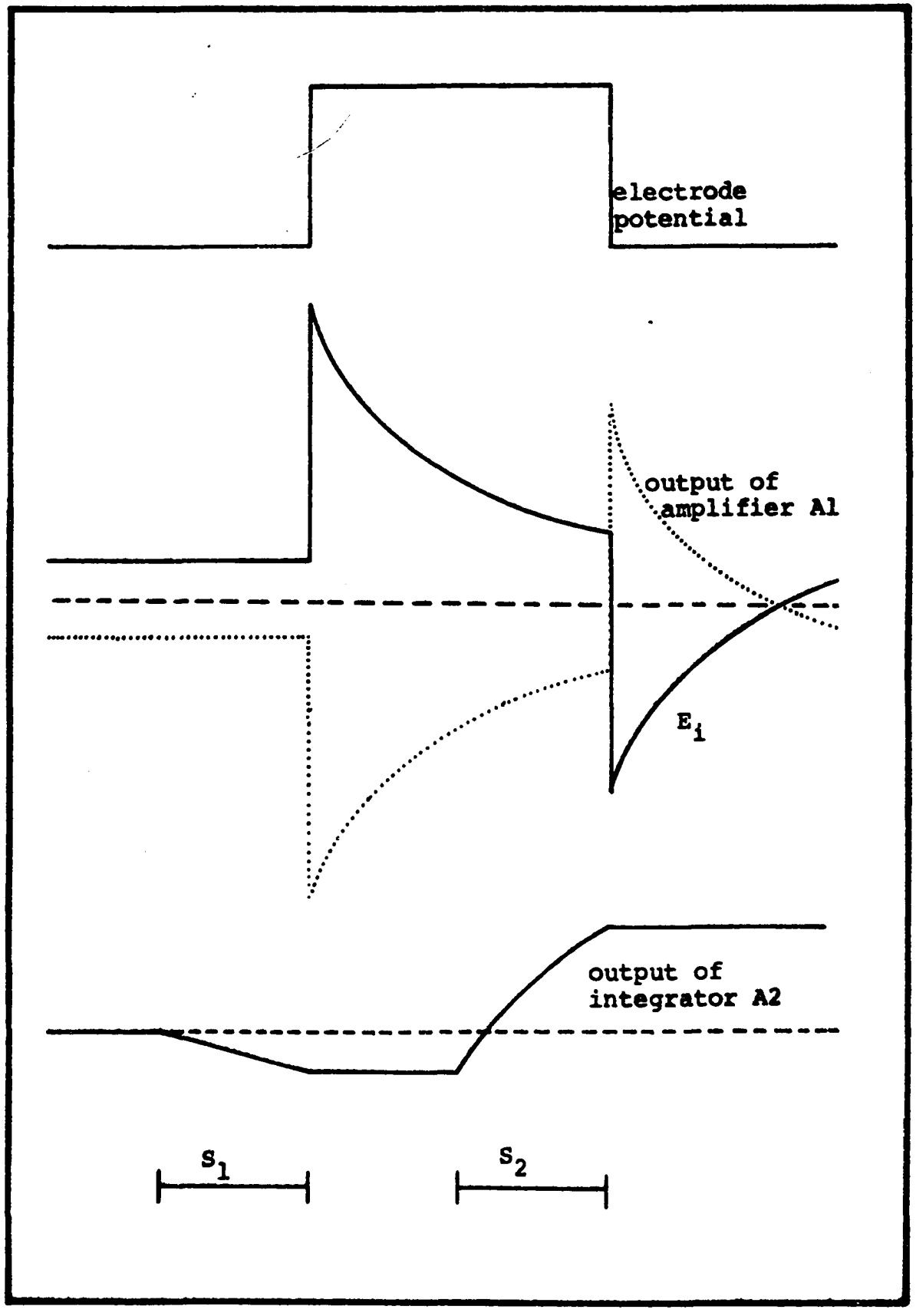
electrode
potential
output of
amplifier A1
E_i
output of
integrator A2
S_1
S_2

The Control Unit commands switch SW 4 to close and the difference in the value computed by the integrator is transferred to the sample-and-hold circuit of amplifier A3, where the signal is held at the output of the Sample-and-Hold Unit until being updated in the next cycle of operation. During the first half of the next cycle, the integrator is reset by command to close switch SW 3.

Amplifier A1 was an Analog Devices AD504 which was chosen for high stability. The input and feedback resistors for amplifier A1 were 1% precision resistors rated at 1% selected which were matched to 0.1% to insure that the circuit would invert the signal without any change in the absolute value of the signal. Amplifiers A2 and A3 were Analog Devices AD503 and AD540 respectively. Both were chosen for their low bias currents. The capacitors were low leakage, polystyrene or mylar capacitors. The digitally driven, analog switches were type DG200BA from Siliconix.

4. Potentiostat Unit

The potentiostat was described in Section III.A.1. The only modification of the potentiostat circuit necessary for this application was the inclusion of two 10-V Zener diodes placed back to back in the feedback circuit of the current follower amplifier. The zener diodes were used so that the initial spike of charging current, which occurs at the beginning of the pulse, would not drive the amplifier to its

output voltage limit. Before the amplifier would reach the voltage limit, the zener diodes would conduct the excess current around the feedback resistor. Although the current follower was not performing the predicted current to voltage conversion when the zener diodes were conducting, this fact is of no consequence because the current is not sampled during the initial charging phenomenon. Without the zener diodes in the circuit, large charging current spikes would cause limiting of the amplifier output and would inhibit the rapid decay of the charging current.

5. Voltage Unit

The function of the Voltage Unit is to provide the various potentials on command from the Control Unit, to the potentiostat so that the working electrode is potentiostated at required potentials during the cycle of operation. A schematic diagram of the circuit is shown in Figure VI.9.

A stable, reference voltage source was prepared from a temperature-compensated zener diode, which has a nominal break-down voltage of 9 V. The zener voltage is applied to the positive input terminal of a non-inverting amplifier (A1) with gain. The circuit gain is trimmed so that the zener voltage is amplified to exactly +10.00 V. The circuit, unlike the zener diode above, is capable of providing power to the other circuit elements without degradation of the

Figure VI.9. Schematic diagram of Voltage Unit

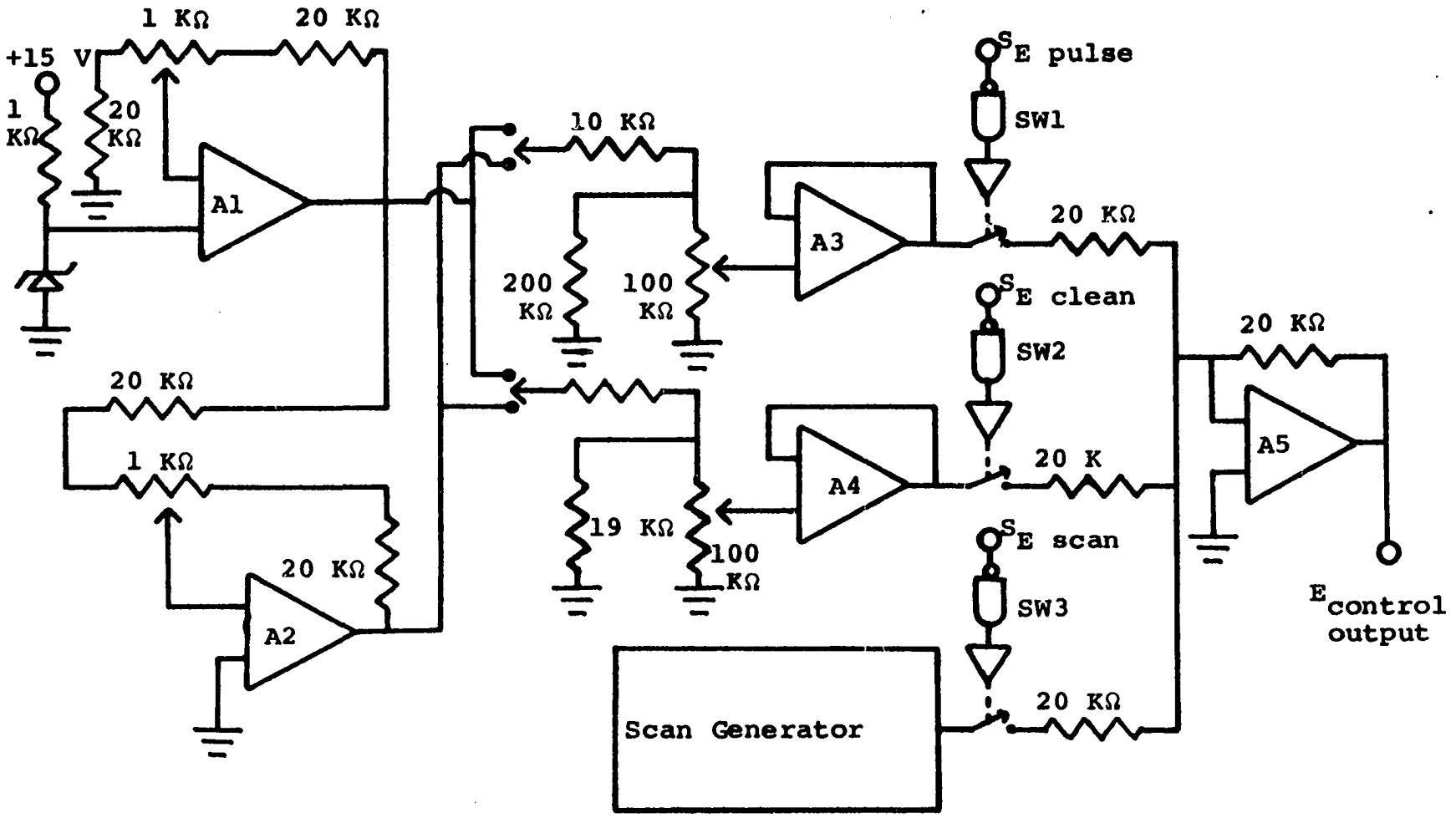
+15 V
1 KΩ
20 KΩ
1 KΩ
20 KΩ
A1
10 KΩ
200 KΩ
100 KΩ
A3
S E pulse
SW1
20 KΩ
S E clean
SW2
20 KΩ
20 KΩ
1 KΩ
A2
19 KΩ
100 KΩ
A4
20 K
A5
S E scan
SW3
E control output
Scan Generator
20 KΩ

voltage level. The +10.00-V output is inverted by amplifier A2 to provide a source at -10.00 V.

The positive or negative reference voltage is selected by single-pole double-throw switches and attenuated by adjustable divider networks to provide a signal of ±0 to 200 mV for application as the potential pulse and a signal of ±0 to 1 V for application as the cleaning potential. The voltages from the voltage dividers are buffered by amplifiers A3 and A4 wired as voltage followers so that power can be drawn from the circuit without degrading the voltage levels.

The potential pulse, cleaning potential, and the scanning potential are linearly combined by the summing circuit of amplifier A5. The inputs to amplifier A5 are controlled by digitally driven analog switches. The Control Unit controls the combination of the signal potentials for cleaning, pulsing, or scanning which are summed and presented at the output of the Voltage Unit to provide the signal for controlling the electrode potential. The amplifiers were Analog Devices AD504 or their equivalent with high stability. The analog switches were IH 5010 and 7347 from Intersil. All fixed resistors were 1% precision resistors.

6. General construction

The circuits were constructed on printed circuit boards which were prepared by the Iowa State University Electronics

shop from positive artwork prepared by the author. Each of the above units is individually contained in an aluminum chassis mounted in a standard 19-inch rack. Each unit has its own power supply and is capable of independent operation.

VII. A COMPARATIVE EVALUATION OF CONSTANT POTENTIAL AMPEROMETRY AND DIFFERENTIAL PULSE AMPEROMETRY FOR DETECTION IN LIQUID CHROMATOGRAPHY

A. Introduction

1. Flow-rate dependence

The efficiency of the coulometric electrode (Detector C) was determined to be independent of the fluid flow rate, V_f, for $V_f < 3$ ml/min as predicted by Equation II.10 (see Chapter IV). Amperometric detection at constant potential using an open tubular electrode (non-coulometric) has a response which is a function of V_f. The diffusion layer thickness, δ, and, hence, the sensitivity of an open tubular electrode is controlled by the hydrodynamic conditions within the electrode. Consequently, to keep the sensitivity of a tubular detector constant, the fluid flow rate must be precisely controlled.

Detection with an open tubular electrode operated under conditions of potential pulse amperometry is expected to be less sensitive to variation of V_f than is DC amperometric detection. Furthermore, the analytical sensitivity for pulse amperometric detection should be greater than for DC detection. The pulse technique owes its greater analytical sensitivity and decreased dependence on V_f to the fact that the diffusion layer thickness, following a potential step

from a value for no electrolysis to a value for which electrolysis occurs, is initially described by Fick's first law of diffusion as given by Equation VII.1.

$$\delta = (\pi Dt)^{1/2} \qquad \text{(VII.1)}$$

In Equation VII.1: δ = diffusion layer thickness (cm);

D = diffusion coefficient (cm^2/sec);

t = time (sec).

Consider application of a potential step from a value where no electrolysis occurs to a value for which the concentration of the analyte at the electrode surface is zero; this is the mass transport-limited case. The resulting faradaic current immediately after application of the potential step is inversely proportional to $t^{1/2}$ as given by Equation VII.2.

$$I_f = nF\pi^{1/2}R^2LD^{1/2}C^b/t^{1/2} \qquad \text{(VII.2)}$$

In Equation VII.2: R = radius of tubular electrode (cm);

L = length of electrode (cm);

C^b = bulk concentration of electroactive analyte ($mole/cm^3$).

The value of δ increases with time following the potential step, as described by Equation VII.1, until being limited by the hydrodynamic conditions resulting from fluid flow in the tube. The limiting (steady-state) value of δ is given by Equation VII.3 for the tubular electrode. The resulting,

$$\delta = 0.579R^{4/3}(DL/V_f)^{1/3} \qquad \text{(VII.3)}$$

limiting faradaic current for the tubular electrode is given

by Equation VII.4.

$$I_f = 5.43nFD^{2/3}R^{2/3}L^{2/3}v^{1/3}C^b \qquad \text{(VII.4)}$$

To summarize: for small values of t following application of the potential step, I_f is described by Equation VII.2 and is independent of V_f. For large values of t, I_f reaches a steady-state value proportional to $V_f^{1/3}$. For intermediate values of t, I_f should be a function both of t and V_f.

Flanagan and Marcoux (105) used the computational technique of digital simulation to predict the value of t for transition from Equation VII.2 to VII.4. These authors demonstrated that Equation VII.2 is valid for $t < 0.4\ t'$, where

$$t' = 0.43R^2L^{2/3}D^{-1/3}V_f^{-2/3} \qquad \text{(VII.5)}$$

and Equation VII.4 is valid for $t > 2.0\ t'$.

2. Analytical sensitivity

DC amperometric detection is generally applied with a value of electrode potential in the range for a mass transported-limited electrode reaction, i.e., the value of I_f is the so-called "limiting current." When the electrode reaction is transport limited, the faradaic current is independent of the electrode potential. This situation is characterized by a wave-like voltammogram with a plateau region corresponding to the transport-limited reaction. An amperometric detector will have a maximum and constant analytical sensitivity at all values of potential within the range of the limiting current plateau. For values of

electrode potential in the region of the rising portion of the voltammetric wave, the sensitivity of the electrode is very dependent on the potential value chosen. Maximum sensitivity for several electroactive species can be obtained at one electrode potential so long as that potential corresponds to a value in the limiting-current region of the voltammetric waves for all the species.

In contrast to DC amperometric detection, pulse detection has maximum sensitivity only at a potential nearly equal to the $E_{1/2}$ for the voltammetric wave (103). Hence, pulse detection is more selective than DC amperometric detection. For small values of potential pulse, ΔE, the differential current, ΔI, is given by Equation VII.6.

$$\Delta I = \frac{n^2F^2}{RT} AC^b \Delta E \left(\frac{D}{\pi t}\right)^{1/2} \frac{P}{(1 + P)^2} \qquad \text{(VII.6)}$$

In Equation VII.6: $P = \exp\{nF(E - E_{1/2})/RT\}$;

A = electrode area (cm^2);

E = applied potential (V).

The maximum current signal, ΔI_{max}, is obtained at $E = E_{1/2}$ ($P = 1$) and is given by Equation VII.7.

$$\Delta I_{max} = \frac{n^2F^2}{4RT} AC^b \Delta E \left(\frac{D}{\pi t}\right)^{1/2} \qquad \text{(VII.7)}$$

The width of a signal peak measured at half peak height, $W_{1/2}$, obtained by the differential pulse method is given by Equation VII.8. The value of $W_{1/2}$ is 90.4, 45.2 and

$$W_{1/2} = 3.52\frac{RT}{nF} \qquad \text{(VII.8)}$$

30.1 mV for electrode reactions with n = 1, 2, and 3, respectively.

3. Literature

McDonald and Duke compared the application of amperometric detection at constant potential (DC) with potential pulse amperometric detection for p-aminophenol at a solid electrode (106). They reported that, under stopped-flow operation for the reaction of the p-aminophenol at the Pt electrode, the pulse technique gave a 20X increase in the analytical sensitivity over the DC amperometric technique. The DC technique was placed at a definite disadvantage under the stopped-flow conditions because the current will eventually decay to zero in the absence of fluid flow. The comparison of the two techniques would be better if performed with continuous fluid flow. A condition of continuous flow would prevail if these detectors were applied to liquid chromatography.

McDonald and Duke also reported that the short-term stability of the electrode was greatly improved when operating with the pulse technique as compared with the DC technique. Based on their results, McDonald and Duke concluded that the electrode surface was deactivated when continuously operating at constant potential by adsorption of impurities or products

of the electrode reaction. For the pulse technique, the electrode potential is held at an initial value for 90-99% of the pulse cycle with no electrode reaction occurring. Apparently, the initial potential allows "cleaning" of the electrode surface by desorption of the contaminating species.

McDonald and Duke reported that the detection by the potential pulse technique was much less affected by changes in fluid flow rate than for the DC technique.

The technique of differential pulse amperometric detection, described in the previous chapter, operates in a manner similar to pulse voltammetry and should show the same advantages over DC amperometric detection reported by McDonald and Duke. In addition, the differential pulse technique can resolve the faradaic current due to the analyte of interest from that due to interfering species which are reacting at the electrode at diffusion-limited rates. The additional selectivity of an electrode operated in the differential pulse mode should reduce the number of interferences which must be separated by the chromatograph.

Swartzfager (67) compared the use of pulse voltammetry, differential pulse voltammetry, and DC voltammetry for the detection of organic compounds at a carbon paste electrode. He demonstrated that, in contrast to DC voltammetry, the sensitivity of pulse and differential pulse voltammetry remained relatively independent of flow rate for flow rates

less than 1 ml/min. Chromatograms for sulfanilamide, DL-3,4-dihydroxyphenylalanine, and p-aminophenol were obtained with detection by differential pulse and DC voltammetry. The use of differential pulse voltammetry dramatically increased the selectivity of the electrochemical detector. However, Swartzfager also reported that the detection limit for the differential pulse techniques was far inferior to the DC amperometric technique because the non-faradaic residual current did not decay to a value of zero before the electrode current was sampled in the pulse and the differential pulse modes. When using the differential pulse technique, an increase in selectivity can be obtained at the expense of a decrease in sensitivity by decreasing the amplitude of the pulse, ΔE.

Differential pulse voltammetry at Detector A (open tube) was applied to the detection of Cu(II) and Fe(III) in the effluent of the liquid chromatograph using the separation previously described. The attempt to dramatically improve sensitivity and to gain independence from the separation parameters was not totally successful. The investigation was productive, however, for elucidating those experimental parameters which must be considered when applying differential pulse voltammetry for electrolysis in fluid streams.

B. Experimental

The instrument and associated techniques have been described in Chapters III and VI.

C. Results and Discussion

1. Detection range

Current-voltage curves of Cu(II) and Fe(III) in 5 M HBr at a Pt RDE using differential pulse voltammetry are shown for comparison in Figures VII.1 and VII.2. In both figures, Curve A is the differential pulse voltammogram and Curve B is the DC voltammogram. From examination of the curves it can be seen that using DC amperometry for detection at any potential less than 0.35 will give constant and maximum sensitivity for both the Cu(II) and the Fe(III). The differential pulse technique, however, would give a maximum response at a much smaller range of potentials. Furthermore, the range is different for the Cu(II) and the Fe(III). The problem can be better appreciated by examining Figure VII.3 where the differential pulse voltammograms of Cu(II) and Fe(III) are shown superimposed on the blank. A potential which gives a maximum response for Cu(II) will not give a maximum response for Fe(III). In addition, if an attempt is made to choose a compromise potential, for example 0.40 V, the potential will be on the sloping region of the current voltage curves for both metals. Any shift in the half wave

Figure VII.1. I-E curves for 1.6×10^{-4} M Cu^{+2} in 5 M HBr

Annodic scan. Scan rate 0.5 V/min. Pt RDE.
Rotational velocity 1600 rev/min.

a Differential pulse voltammetry

Pulse amplitude 40 mV

Pulse duration 33.3 msec

b DC voltammetry

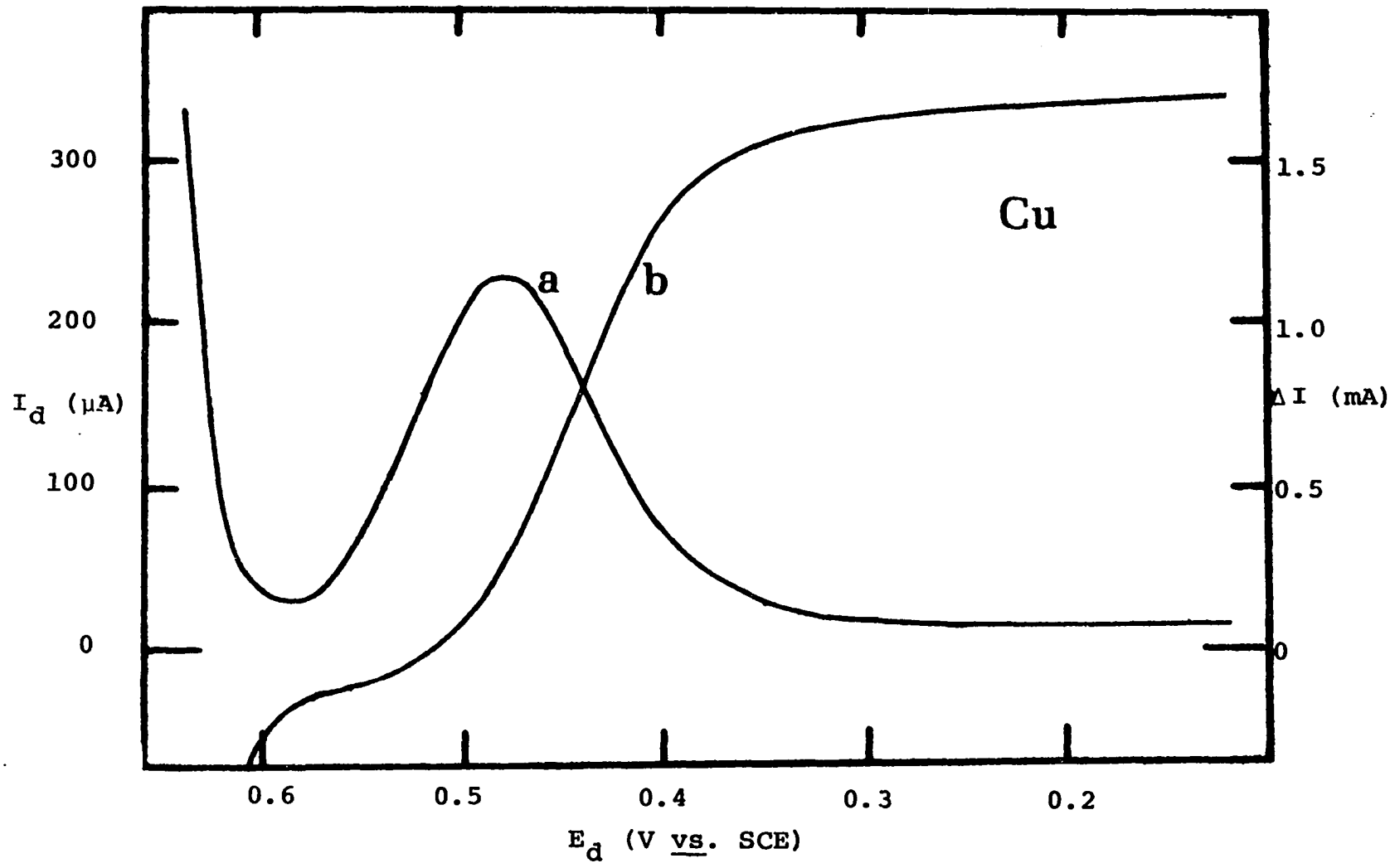
300
200
100
0
I_d (μA)
1.5
1.0
0.5
0
ΔI (mA)
Cu
a
b
0.6
0.5
0.4
0.3
0.2
E_d (V vs. SCE)

Figure VII.2. I-E curves for 1.8×10^{-4} M Fe^{+3} in 5 M HBr

Anodic scan. Scan rate 0.5 V/min. Pt RDE.
Rotational velocity 1600 rev/min.

a Differential pulse voltammetry

Pulse amplitude 40 mV

Pulse duration 33.3 msec

b DC voltammetry

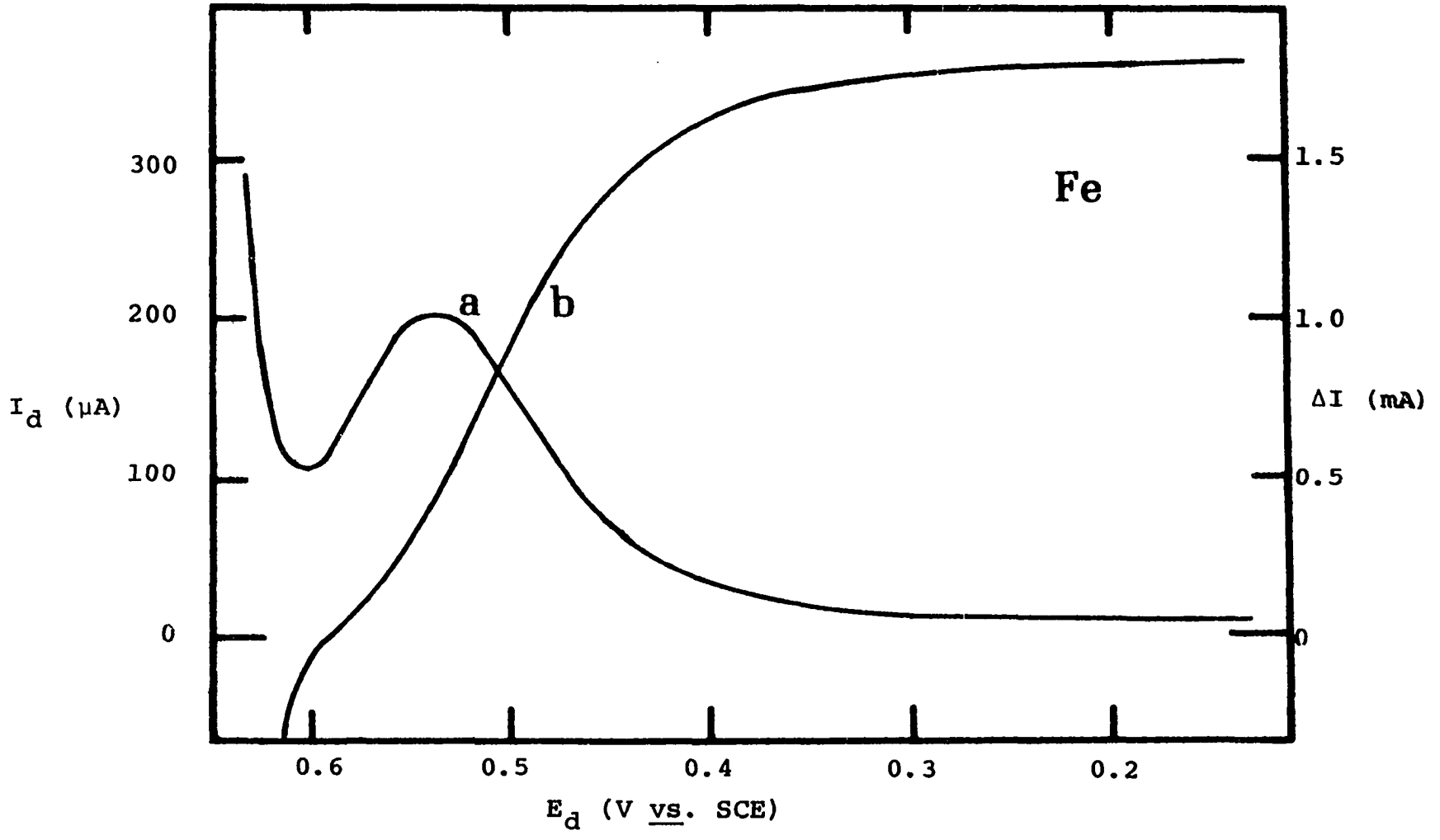
Fe
a
b
300
200
100
0
I_d (μA)
1.5
1.0
0.5
0
ΔI (mA)
0.6
0.5
0.4
0.3
0.2
E_d (V vs. SCE)

Figure VII.3. Differential pulse voltammograms for 1.6×10^{-4} M Cu^{+2} and 1.8×10^{-4} M Fe^{+3} in 5 M HBr and blank

Anodic scan. Scan rate 0.5 V/min. Pt RDE. Rotational velocity 1600 rev/min. Pulse amplitude 40 mV. Pulse duration 33.3 msec.

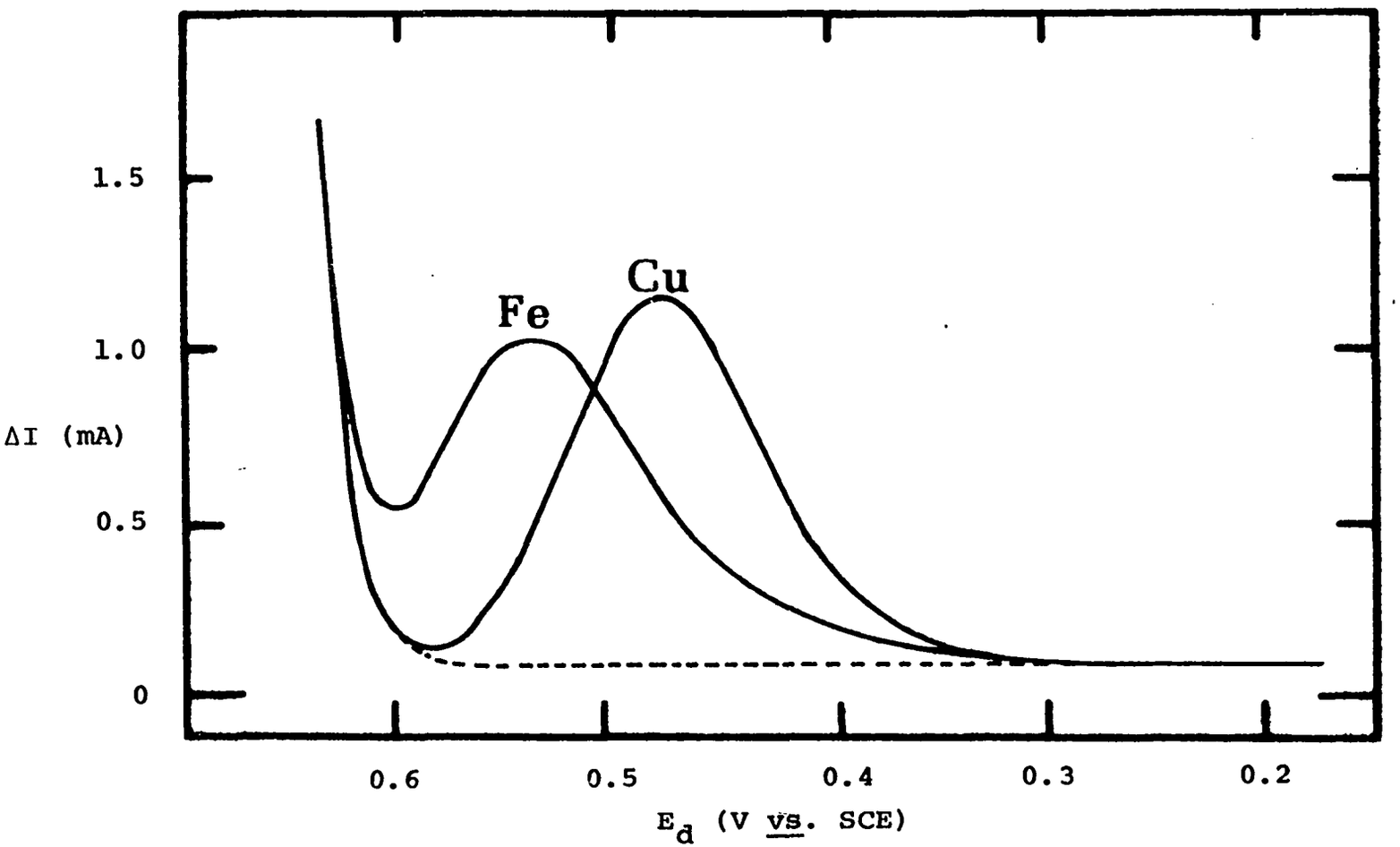
1.5
1.0
0.5
0
ΔI (mA)
Fe
Cu
0.6
0.5
0.4
0.3
0.2
E_d (V vs. SCE)

potentials will shift the peak positions and will result in great changes in sensitivities. The shifting of half wave potentials is frequently observed.

Another problem is that the more anodic pctentials used in differential pulse voltammetry lie near the potential at which Br^- is oxidized. The oxidation of Br^- sets the positive limit of the useful potential range and is responsible for the signal increasing for $E > 0.6$ V. The technique of differential pulse voltammetry outputs signals of the same polarity for oxidations and reductions. A negative pulse potential increases the degree of cathodic polarization but decreases the degree of anodic polarization. A decrease in anodic current gives a difference in current, ΔI, which is the same in polarity as an increase in cathodic current. The tail of the Br^- oxidation lies under parts of the Cu(II) and Fe(III) peak. The potential at which bromide would be detected at maximum sensitivity is different enough from the potential used for Cu(II) and Fe(III) that if the bromide were present at similar concentrations as the Cu(II) and Fe(III) the bromide reduction would not interfere at all. However due to the large amounts of Br^- in the electrolyte even the very small sensitivity to Br^- at these potentials is enough to give a considerable baseline, which will change with Br^- concentration. In DC amperometry this problem is nonexistent as the maximum sensitivity for Cu(II)

and Fe(III) is at potentials which are very far removed from that sufficient to oxidize Br^-.

It must be remembered that differential pulse voltammetry is one of the best methods of resolving and detecting compounds when the current is measured as a function of voltage. The ability to resolve the signals as a function of voltage, however, limits the potential range which can be used for detection. That the range is limited means that the technique is more selective and will have a low sensitivity to compounds which have half-wave potentials which differ from the detector potential by more than 0.15/n V. Thus responses to many interferences may be eliminated.

2. Effect of change in electrolyte

Figure VII.4 is a series of differential pulse voltammograms for HBr at different concentrations. An examination of the eV curves leads one to expect that any response to the HBr, which is used as the eluent and electrolyte will be a function of the HBr concentration. Differential pulse voltammetry at Detector A was used for detection of Cu(II) and Fe(III) using the separation previously described in Section V.B.3.d. When the detector potential was set at 0.50 V to obtain optimum sensitivity for Cu(II) and Fe(III), baseline changes were observed with changes in the eluent concentration. When the potential of the detector was changed to 0.45 V in an attempt to change the detector to

Figure VII.4. Differential pulse voltammograms for HBr

Anodic scan. Scan rate 0.5 V/min. Pt RDE. Rotational velocity 1600 rev/min. Pulse amplitude 40 mV. Pulse duration 33.3 msec.

a 0.1 M HBr

b 0.5 M HBr

c 2.5 M HBr

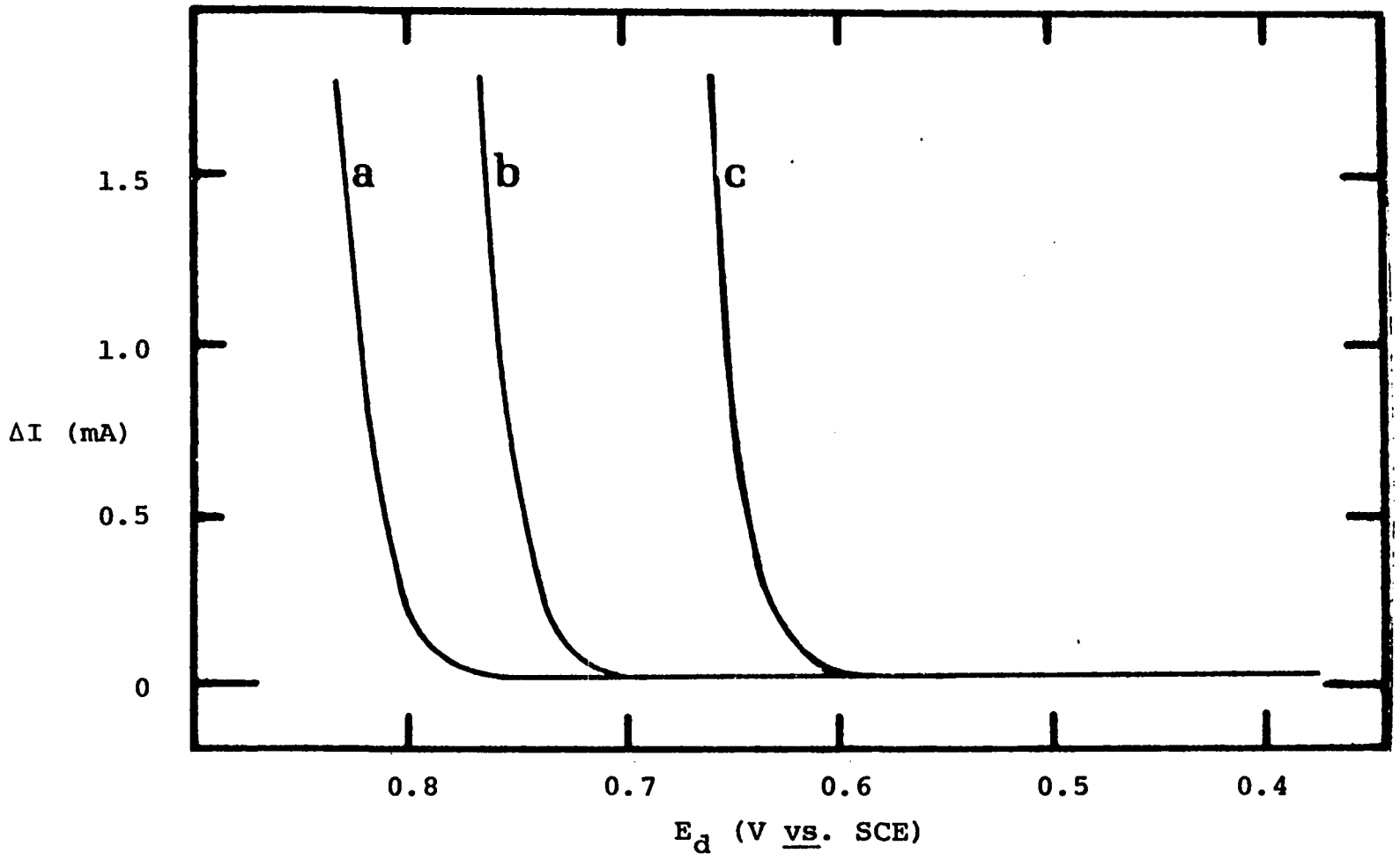
a
b
c
1.5
1.0
0.5
0
ΔI (mA)
0.8
0.7
0.6
0.5
0.4
E_d (V vs. SCE)

a potential which would be less sensitive to the oxidation of bromide, much smaller changes in baseline were observed when switching eluents. But at this potential the sensitivity for the Cu(II) and especially the Fe(III) was reduced.

The change in eluent/electrolyte composition can also lead to a shift in the half-wave potential and a consequent change in the sensitivity of the differential pulse technique. Figure VII.5 shows a differential pulse voltammogram of 5×10^{-4} M Fe(III) at a rotating platinum disk electrode in 0.2 HCl and 5.0 M HCl. The maximum, which corresponds to the half-wave potential, was shifted about 0.1 V more positive with the decrease in electrolyte concentration. Clearly the sensitivity of the differential pulse technique when used for detection could be greatly influenced by changes in electrolyte composition. In contrast, simple DC amperometric or pulse (not differential pulse) detection will have a constant sensitivity with changes in half-wave potential as long as the detector potential remains on the convective diffusion limited plateau of the current voltage curve.

3. Effect of adsorbed species

Iodide is known to adsorb strongly to platinum electrodes and cause marked changes in the electrochemistry at the platinum surface. This phenomenon has been well documented (99, 107). Iodide has also been observed to strongly adsorb to gold electrodes and to markedly influence the

Figure VII.5. Differential pulse voltammograms for 1.8×10^{-4} M Fe^{+3} in HCl

Anodic scan. Scan rate 0.5 V/min. Pt RDE. Rotational velocity 1600 rev/min.

a 0.2 M HCl

b 5.0 M HCl

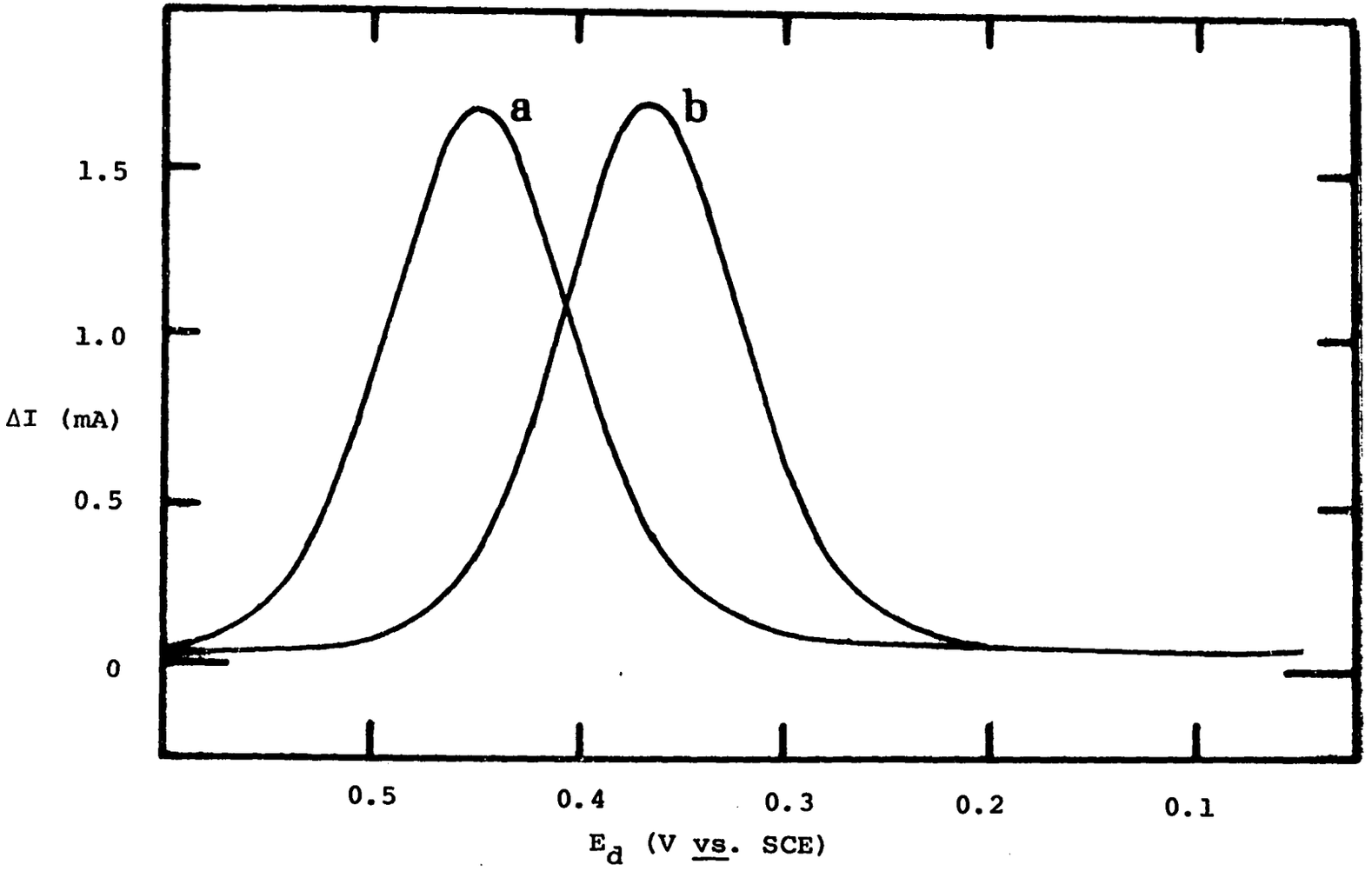
a
b
1.5
1.0
ΔI (mA)
0.5
0
0.5
0.4
0.3
0.2
0.1
E_d (V vs. SCE)

electrochemistry at the gold surface. It is interesting to note that the effect of the adsorbed iodide cannot be generalized. For example, iodide decreases the overpotential for the reduction of Cr(VI) at a platinum electrode but increases the overpotential for the reduction of Cr(VI) at a gold electrode.

Curve a of Figure VII.6 is a differential pulse voltammogram for 1.8×10^{-4} M Fe(III) in 1 M HCl at a rotating gold disk electrode which has just been polished. Curve b of Figure VII.6 was obtained under the same conditions except the electrode had been previously dipped into a dilute solution of NaI and rinsed with distilled water to remove excess iodide. The I^- which is strongly adsorbed by the gold surface, clearly changed the nature of the differential pulse voltammogram. Not only has the maximum of the peak been shifted but the peak height has been greatly reduced. Therefore we would expect that if Fe(III) was being detected at a gold tubular detector employing differential pulse amperometry at a potential which gives maximum sensitivity for a clean gold electrode, the adsorption of impurities such as iodide would result in a continuous decrease in sensitivity to approximately 25% of the original value.

The specific adsorption of iodide at the gold electrode is only one example of how changes in the interfacial region of the electrode can influence the electrochemistry. The

Figure VII.6. Differential pulse voltammogram for 1.8×10^{-4} M Fe^{+3} in 1.0 M HCl

Anodic scan. Scan rate 0.5 V/min. Au RDE. Rotational velocity 2500 rev/min.

a without I^-

b surface adsorbed I^-

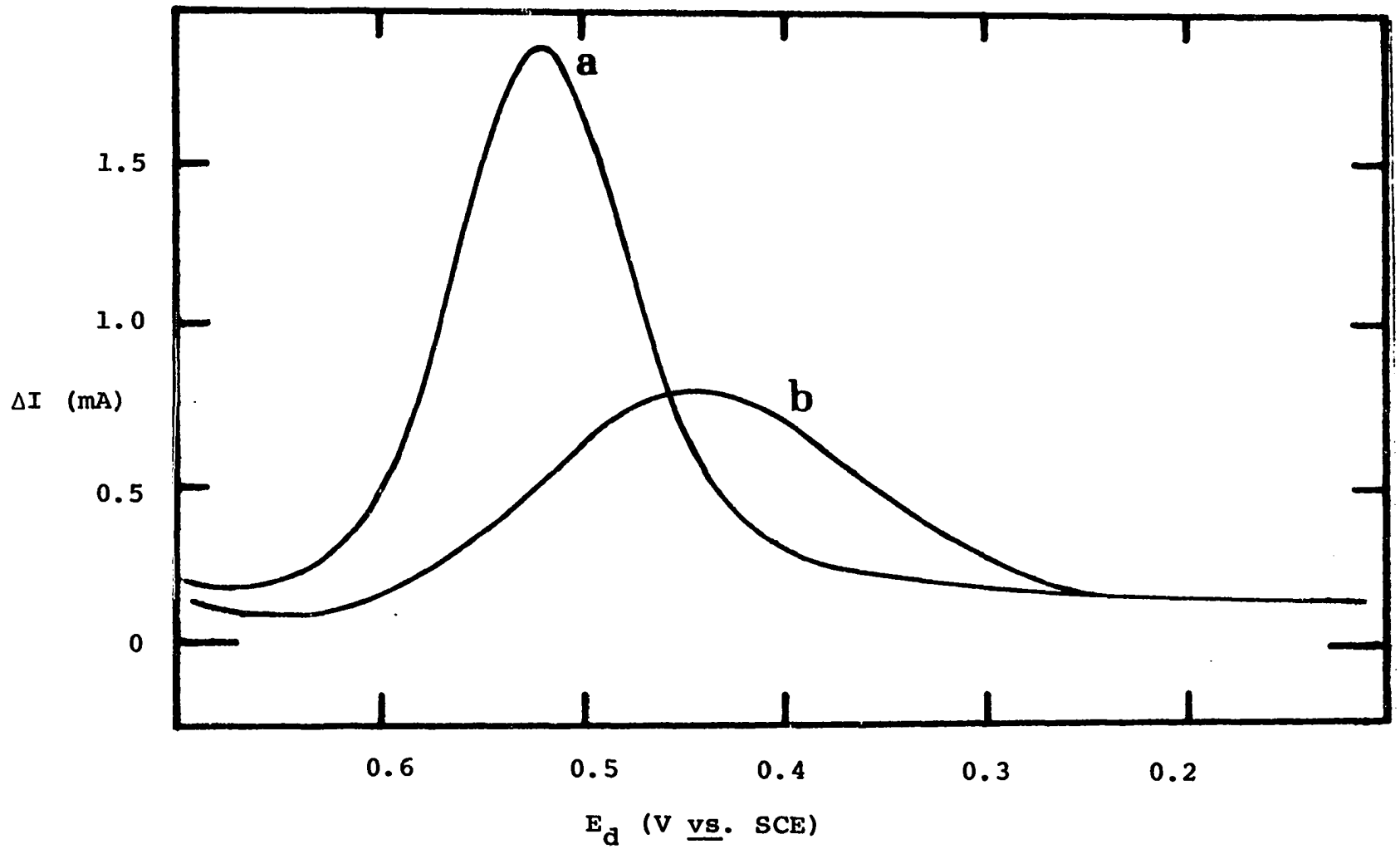
a
b
1.5
1.0
0.5
0
ΔI (mA)
0.6
0.5
0.4
0.3
0.2
E_d (V vs. SCE)

interfacial region may also be altered by changes in the electrolyte composition or by adsorption of reactants or products of previous determinations as well as the adsorption of trace impurities. The effect of such alterations in the interfacial region must be seriously considered in any analytical scheme employing electrochemical detection.

Impurities exist even in the most carefully prepared reagents. When impurities which can adsorb onto the electrode and which change the electrochemistry at the surface are present at extremely low concentrations, they may adsorb and slowly alter the electrochemistry. Figure VII.7 compares the differential pulse and DC voltammograms of 1.8×10^{-4} M Fe(III) at a rotating platinum disk electrode in 5 M HBr which had been polished as described in Section V.B.3.a. The solid lines are voltammograms which were run on a freshly polished electrode. The dashed lines are voltammograms which were run after the electrode had been left rotating in the solution for an hour. Again a shift and decrease in peak height is observed in the differential pulse voltammogram. The DC voltammogram although changed still has a convective diffusion limited plateau which would still give the same sensitivity as the electrode originally had. This figure demonstrates that although the sensitivity of a detector employing differential pulse voltammetry would change with time, a detector employing DC voltammetry at a

Figure VII.7. I-E curves for 1.8×10^{-4} M Fe^{+3} in 5 M HBr

Anodic scan. Scan rate 0.5 V/min. Pt RDE. Rotational velocity 2500 rev/min.

a Differential pulse voltammogram using a freshly polished electrode. Pulse amplitude 40 mV. Pulse duration 33.3 msec.

b DC voltammogram using a freshly polished electrode.

c Same as b but after 1 hr of use.

d Same as a but after 1 hr of use.

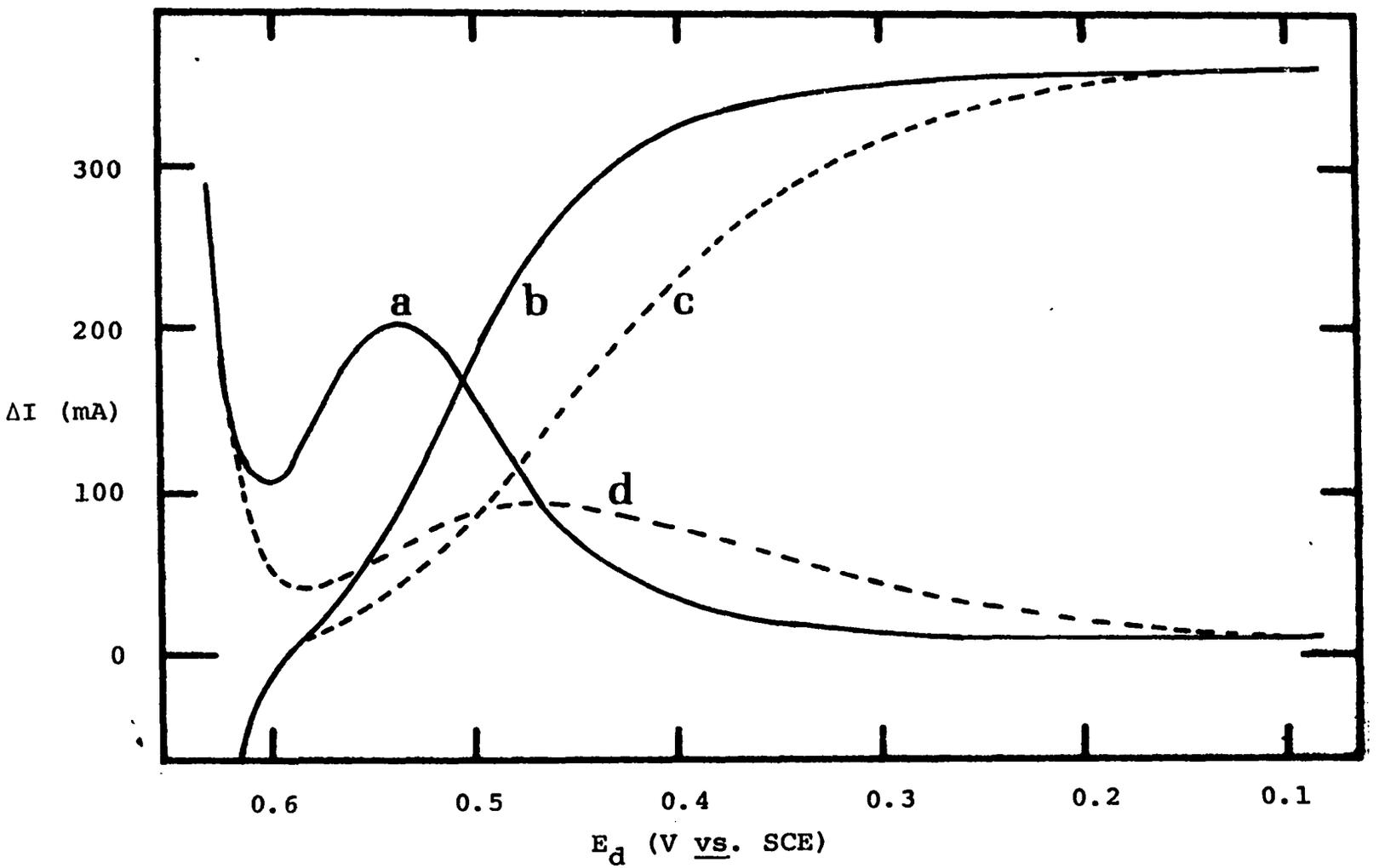
300
200
100
0
ΔI (mA)
a
b
c
d
0.6
0.5
0.4
0.3
0.2
0.1
E_d (V vs. SCE)

potential of 0.15 V would have a sensitivity which would have remained virtually unchanged.

4. Conclusions

Differential pulse voltammetry gives a voltammogram which is a peak, the geometry of which is a function of the above described parameters. It is therefore recommended that the use of differential pulse voltammetry for detection in liquid chromatography be limited to those situations where the parameters affecting the electrochemistry could be rigidly controlled.

Techniques such as pulse and DC voltammetry give voltammograms which have convective diffusion limited plateaus. The height of the plateau is a function only of the physical processes of convection and diffusion. Amperometric detectors operating on this plateau will have a constant sensitivity as long as the hydrodynamic conditions such as flow-rate and temperature are kept constant. Indeed the coulometric detector operates with constant and maximum sensitivity within a range of hydrodynamic and electrochemical conditions.

However, it must be recognized that differential pulse voltammetry still may be used to advantage when the electrochemistry can be stabilized and one compound or a class of compounds which have nearly the same half-wave potentials is

to be determined in the presence of interferences which have different half-wave potentials.

VIII. THE DETERMINATION OF CHROMIUM(VI)

A. Introduction

Compounds of Cr(VI) are extensively used by industry for a variety of purposes including chrome plating, corrosion control, "chrome dying" of cloth, pigmentation, tanning of leather and the preservation of wood. All too often, solutions of unused Cr(VI) from these processes are discharged without treatment and the Cr(VI) can subsequently enter into streams and water supplies. The concentration of Cr(VI) in drinking water in the United States has been reported to vary between 0.0003 μg/ml and 0.04 μg/ml with a mean of 0.0032 μg/ml (108). The maximum concentration of Cr(VI) presently permitted in potable water by the Safe Drinking Water Act (109) is 0.05 μg/ml.

The toxic properties of Cr are primarily confined to the hexavalent oxidation state of the element. Chromium(VI) is toxic at low concentrations, and exerts an irritative and corrosive effect on biological systems. Furthermore, Cr(VI) is suspected of having carcinogenic properties (108, 110). Because Cr(III) is much less toxic, analytical techniques for trace Cr should be specific for the hexavalent oxidation state.

B. Experimental

1. Chemicals and reagents

A standard stock solution of 0.100 N (0.0167 M) $K_2Cr_2O_7$ was prepared by dissolving 1.2267 g of Baker Reagent Grade $K_2Cr_2O_7$ and diluting to 250 ml with triply distilled water. Other solutions of $K_2Cr_2O_7$ were prepared by diluting this standard stock solution.

The chromatographic eluents and reagents were prepared by diluting Baker Reagent Grade HCl with deionized water. The deionized water was prepared by passing distilled water from the building supply through a mixed-bed ion-exchange column. The eluents and reagents were subsequently deaerated for 15 min with dispersed N_2 from Air Products Corp.

2. Water sample

The water sample (VDL 10334) was obtained from Mrs. Rhonda Snider of the Veterinary Diagnostic Laboratory (VDL) at Iowa State University. The original source of the sample was the waste effluent of a tannery. The raw sample was prepared for analysis at the VDL by evaporating a 50-ml aliquot of the raw sample to dryness and ashing at 500 °C overnight. The residue was taken up in concentrated HCl and then diluted to 25 ml in a volumetric flask.

The Cr(VI) in the sample was determined at the VDL by atomic absorption spectrophotometry. The instrument used

was a Perkin Elmer Model 303 atomic absorption spectrophotometer with a Perkin Elmer Intensitron hollow cathode lamp operated at 25 mA. The 358-nm resonance line was selected for the analysis. An air-acetylene flame was used with a three-slit burner. The Cr(VI) in the sample was extracted into methyl isobutyl ketone and aspirated into the flame. A calibration curve was prepared by determining the Cr(VI) in standards containing from 0.2 ppm to 1.4 ppm Cr(VI). The concentration of the Cr(VI) in the ashed sample was determined to be 0.6 ppm by the VDL.

I received for analysis the ashed water sample containing 10% HCl. The large amount of HCl in the sample was undesirable for my analytical method as it displaced the Cr(VI) from the chromatographic column. The sample therefore was diluted 1:50 with distilled water prior to analysis.

3. Experimental procedure

a. Voltammetry Cyclic voltammograms were obtained in the manner described in Section VI.B using a Pt RDE with an electrode area of 0.47 cm^2. The electrode was constructed by Pine Instrument Co. and was rotated in a PIR rotator also from Pine Instrument Co.

Plots of detector sensitivity as a function of detector potential were obtained by integrating the electrolysis current for samples of $K_2Cr_2O_7$ passing through the detector at fixed values of detector potential. Samples (0.504 ml)

of 1.00×10^{-4} N $K_2Cr_2O_7$ were injected into a stream of deionized water flowing at 0.5 ml/min. The sample stream was mixed with a 4 M solution of HCl flowing at 3.0 ml/min. The resulting mixed stream passed through the detector which was potentiostated at the specified potential. The integral of the electrolysis current (coulombs) was plotted against the detector potential.

b. Electrode pretreatment At the beginning of each experimental day the detector was pretreated by the passage of 4 M HCl through the detector while cycling the electrode potential between 1.60 V and -0.40 V at a scan rate of 0.1 V/min for approximately 15 min. The electrode potential was then set at 0.00 V and several 0.5-ml samples of 0.1 M KI were injected into the electrolyte stream passing through the detector. The potential was then adjusted to the desired value for subsequent experimentation. This treatment of the Pt electrode with I^- resulted in adsorption of iodine on the detector surface. The adsorbed iodine serves to electrocatalyze the reduction of $Cr_2O_7^=$ in acidic media and is not desorbed for detector potentials in the approximate range of 1.0 to -0.2 V vs. SCE.

c. Linear dynamic range The linear dynamic range of Detector C without chromatographic separation was determined by injecting 0.504-ml samples of standard solutions of $K_2Cr_2O_7$, ranging in concentration from 5×10^{-9} N to 0.1 N,

into a stream of deionized water flowing at a rate of 0.1 ml/min. The sample stream was mixed with a stream of 4 M HCl and the resulting stream passed through Detector C which was potentiostated at 0.250 V. The electrolysis current was integrated with the electronic integrator. The linear dynamic range of the total chromatographic system was determined in a similar manner using standard solutions of $K_2Cr_2O_7$. Details of the separation procedure are given in the following section.

d. Chromatographic separation The construction of the liquid chromatograph was described in Section III.B. The separation of complex samples containing $Cr_2O_7^=$ was performed on a 2 x 80-mm column of alumina. The column was prepared from Fisher A-540 adsorption alumina which was ground wet with a mortar and pestle. The alumina was then sieved under a stream of deionized water. The 180-250 mesh fraction of alumina was placed in the chromatographic column as an aqueous slurry.

The sample was placed onto the column by injection into an eluent stream of 0.18 M HCl which was flowing at a rate of 0.5 ml/min. Seven minutes after sample injection, the eluent was switched to 1.8 M HCl and the $Cr_2O_7^=$ was eluted from the column. The elution of $Cr_2O_7^=$ was complete 5 min after switching eluents. The eluent was then changed to 4 M HCl for 4 min and then switched back to 0.18 M HCl for 4 min

before injection of the next sample. The 4 M HCl served to clean the column of any metal ions still retained after the elution of the $Cr_2O_7^=$ with 1.8 M HCl. The column effluent was mixed with 4 M HCl before passage through the detector. The detector potential was 0.250 V.

e. Detector efficiency The efficiency of the detector was determined as a function of flow rate by passing samples of $Cr_2O_7^=$ through the detector at various flow rates while integrating the resulting electrolysis current. A series of 0.504-ml samples of 1.00×10^{-4} N $Cr_2O_7^=$ were injected into a stream of deionized water flowing at a rate of 0.1 ml/min. The sample stream was mixed with a stream of 4 M HCl before passage through the detector. The potential of the detector was 0.250 V. The flow rate of the mixed stream was controlled in the range of 0.1 - 5.5 ml/min. The selection of flow rates was made at random and had no natural sequence.

f. Analysis of water sample The analysis of the water sample for Cr(VI) was conducted by the method of standard additions. A 1.00-ml aliquot of unknown was pipetted into each of six 50-ml volumetric flasks. The sample in the first flask was diluted to volume with triply distilled water and contained only the diluted sample. Aliquots of volume between 0.25 ml and 2 ml of a standard solution of 1.00×10^{-4} N $Cr_2O_7^=$ were added to the other 50-ml volumetric flasks with a Gilmont micrometer burette. The contents of each flask

were diluted to volume with triply distilled water. These solutions were analyzed by the method of separation described above with a detector potential of 0.250 V.

C. Results and Discussion

1. Voltammetry

The reduction of $Cr_2O_7^=$ at a Pt electrode in acidic solutions was discovered to be electrocatalyzed by iodide adsorbed at the electrode surface. Current-potential (I-E) curves are shown in Figure VIII.1 which were obtained at a RPDE for 2×10^{-4} M $Cr_2O_7^=$ in 1.0 M HCl. Curve a is for the reduction of the $Cr_2O_7^=$ in the absence of adsorbed iodine. The reduction is extremely irreversible and exhibits no limiting current plateau. The observed value of $E_{1/2}$ is approximately 0.00 V vs. SCE whereas the value predicted for a reversible reduction is 0.76 V. Curve b is for the same solution after the electrode was immersed in 0.01 M NaI followed by a rinse with triply distilled water. The increased reversibility for the reduction of $Cr_2O_7^=$ is the direct consequence of the electrode pretreatment. Iodine is known to be irreversibly adsorbed at Pt and has been observed to electrocatalyze certain irreversible electrochemical reactions at Pt electrodes (99). The observed value of $E_{1/2}$ for the electrocatalyzed reaction is 0.50 V. A current plateau in the range of 0.4 to 0.1 V vs. SCE exists for the iodine-catalyzed reduction.

Figure VIII.1. I-E curves for 2 x 10^{-4} M $Cr_2O_7^{=}$ in 1 M HCl

Scan rate 2.0 V/min. Pt RDE. Rotational velocity 6400 rev/min.

A No adsorbed iodine.

B Presence of adsorbed iodine at electrode surface.

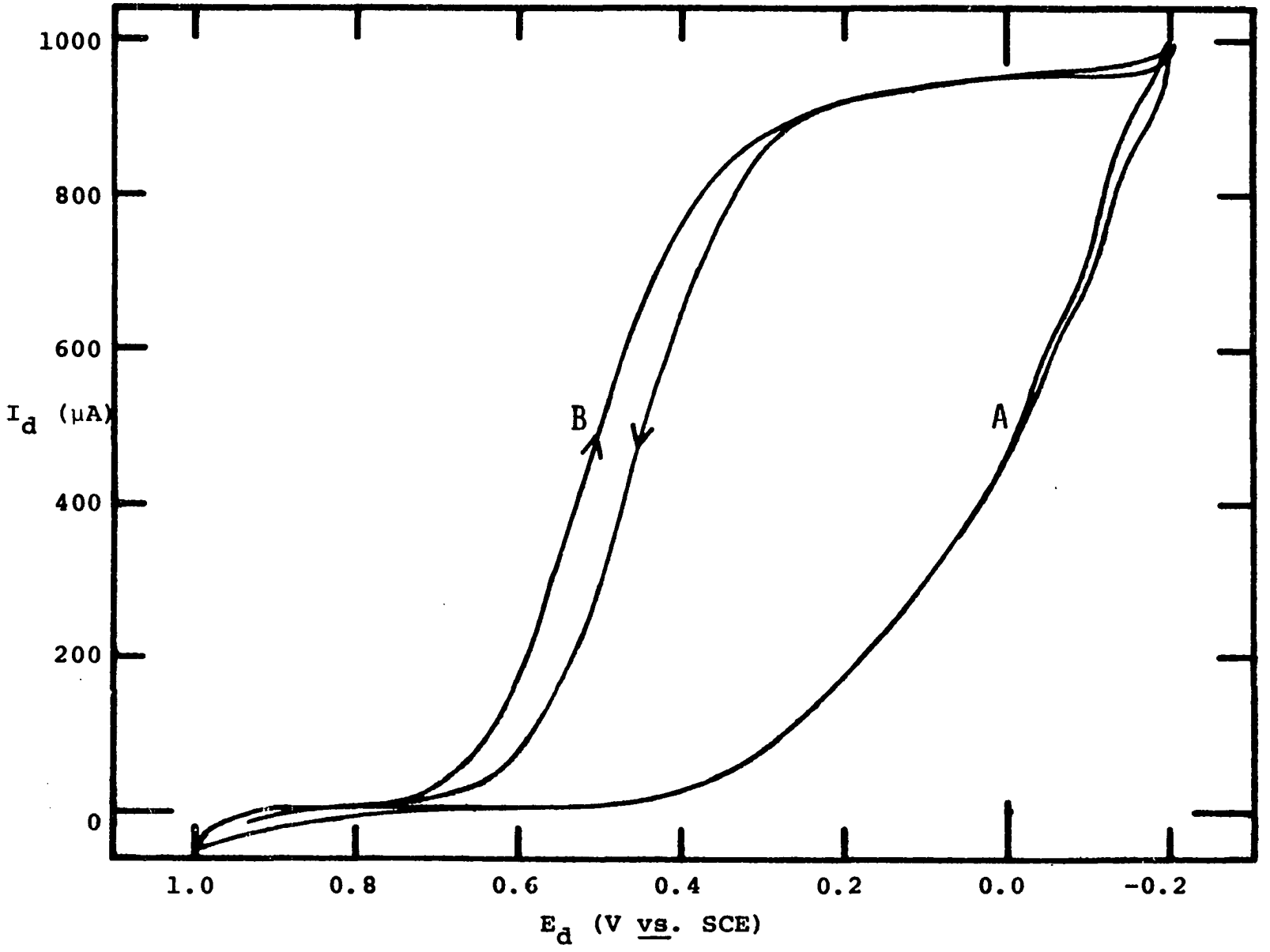
1000
800
600
400
200
0
I_d (μA)
B
A
1.0
0.8
0.6
0.4
0.2
0.0
-0.2
E_d (V vs. SCE)

The equation predicting the convective-diffusion limited current at a RDE was derived by Levich (26) and is given by Equation VIII.1.

$$I_\ell = 0.62nFAD^{2/3}\nu^{-1/6}\omega^{1/2}C^b \qquad \text{(VIII.I)}$$

In Equation VIII.1: I_ℓ = limiting current (mA);

n = equivalents per mole;

F = Faraday constant (96,487 coulombs/ equivalent);

A = geometric area of electrode (cm^2);

D = diffusion coefficient of electro-active species (cm^2/sec);

ν = kinematic viscosity of solution (cm^2/sec);

ω = rotational velocity of electrode (rad/sec);

C^b = bulk concentration of electroactive species (mol/liter).

According to Equation VIII.1, I_ℓ is proportional to $\omega^{1/2}$. A diagnostic verification of the condition of mass-transport limitation for an electrode current is the linearity of a plot of I vs. $\omega^{1/2}$. Such plots will deviate from linearity at high values of ω for which the rate of mass transport exceeds the rate of the heterogeneous electrochemical reaction. I-E curves for the reduction of $Cr_2O_7^=$ obtained for several values of ω are shown in Figure VIII.2.

Figure VIII.2. I-E curves for 2×10^{-4} M $Cr_2O_7^{=}$ at a Pt RDE in 1 M HCl

Anodic scan. Scan rate 2.0 V/min.

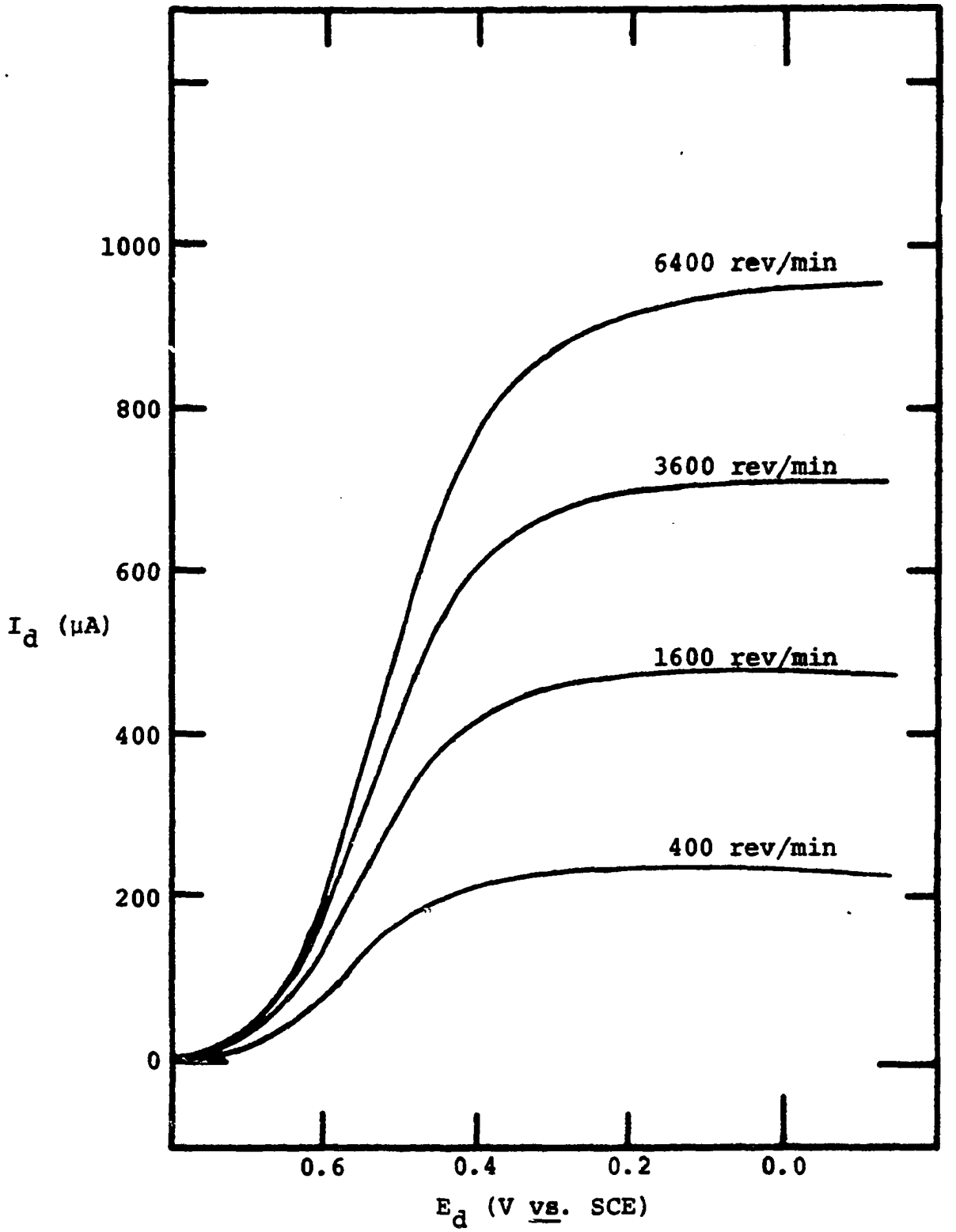
1000
800
600
400
200
0
I_d (μA)
6400 rev/min
3600 rev/min
1600 rev/min
400 rev/min
0.6
0.4
0.2
0.0
E_d (V vs. SCE)

A plot of current vs. $\omega^{1/2}$, measured on the current plateau at 0.00 V, is shown in Figure VIII.3. The plot is approximately linear with a zero intercept for $\omega < 900$.

The fact that $Cr_2O_7^{=}$ is reduced at a rate limited by mass-transport for low values of ω was taken as evidence that the reduction of $Cr_2O_7^{=}$ would be mass-transport controlled at the low flow rates typical for a tubular Pt chromatographic detector.

The voltammetric behavior of $Cr_2O_7^{=}$ in Detector C was studied by measuring the current-time integral as a function of detector potential. The electrode surface had previously been pretreated by injection of several samples of 0.01 M NaI. The plot of the percent Cr(VI) electrolyzed vs. E is shown in Figure VIII.4. This plot has a plateau which apparently corresponds to convective-diffusion limited mass transport to the electrode surface. Application of Detector C for quantitative determination of $Cr_2O_7^{=}$ should be possible with a detector potential in the region of this plateau.

2. Detector efficiency

The electrolytic efficiency of Detector C was calculated for reduction of $Cr_2O_7^{=}$ according to Equation VIII.2. and is plotted in Figure VIII.5 as a function of the flow rate of the electrolyte stream. Only at slow flow rates does the

$$Cr_2O_7^{=} + 14H^{+} + 6e \rightarrow 2Cr^{+3} + 7H_2O \qquad \text{(VIII.2)}$$

Figure VIII.3. I_ℓ *vs.* $\omega^{1/2}$ for 2×10^{-4} M $Cr_2O_7^=$ at a Pt RDE in 1 M HCl

E_d = 0.00 V *vs.* SCE

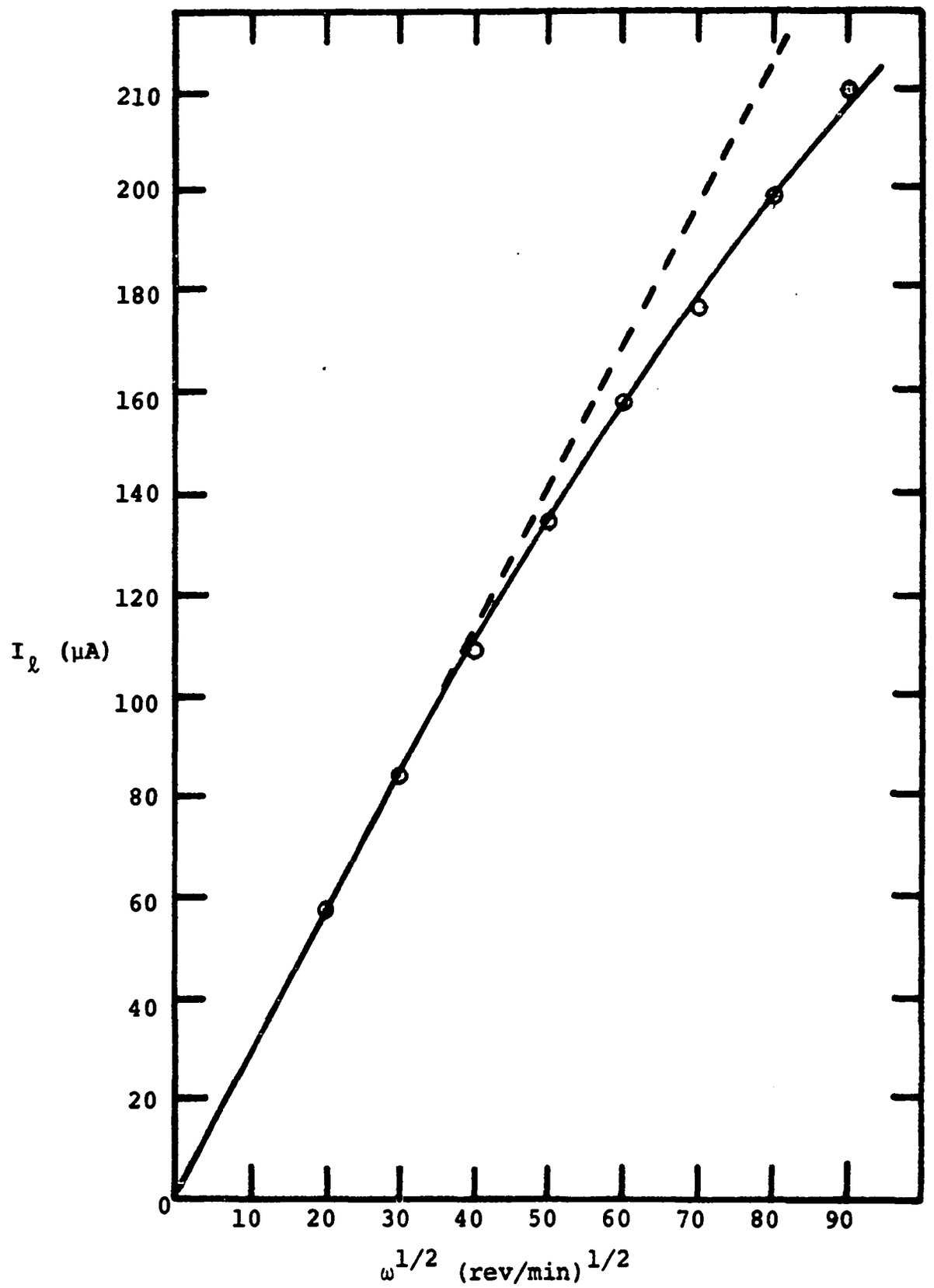
210
200
180
160
140
120
100
80
60
40
20
0
I_ℓ (μA)
10
20
30
40
50
60
70
80
90
$\omega^{1/2}$ (rev/min)$^{1/2}$

Figure VIII.4. Percent $Cr_2O_7^=$ electrolyzed *vs.* E
Detector C. Pretreated with I^-.
0.504 ml of 1.00×10^{-4} M $Cr_2O_7^=$
injected into 4 M HCl.

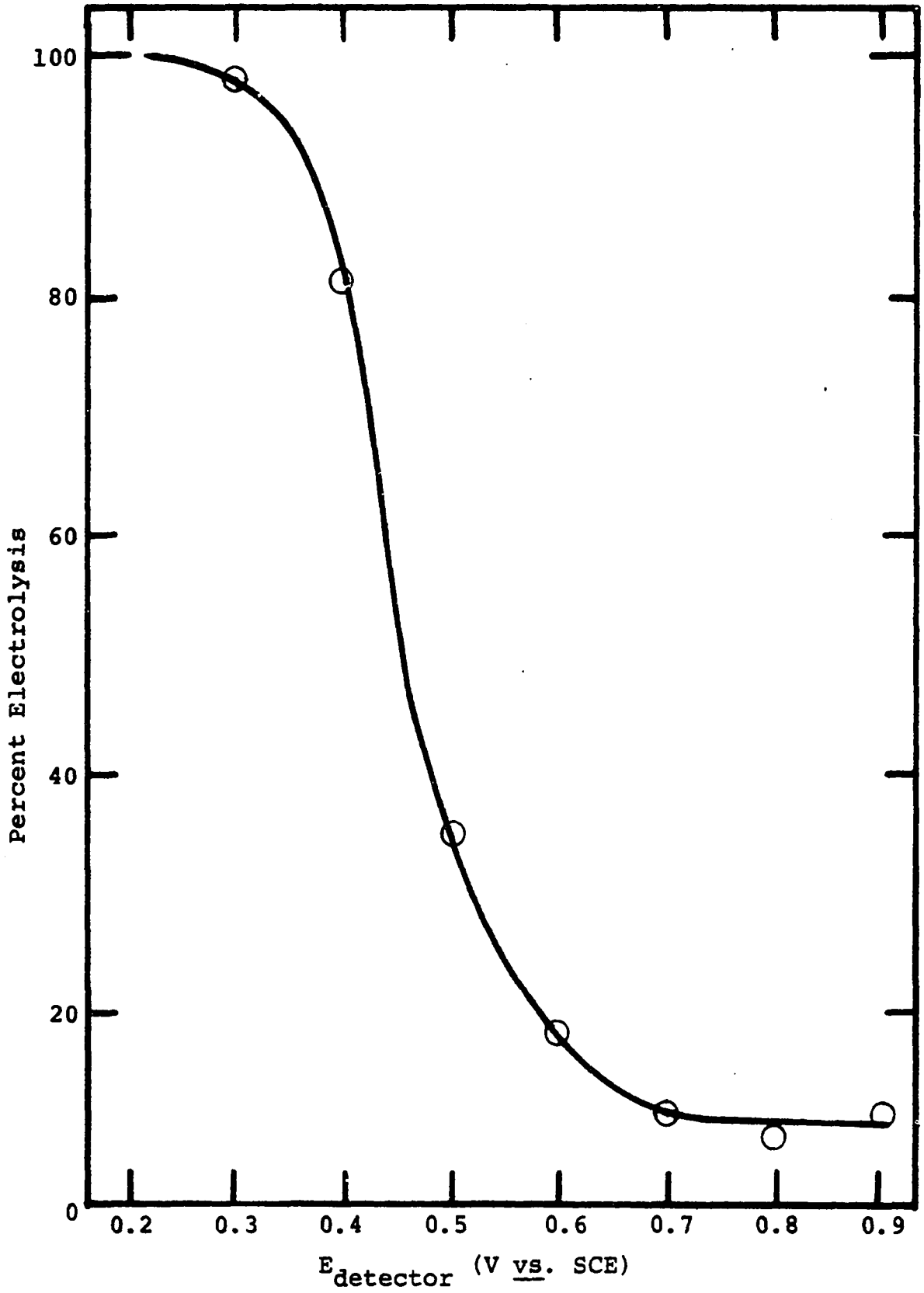
100
80
60
40
20
0
Percent Electrolysis
0.2
0.3
0.4
0.5
0.6
0.7
0.8
0.9
E detector (V vs. SCE)

Figure VIII.5. Percent $Cr_2O_7^=$ electrolyzed *vs.* flow rate Detector C. Pretreated with I^-. 0.504 ml of 1.00×10^{-4} M $Cr_2O_7^=$ injected into 4 M HCl. Electrode potential 0.25 V *vs.* SCE.

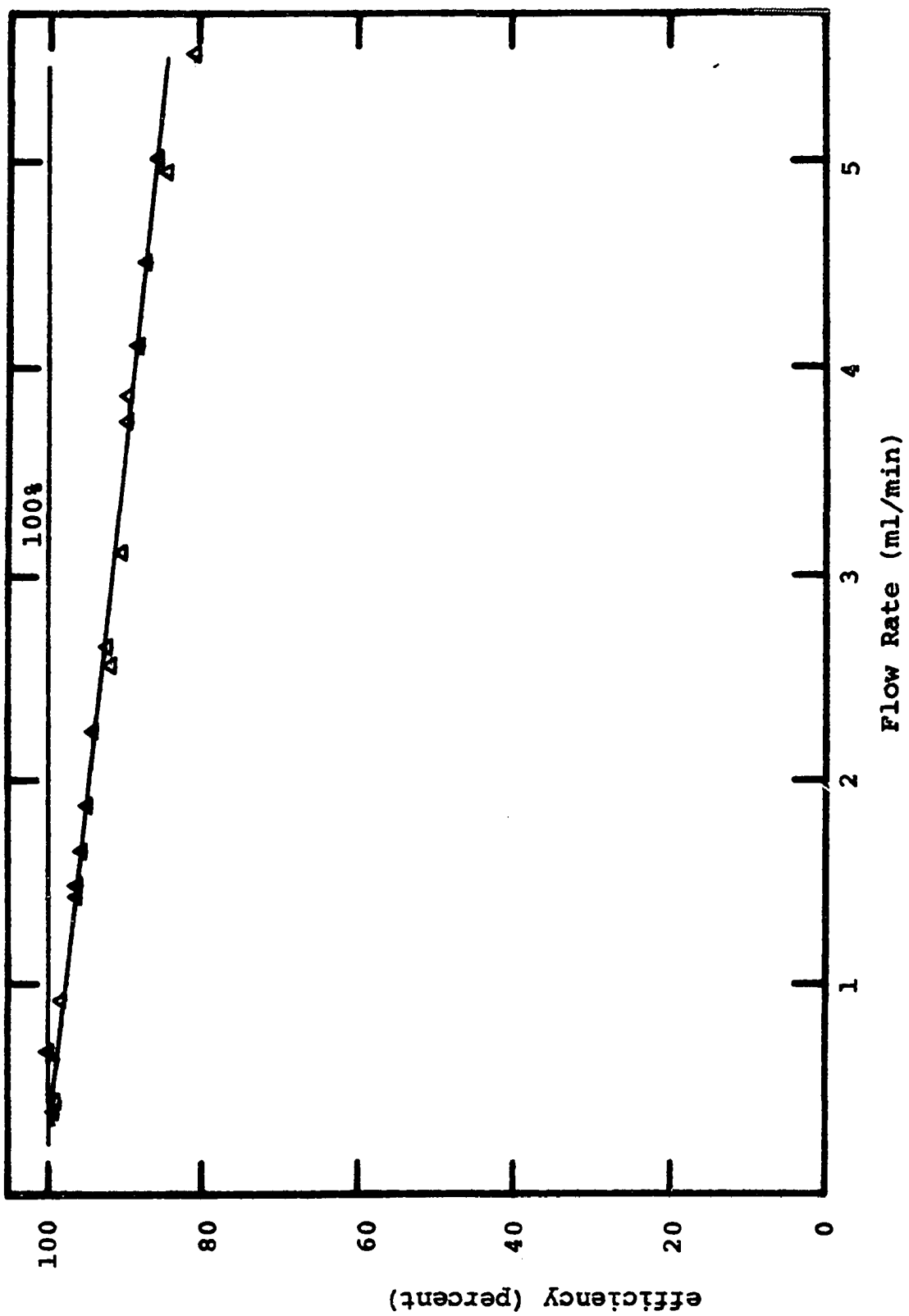
100%
efficiency (percent)
0
20
40
60
80
100
1
2
3
4
5
Flow Rate (ml/min)

efficiency approach 100%. I conclude from the data presented in Figure VIII.3 that at high mass-transport rates the reduction would be partly limited by the rate of the electrode reaction. Therefore the non-coulometric response of the detector when reducing $Cr_2O_7^{=}$ at high flow rates is qualitatively consistent with the data obtained with the RPtDE. Nevertheless Detector C can be used for accurate and precise analysis even when the efficiency is not 100% provided the efficiency is constant (i.e. flow rate is carefully controlled) and calibration is achieved with a standard solution of Cr(VI). According to Figure VIII.5, a change of only 3% is observed in sensitivity for a 10% change of flow rate. Control of flow rate within 10% limit is easily achieved for the chromatograph described.

A major concern when using solid electrodes for analysis is that deactivation of a significant fraction of the surface area can result from adsorption of solution impurities. In this specific case where activation of the electrode requires adsorption of iodide, deactivation could result from slow desorption of iodide. Because the data shown in Figure VIII.5 was obtained in a random fashion over a period of 3 hr, the fact that the data coincides satisfactorily with a smooth curve is an indication that deactivation did not occur to a significant extent during the 3-hr period.

3. Detection range

Values of pQ are plotted in Figure VIII.6 as a function of pCr(VI) in the range 1.8 - 8.8. Linearity exists for data in the pCr(VI) range 2.5 - 7.8 which corresponds to 0.4 ng - 80 μg Cr. The sample loop had a volume of 0.504 ml and 0.4 ng corresponds to 0.8 parts per billion. The response of Detector C is shown in Figure VIII.7 for injections of 1.33×10^{-8} M and 1.67×10^{-9} M Cr(VI) as well as for injection of a water blank.

The fact that a linear calibration curve is applicable for this detector over nearly six decades in the concentration range is evidence that the electrochemical detector is unique among inexpensive detectors for liquid chromatography. By way of comparison, spectrophotometric detection at 0.001 absorbance unit of Cr(VI) at a concentration of 0.8 ppb in a 1-cm cell would be possible only if a color-forming reagent was available to produce a compound with a molar absorptivity equal to approximately 7×10^{4} liter/mol-cm.

4. Precision

Replicate analyses of samples containing $Cr_2O_7^{=}$ in the range 5×10^{-9} - 2×10^{-7} N yielded results with average deviations of 1.5%. Areas of the electrolysis peaks for this study were measured on the recorder chart with a planimeter. Accurate electronic integration was possible for

Figure VIII.6. Calibration plot for Cr(VI) with Detector C Pretreated with I^-. Samples of $Cr_2O_7^=$ injected into 4 M HCl. Flow rate 3 ml/min. Detector potential 0.25 V vs. SCE.

———— Theoretical curve

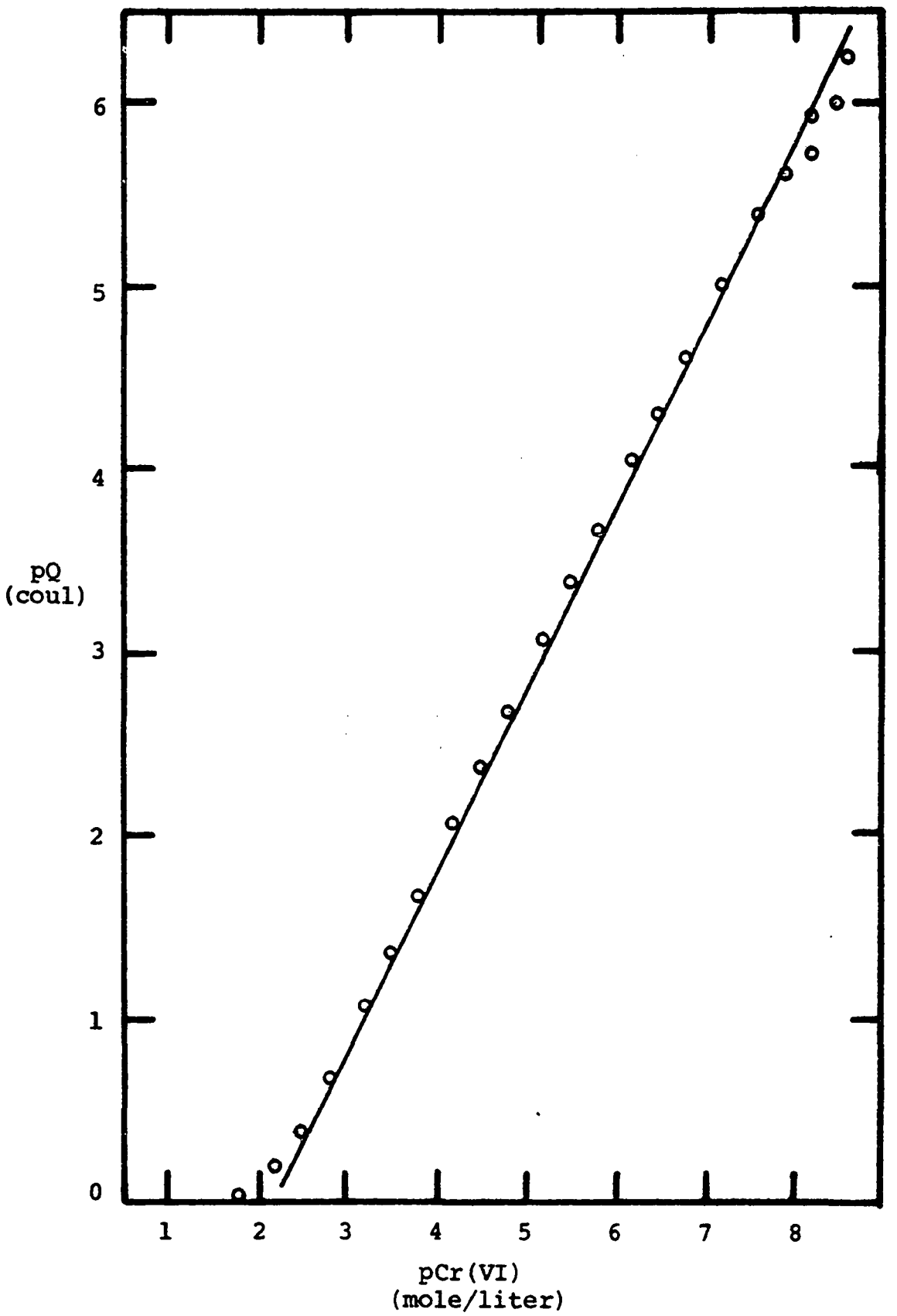
pQ
(coul)
0
1
2
3
4
5
6
1
2
3
4
5
6
7
8
pCr(VI)
(mole/liter)

Figure VIII.7. Detector response for blank and low concentrations of $Cr_2O_7^{=}$

Detector C. Pretreated with I^-. 0.504 ml samples of $Cr_2O_7^{=}$ injected into 4 M HCl. Flow rate 3 ml/min. Detector potential 0.25 V *vs.* SCE.

A 1.33×10^{-8} M Cr(VI)

B 1.67×10^{-9} M Cr(VI)

C Blank

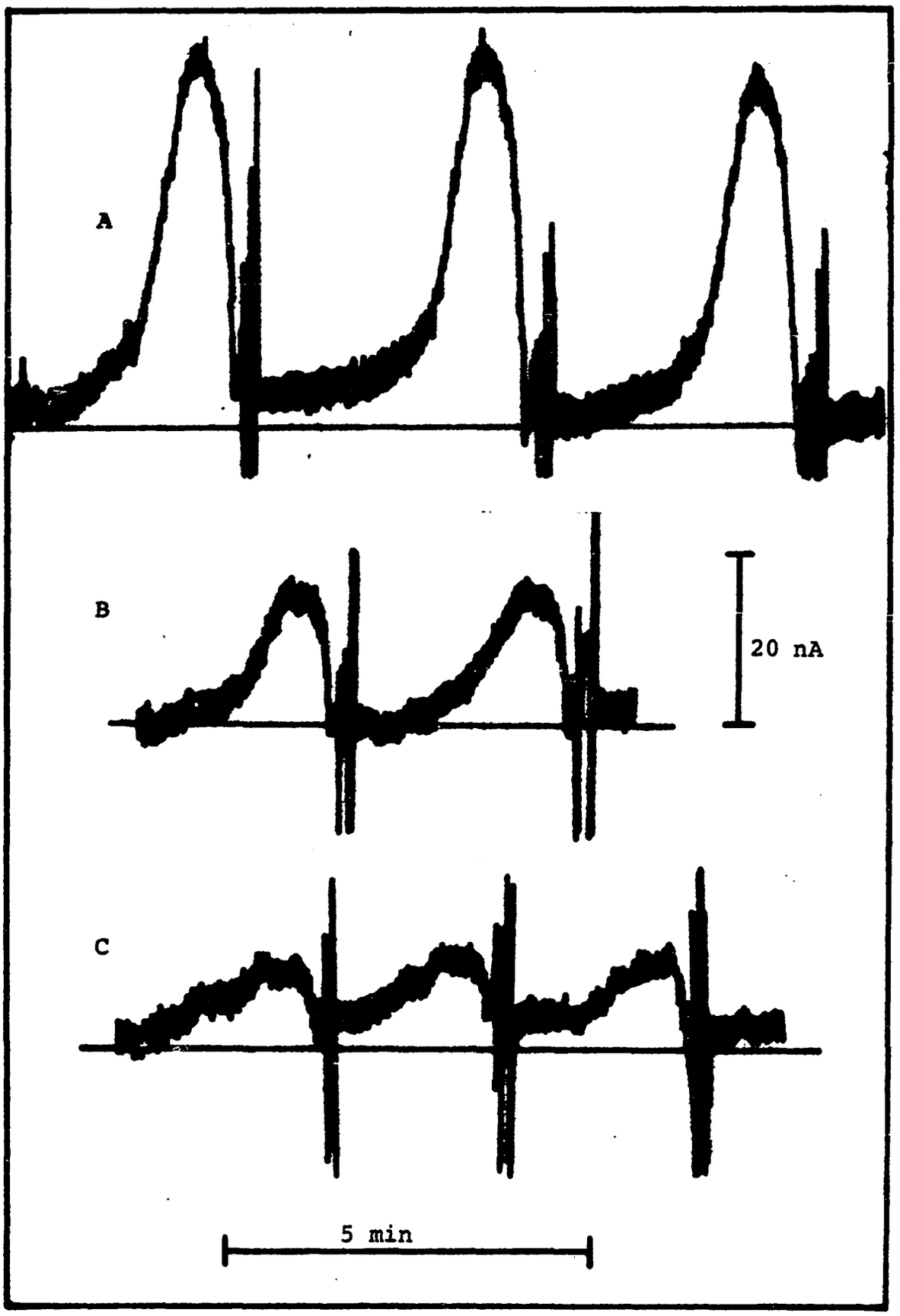
A
B
20 nA
C
5 min

concentrations greater than 5×10^{-7} N. Average deviations for replicate analyses at concentrations above 5×10^{-7} N were approximately 0.3%.

5. Ionic interferences

Cations present in samples of $Cr_2O_7^{=}$ are not retained by the alumina column and, therefore, cannot interfere with the separation. The common monovalent anions NO_3^-, Cl^-, Br^-, I^-, F^-, ClO_4^-, and CH_3COO^- are not electroactive at the detector potential used for this analysis. Furthermore, they are not adsorbed by the alumina column and have no affect on the elution time and peak width for Cr(VI). High concentrations of $SO_4^{=}$, HPO_4^{-2} and PO_4^{-3} were observed to affect the separation by displacement of adsorbed $Cr_2O_7^{=}$.

Of the common electroactive anions NO_2^-, MnO_4^-, BrO_3^- and IO_3^-, only IO_3^- was found to be retained significantly on the alumina column. However, the $Cr_2O_7^{=}$ was resolved from IO_3^- by the prescribed chromatographic procedure.

6. Analysis of water sample

A water sample suspected of containing Cr(VI) was supplied by the Veterinary Diagnostic Laboratory of Iowa State University. The sample had been made 10% concentrated HCl to prevent precipitation of $Fe(OH)_3$ and was consequently diluted 1:50 with triply distilled water prior to analysis. Chromatograms for the sample obtained at two recorder

sensitivities are shown in Figure VIII.8. A large peak was obtained for impurities (predominantly Fe(III)) eluted prior to $Cr_2O_7^{=}$.

The plot of data obtained for analysis of the sample based on the technique of standard additions is shown in Figure VIII.9. The peak area for Cr(VI) is plotted vs. the concentration of added $Cr_2O_7^{=}$. The concentration of Cr(VI) determined for the diluted sample is 20.8 ppb which corresponds to 1.04 ppm for the sample as received.

Figure VIII.8. Chromatogram of water sample

A Electroactive species other than Cr(VI).

B Cr(VI).

a Sample injected.

b Eluent changed from 0.18 M HCl to 1.8 M HCl.

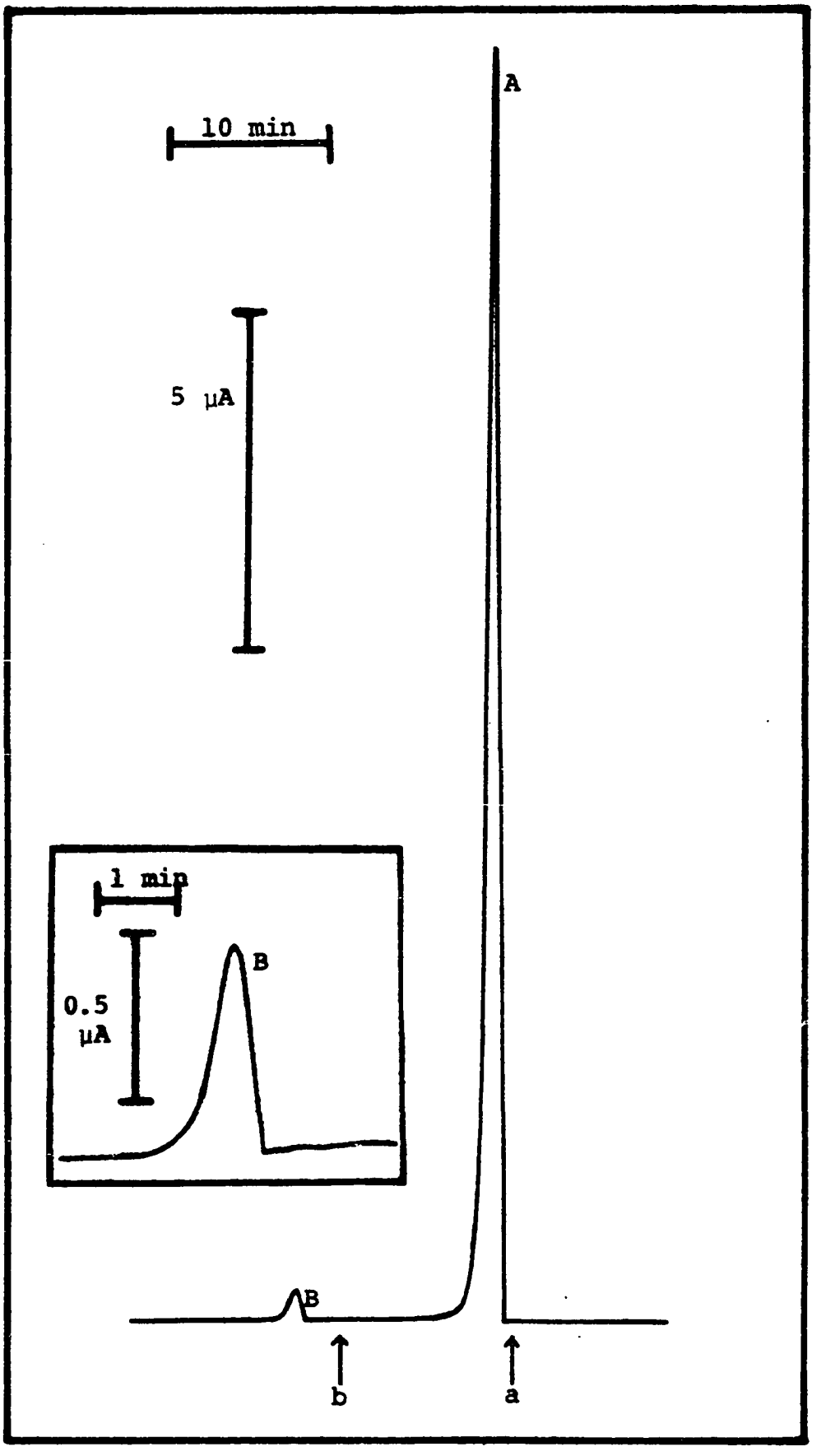
A
10 min
5 µA
1 min
B
0.5 µA
B
b
a

Figure VIII.9. Standard addition plot for the determination of Cr(VI) in the water sample

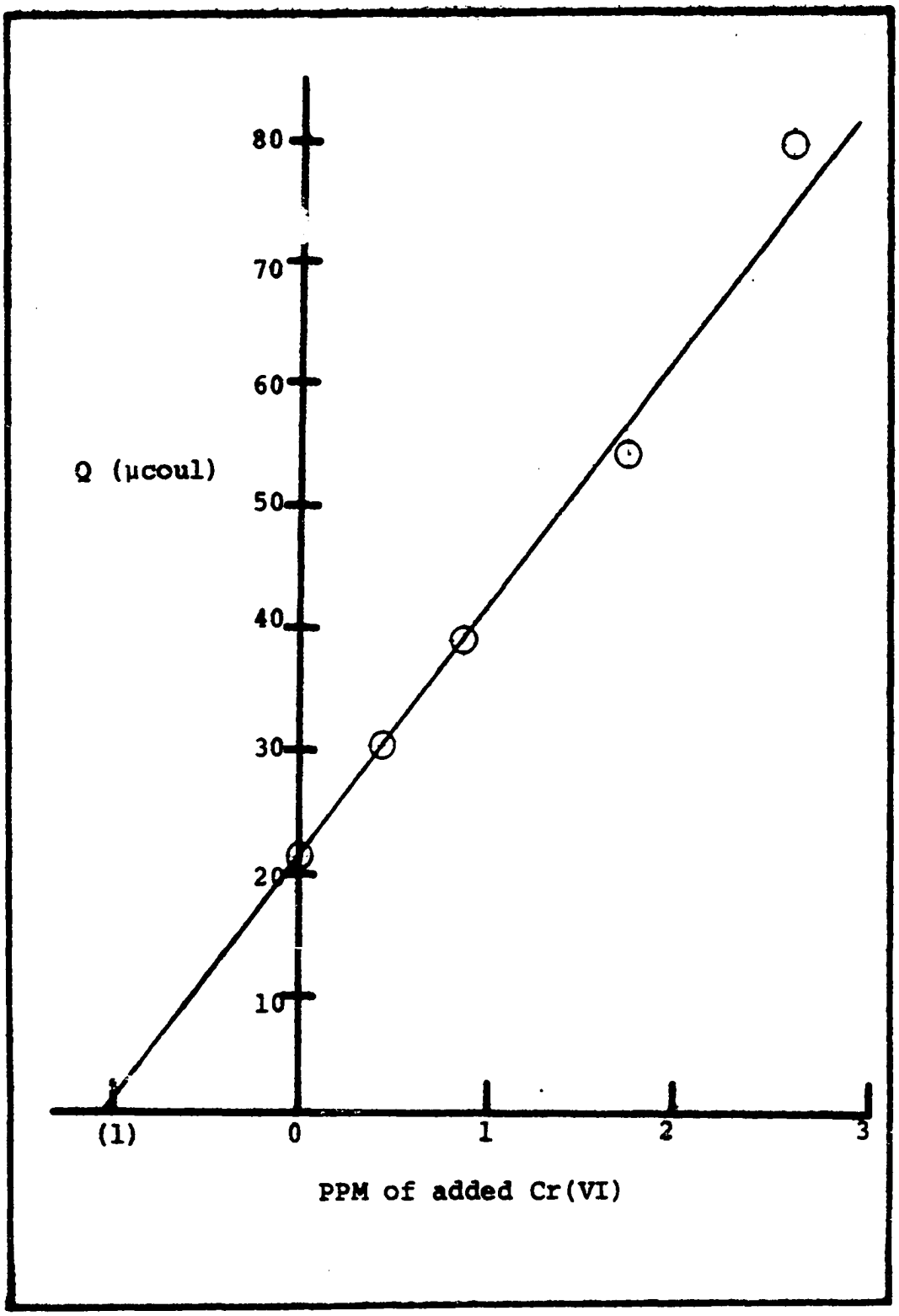
80
70
60
Q (µcoul)
50
40
30
20
10
(1)
0
1
2
3
PPM of added Cr(VI)

IX. SUMMARY

A coulometric electrochemical detector was constructed and evaluated. For electrochemical systems characterized by fast heterogeneous kinetics, the detector operated at an efficiency of 100 ± 1% for a wide range of fluid flow rates suitable for use in liquid chromatography. For example, iodide was quantitatively oxidized to iodine with efficiency $\geq$ 99.7% in the coulometric detector at flow rates less than 2 ml/min. At a constant flow rate, the sensitivity of the coulometric detector measured over an extended period of time changed less than 1 ppt.

Copper(II) and Fe(III) in artificial and standard NBS samples were determined by ion-exchange liquid chromatography with coulometric detection. The results for Cu(II) were identical to the certificate values. An average relative deviation less than 3 ppt was obtained for a sample containing 0.3% Cu by weight.

A differential pulse voltammograph was constructed and tested. Differential pulse amperometric detection with a tubular electrode was compared to detection with a coulometric electrode at constant potential. The quantitative analytical application of the coulometric detection was judged to be superior to the application of the pulsed detection.

The irreversible reduction of Cr(VI) at a Pt electrode in acidic media was discovered to be catalyzed by adsorbed

iodine. A procedure was developed for the separation of Cr(VI) in acidic solutions from various other electroactive ions by liquid chromatography with an alumina column. The detection limit for the chromatographic separation with coulometric detection was 0.1 ng of Cr(VI) in a 0.5-ml sample which corresponds to a concentration of 0.2 ppb.

X. SUGGESTIONS FOR FUTURE WORK

The limit of detection for high performance liquid chromatography with amperometric or coulometric detection is set by the residual current in the detector. Peaks attributed to charging current are observed whenever the composition of the chromatographic effluent flowing through the detector is suddenly changed. Hence, background peaks are observed for sample injection and for the changes of eluent composition required by the separation procedure. In the research described in this thesis, quantitative stripping of a selected analyte from the chromatographic column was accomplished by making a step-wise change in the electrolyte concentration of the eluent. Hence, a sudden change in the ionic strength of the effluent passing through the detector accompanies the elution peak for the analyte. The resultant background peak was diminished somewhat by mixing the effluent stream with a very concentrated solution of electrolyte to "buffer" the ionic strength of the solution passing through the detector. Use of the buffering reagent at high concentration requires virtually complete removal of electroactive impurities from the reagent. Another approach to minimize the effect of charging peaks would be the application of gradient elution rather than step-wise elution. The resulting background signal would be non-zero but would vary in a

smooth manner with time. Hence, estimation of background current when determining the area of a chromatographic peak would be made more accurate.

A current spike was frequently observed simultaneously with the injection of a sample or the switching of a control value in the chromatographic system. This phenomenon was apart from a background peak for charging which was observed when the ionic front had reached the detector after the act of changing a valve. The magnitude of the current spike was dependent on the identity of the electrolyte in the detector, the electrode potential, and the flow rate previous to the switching action. Random fluctuations of the residual current were also frequently observed during continuous flow of an electrolyte solution through the detectors. The extent of the fluctuations seemed to be a function of the identity of the electrolyte. An investigation into the mechanism of noise generation in electrochemical detectors is recommended. Such a study is likely to be difficult but the conclusions would undoubtedly be helpful for improving the detection limits for routine applications of amperometric and coulometric detectors to high performance liquid chromatography.

Chromium(VI) ions are readily adsorbed on the surfaces of containers and are easily reduced by a large variety of reducing agents including many organic compounds. Therefore,

the handling and storage of water samples containing traces of Cr(VI) may lead to serious error in the analytical results. The alumina columns used for the determination of Cr(VI) in this research are inexpensive and easily prepared. It is suggested that water can be sampled directly by drawing a measured quantity through the column with a syringe. The adsorbed Cr(VI) could then be transported and stored on the column for subsequent analysis following connection of the sample column into a chromatographic system.

Manganese(VII) and Fe(III) are quantitatively reduced to Mn(II) and Fe(II) under the conditions described here for determination of Cr(VI). The Fe(III) is not adsorbed by the alumina column and Mn(VII) is adsorbed very weakly. Hence, mixtures of Fe(III), Mn(VII) and Cr(VI) are easily separated and detected. A method should be developed for the simultaneous determination of Fe, Mn and Cr in stainless steel. The development must contend with large concentrations of anionic sulfate. The usual procedure for oxidizing Mn(II) and Cr(III) in acidic solutions of the steel samples uses $S_2O_8^=$ with subsequent destruction of excess $S_2O_8^=$ by boiling. As a result, the large concentration of $SO_4^=$ produced from the $S_2O_8^=$ may interfere with the separation scheme.

XI. BIBLIOGRAPHY

1. C. Morris and P. Morris, "Separation Methods in Biochemistry," Interscience, New York, 1963.

2. C. I. Sjoberg and G. Agren, Anal. Chem., 36, 1017 (1964).

3. J. H. Van Diqk, J. Chromatog. Sci., 10, 31 (1972).

4. B. J. Bulhin, K. Dill and J. J. Dannenberg, Anal. Chem., 43, 974 (1971).

5. T. Tsuda, Y. Ojika, M. Izuda, I. Fujishima and T. C. Ishii, J. Chromatog., 69, 194

6. H. W. Johnson, V. A. Campanile and H. A. LeFebre, Anal. Chem., 39, 33 (1967).

7. J. C. Steinberg and L. M. Carson, J. Chromatog., 2, 53 (1959).

8. J. W. O'Laughlin and C. V. Banks, Anal. Chem., 36, 1222 (1964).

9. N. Farnstedt and J. Porath, J. Chromatog., 42, 376 (1969).

10. V. G. Myerhoff, Makromol. Chem., 118, 265 (1968).

11. N. Haden et al., "Basic Liquid Chromatography," Varian Aeorgraph, Walnut Creek, CA, 1972.

12. S. H. Byrne, "Modern Practices of Liquid Chromatography," J. J. Kirkland, ed., Wiley Interscience, New York, 1954.

13. J. Polesuk and D. G. Howery, J. Chromatog. Sci., 11, 226 (1973).

14. H. F. Walton, Anal. Chem., 48, 60R (1976).

15. T. Takeuchi and N. Kaguku, Zokan, 120, 65 (1973).

16. G. Zweig and J. Sherma, Anal. Chem., 46, 79R (1974).

17. H. Veening, J. Chem. Ed., 47, 549 (1970).

18. G. Zweig and J. Sherma, Anal. Chem., 44, 42R (1972).

19. S. Haderka, J. Chromatog., 91, 167 (1974).

20. M. Krejici and P. Nadezda, J. Chromatog., 73, 105 (1972).

21. M. N. Munk, J. Chromatog. Sci., 8, 491 (1970).

22. R. A. Keller, J. Chromatog. Sci., 11, 223 (1973).

23. J. F. K. Huber, J. Chromatog. Sci., 7, 172 (1969).

24. D. R. Baker, R. C. Williams and J. C. Steichen, J. Chromatog. Sci., 12, 499 (1974).

25. V. A. Tyagai, Elektrokhimiya, 10, 3 (1974).

26. V. G. Levich, "Phsicochemical Hydrodynamics," Prentice-Hall, Englewood Cliffs, NJ, 1962.

27. W. J. Blaedel and L. N. Klatt, Anal. Chem., 38, 879 (1971).

28. L. N. Klatt and W. J. Blaedel, Anal. Chem., 40, 512 (1968).

29. W. J. Blaedel and S. L. Boyer, Anal. Chem., 43, 1538 (1971).

30. O. H. Müller, J. Am. Chem. Soc., 69, 2992 (1974).

31. W. Kemula, Raczniki Chem., 26, 281 (1952); Chem. Abstr., 51, 18479b (1947).

32. L. D. Wilson and R. J. Smith, Anal. Chem., 25, 218 (1953).

33. J. A. Lewis and K. C. Overton, Analyst, 79, 293 (1954).

34. R. Tamamushi, S. Moniyama and N. Tanaka, Anal. Chim. Acta, 23, 585 (1960).

35. W. J. Blaedel and J. H. Strohl, Anal. Chem., 33, 1631 (1961).

36. W. J. Blaedel and J. H. Strohl, Anal. Chem., 36, 445 (1964).

37. Y. Takemori and M. Honda, Rev. Polarog. Jap., 16, 96 (1970).

38. E. Scarno, M. G. Bonicelli and M. Forina, Anal. Chem., 42, 1470 (1970).

39. W. Kemula, Pure Appl. Chem., 25, 763 (1971).

40. L. D. Wilson and R. J. Smith, Anal. Chem., 25, 334 (1953).

41. H. W. Bertran, M. W. Larner, G. J. Petretic, E. S. Roszkowski, and C. J. Rodden, Anal. Chem., 30, 354 (1958).

42. W. J. Parker, Metal Ind., 2, 82 (1962).

43. L. Gierst and W. Dubru, Bull. Soc. Chim. Belges., 68, 379 (1954).

44. C. K. Mann, Anal. Chem., 29, 1385 (1957).

45. R. L. Rebertus, R. J. Cappell, and G. W. Bond, Anal. Chem., 30, 1825 (1958).

46. W. J. Blaedel and J. W. Todd, Anal. Chem., 30, 1821 (1958).

47. T. Fuginaga, S. Vugai, T. Okazaki and C. Takagi, Nippon Kagaku Zasshi, 84, 941 (1963).

48. M. Mohnke, R. Schmunk and H. Z. Schütze, Z. Anal. Chem., 219, 137 (1966).

49. W. Kemula and J. Witwicki, Roczniki Chem., 29, 115 (1955).

50. W. J. Blaedel and J. W. Todd, Anal. Chem., 33, 205 (1961).

51. B. Drake, Acta Chem. Scand., 4, 554 (1950).

52. J. G. Koen, J. F. K. Huber, H. Poppe and G. den Boef, J. Chromatog. Sci., 8, 192 (1970).

53. E. Sandi, Z. Anal. Chem., 167, 241 (1959).

54. W. Kemula, K. Bulkiewicz and Sybilska, "Modern Aspects of Polarography," Plenum Press, New York, 1966.

55. W. Kemula and Z. Stachurski, Roczniki Chem., 30, 1285 (1956).

56. D. C. Johnson and J. H. Larochelle, Talanta, 20, 959 (1973).

57. R. N. Adams, Life Sci., 14, 311 (1974).

58. P. T. Kissinger, C. Refshauge, R. Dreiling and R. N. Adams, Anal. Letters, 6, 465 (1973).

59. T. Fujinaga, Pure Appl. Chem., 25, 709 (1971).

60. P. L. Joyness and R. J. Moggs, J. Chromatog. Sci., 8, 427 (1970).

61. E. Pungor, Zs. Feher and G. Nagy, Anal. Chim. Acta, 51, 417 (1970).

62. G. Nagy, Zs. Feher, and E. Punger, Anal. Chim. Acta, 52, 47 (1970).

63. U. R. Tjaden, J. Lankelma, H. Poppe and G. Muusze, J. Chromatog., 125, 275 (1976).

64. R. M. Riggin, A. L. Schmidt and P. T. Kissinger, J. Pharm. Sci., 64, 680 (1975).

65. K. V. Thrivikraman, C. Refshauge and R. N. Adams, Life Sci., 15, 1335 (1974).

66. R. J. Maggs, Proc. in Anal. Chem., May, 103 (1972).

67. D. G. Swartzfager, Anal. Chem., 48, 2189 (1976).

68. C. Refshauge, P. T. Kissinger, R. Dreiling, L. Blank, R. Freeman and R. N. Adams, Life Sci., 14, 311 (1974).

69. R. M. Riggin, L.-D. Rau, R. L. Alcorn and P. T. Kissinger, Anal. Letters, 7, 791 (1974).

70. P. T. Kissinger, L. J. Felice, R. M. Riggin, L. A. Pachla and D. C. Wenke, Clin. Chem., 20, 992 (1974).

71. L. A. Pachla and P. T. Kissinger, Clin. Chim. Acta, 59, 309 (1975).

72. W. D. Slaunwhite, L. A. Pachla, D. C. Wenke and P. T. Kissinger, Clin. Chem., 21, 1427 (1975).

73. P. T. Kissinger, R. M. Riggin, R. L. Alcorn and L.-D. Rau, Biochem. Med., 13, 299 (1975).

74. R. M. Riggin, M. J. McCarthy and P. T. Kissinger, Agric. Food Chem., 24, 189 (1976).

75. R. M. Riggin, R. L. Alcorn and P. T. Kissinger, Clin. Chem., 22, 782 (1976).

76. C. L. Balnk, J. Chromatog., 117, 35 (1976).

77. P. T. Kissinger, L. J. Felice, W. P. King, L. A. Pachla, R. M. Riggin and R. E. Shoup, J. Chem. Ed., 54, 50 (1977).

78. J. Yamada and H. Matsuda, J. Electroanal. Chem. Interfac. Electrochem., 44, 189 (1973).

79. H. Matsuda, J. Electroanal. Chem., 16, 153 (1968).

80. B. Fleet and C. J. Little, J. Chromatog. Sci., 12, 747 (1974).

81. E. L. Eckfeldt, Anal. Chem., 31, 1453 (1959).

82. A. J. Bard, Anal. Chem., 35, 1124 (1963).

83. G. Johansson, Talanta, 12, 163 (1965).

84. E. L. Eckfeldt and E. W. Shaffer, Anal. Chem., 36, 2008 (1964).

85. J. D. Voorhies and S. M. Davis, Anal. Chem., 32, 1855 (1960).

86. J. Molnar, Magy. Kem. Foly., 68, 504 (1962); Chem. Abstr., 58, 8943 (1963).

87. W. J. Blaedel and J. H. Strohl, Anal. Chem., 36, 1245 (1964).

88. R. E. Sioda, Electrochim. Acta, 13, 375 (1968).

89. J. H. Strohl and T. A. Polutanovich, Anal. Letters, 2, 423 (1969).

90. R. L. Bamberger and J. H. Strohl, Anal. Chem., 41, 1450 (1969).

91. D. K. Roe, Anal. Chem., 36, 2371 (1964).

92. R. E. Sioda, Electrochim. Acta, 13, 1559 (1968).

93. J. A. Shropshire, J. Electroanal. Chem., 9, 90 (1965).

94. P. A. Shaffer, A. Briglio and J. A. Brockman, Anal. Chem., 20, 1008 (1948).

95. L. R. Taylor and D. C. Johnson, Anal. Chem., 46, 262 (1974).

96. Y. Takata and G. Muto, Anal. Chem., 45, 1864 (1973).

97. M. D. Seymour, J. P. Sickafoose and J. S. Fritz, Anal. Chem., 43, 1734 (1971).

98. W. J. Blaedel, C. L. Olsen and R. L. Sharma, Anal. Chem., 35, 2100 (1963).

99. D. C. Johnson, J. Electrochem. Soc., 119, 331 (1972).

100. J. Heyrovsky, Chem. Listy, 16, 256 (1922).

101. G. C. Barker, R. L. Faircloth and A. W. Gardner, At. Energy Res. Establ. (G. Brit.) AERE Harwell C/R 1786 (1955).

102. G. C. Barker and A. W. Gardner, At. Energy Res. Establ. (G. Brit.) AERE, Harwell C/R (1958).

103. E. D. Parry and R. A. Osteryoung, Anal. Chem., 37, 1634 (1965).

104. B. H. Vassos and R. A. Osteryoung, Chem. Instr., 5, 257 (1974).

105. J. B. Flanagan and L. Marcoux, J. Phys. Chem., 78, 718 (1974).

106. A. MacDonald and P. D. Duke, J. Chromatog., 83, 331 (1973).

107. A. T. Hubbard, R. A. Osteryoung and F. C. Anson, Anal. Chem., 38, 692 (1966).

108. C. A. Hampel, "Encyclopedia of the Chemical Elements," Reinhold Book Corp., New York, 1968.

109. Federal Register, 40, No. 248 (1975).

110. American Public Health Association, "Standard Methods for Examination of Water and Wastewater," 12th ed., American Public Health Assoc., New York, 1965.

XII. ACKNOWLEDGEMENTS

The author would like to thank Dr. Dennis C. Johnson not only for his assistance and guidance in the direction of this research and the preparation of this manuscript, but also for the personal guidance and interest he displayed in my growth as a person as well as a professional. The interest he shows in the welfare of his students goes way beyond that required of him as a teacher.

The author is indebted to Dr. James S. Fritz and the members of his research group for the assistance given in the assembly of the chromatograph and the development of the chromatographic separations.

The author thanks the National Science Foundation, and Pine Instrument Company, Grove City, Pennsylvania, as well as the Department of Chemistry of Iowa State University for research funds and equipment for this research.

The author would also like to acknowledge the help of his wife, Kathy, in the completion of this work.